

(18) AFOSR TR. 79-0028

(7) 

(14) ERIC-120400-1-F

**LEVEL**

(6)

(7) FINAL REPORT

SEISMIC MEASUREMENTS FOR THE PRE-DICE THROW TI-1 (TNT SHOT),  
PRE-DICE THROW II-2 (AN/FO SHOT) AND DICE THROW EVENTS.

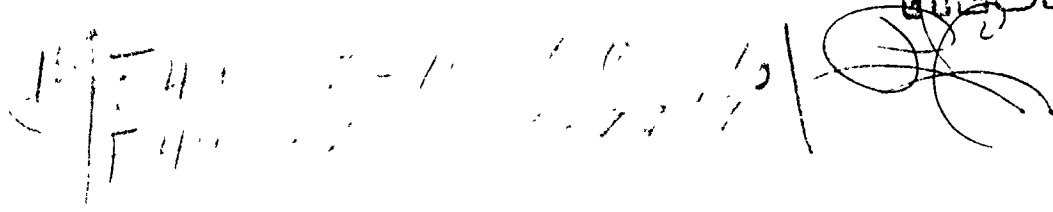
(10) R. M. TURPENING and A. R. LISKOW  
Applications Division  
Resources and Technology Group  
ENVIRONMENTAL RESEARCH INSTITUTE OF MICHIGAN  
P. O. Box 8618  
Ann Arbor, MI 48107

(11) DECEMBER 1978

(12) 136

DDC  
RECEIVED  
FFR 16 1979  
C

Distribution of this document is unlimited



AIR FORCE OFFICE OF SCIENTIFIC RESEARCH  
Building 410, Bolling Air Force Base  
Washington, D. C. 20332  
Contract No. F44620-76-C-0077  
Technical Monitor: Mr. William J. Best

AD AUG 4 605

DDC FILE COPY

9 10

012

## NOTICES

Sponsorship. The work reported herein was conducted by the Environmental Research Institute of Michigan for Air Force Office of Scientific Research, Contract No. F44620-76-C-0077. Contracts and grants to the Institute for the support of sponsored research are administered through the Office of Contracts Administration.

Final Disposition. After this document has served its purpose, it may be destroyed. Please do not return it to the Environmental Research Institute of Michigan.

AIR FORCE OFFICE OF SCIENTIFIC RESEARCH (AFSC)  
NOTICE OF TRANSMITTAL TO DDC  
This technical report has been reviewed and is  
approved for public release IAW AFR 190-12 (7b).  
Distribution is unlimited.

2. BLOSE

## PREFACE

The work reported here was conducted under two Air Force Office of Scientific Research (AFOSR) contracts F44620-76-C-0019 and F44620-76-C-0077. <sup>new</sup> The principal investigator was Dr. Roger Turpening under the direction of the Infrared and Optics Laboratory.

The field crew members who contributed greatly to this multi-year effort are Mr. John Baumler, Mr. Leo Levereault, Mr. Jim Ladd, Mr. William Juodawlkis, Mr. David Zuk, Mr. Richard Valade, Mr. Mark Bondy, Mr. Hugh Bennett, Mr. Ernie Kraudelt. The surveying work of Capt. A. Schenker and Capt. Louis Karably and Dr. Robert Reinke of the Air Force Weapons Laboratory (AFWL) is greatly appreciated.

ACCESSION for

NTIS

on ☒

on ☐

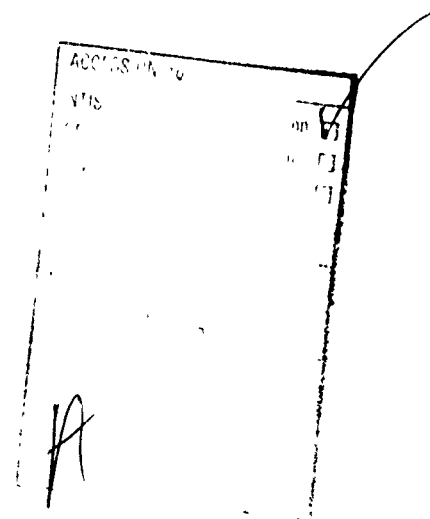
on ☐

A

## PREFACE

The work reported here was conducted under two Air Force Office of Scientific Research (AFOSR) contracts F44620-76-C-0019<sup>new</sup> and F44620-76-C-0077.<sup>new</sup> The principal investigator was Dr. Roger Turpening under the direction of the Infrared and Optics Laboratory.

The field crew members who contributed greatly to this multi-year effort are Mr. John Bauml, Mr. Leo Levereault, Mr. Jim Ladd, Mr. William Juodawlkis, Mr. David Zuk, Mr. Richard Valade, Mr. Mark Bondy, Mr. Hugh Bennett, Mr. Ernie Kraudelt. The surveying work of Capt. A. Schenker and Capt. Louis Karably and Dr. Robert Reinke of the Air Force Weapons Laboratory (AFWL) is greatly appreciated.



## PREFACE

The work reported here was conducted under two Air Force Office of Scientific Research (AFOSR) contracts F44620-76-C-0019 and F44620-76-C-0077. <sup>new</sup> The principal investigator was Dr. Roger Turpening under the direction of the Infrared and Optics Laboratory.

The field crew members who contributed greatly to this multi-year effort are Mr. John Baumler, Mr. Leo Levereault, Mr. Jim Ladd, Mr. William Juodawlkis, Mr. David Zuk, Mr. Richard Valade, Mr. Mark Bondy, Mr. Hugh Bennett, Mr. Ernie Kraudelt. The surveying work of Capt. A. Schenker and Capt. Louis Karably and Dr. Robert Reinke of the Air Force Weapons Laboratory (AFWL) is greatly appreciated.

ACCESSION for	
NTIS	Section <input checked="" type="checkbox"/>
DDC	Section <input type="checkbox"/>
U.S. Army	Section <input type="checkbox"/>
JCS	Section <input type="checkbox"/>
Pr	
A	

## CONTENTS

LIST OF TABLES	iv
LIST OF FIGURES	v
1. INTRODUCTION	1
2. SEISMIC STATIONS	3
2.1 Pre-Dice Throw II-1 (TNT Shot)	
2.2 Pre-Dice Throw II-2 (AN/FO Shot)	
2.3 Dice Throw	
3. STRUCTURE FROM BODY WAVE TRAVEL TIMES	5
3.1 Travel Times from Pre-Dice Throw II-1 (TNT Shot)	
3.2 Travel Times from Pre-Dice Throw II-2 (AN/FO Shot)	
3.3 Travel Times from Dice Throw	
3.4 Structure	
4. AMPLITUDES	9
4.1 Measurement Techniques	
4.2 Discussion of Amplitudes	
4.2.1 Pre-Dice Throw II-1 (TNT Shot)	
4.2.2 Pre-Dice Throw II-2 (AN/FO Shot)	
4.2.3 Dice Throw	
5. SUMMARY	13
REFERENCES	99
APPENDIX - SEISMOGRAMS FROM THE PRE-DICE THROW II-1 (TNT Event), PRE-DICE THROW II-2 (AN/FO Event), AND DICE THROW EVENTS	100
DISTRIBUTION LIST	114

# LIST OF FIGURES

<u>FIGURE</u>	<u>TITLE</u>	<u>PAGE</u>
1	Seismograph Stations for Pre-Dice Throw II-1 (TNT Shot)	21
2	P-Wave Travel Times, Pre-Dice Throw II-1 (TNT Shot), South Sites	22
3	P-Wave Structure in the Queen 15 Area of White Sands Missile Range, Derived from the First Arrivals from the Pre-Dice Throw II-1 (TNT Shot) and Pre-Dice Throw II-2 (AN/FO Shot)	23
4	Description of Measurement Criteria.	24
5	Various Displacement and Particle Velocity Curves Used for Association with Rayleigh Wave Data in this Report	25
6	P-Wave Particle Velocity, Pre-Dice Throw II-1 (TNT Shot) Vertical Component, North Sites	26
7	P-Wave Particle Displacement, Pre-Dice Throw II-1 (TNT Shot), Vertical Component, North Sites.	27
8	P-Wave Particle Velocity, Pre-Dice Throw II-1 (TNT Shot), Longitudinal Component, North Sites	28
9	P-Wave Particle Displacement, Pre-Dice Throw II-1 (TNT Shot), Longitudinal Component, North Sites	29
10	P-Wave Particle Velocity, Pre-Dice Throw II-1 (TNT Shot), Vertical Component, South Sites	30
11	P-Wave Particle Displacement, Pre-Dice Throw II-1 (TNT Shot), Vertical Component, South Sites	31
12	P-Wave Particle Velocity, Pre-Dice Throw II-1 (TNT Shot), Longitudinal Component, South Sites	32
13	P-Wave Particle Displacement, Pre-Dice Throw II-1 (TNT Shot), Longitudinal Component, South Sites	33
14	Rayleigh Wave Particle Velocity, Pre-Dice Throw II-1 (TNT Shot), North Sites	34
15	Rayleigh Wave Particle Displacement, Pre-Dice Throw II-1 (TNT Shot), North Sites	35

<u>FIGURE</u>	<u>TITLE</u>	<u>PAGE</u>
16	Particle Velocity, Pre-Dice Throw II-1 (TNT Shot) Rayleigh Waves, South Sites	36
17	Rayleigh Wave Particle Displacement, Pre-Dice Throw II-1 (TNT Shot), South Sites	37
18	Particle Velocity for Fundamental Mode Rayleigh Wave, Pre-Dice Throw II-1 (TNT Shot), North Sites	38
19	Particle Displacement for Fundamental Mode Rayleigh Wave, Pre-Dice Throw II-1 (TNT Shot), North Sites	39
20	Particle Velocity for Fundamental Mode Rayleigh Wave, Pre-Dice Throw II-1 (TNT Shot), South Sites	40
21	Particle Displacement for Fundamental Mode Rayleigh Wave, Pre-Dice Throw II-1 (TNT Shot), South Sites	41
22	Seismograph Stations for Pre-Dice Throw II-2 (AN/FO Shot)	42
23	P-Wave Travel Times, Pre-Dice Throw II-2 (AN/FO Shot), South Sites	43
24	P-Wave Travel Times, Pre-Dice Throw II-2 (AN/FO Shot), North and Northwest Sites	44
25	P-Wave Travel Times, Pre-Dice Throw II-2 (AN/FO Shot), Northeast Sites	45
26	P-Wave Travel Times, Pre-Dice Throw II-1 (TNT Shot) and II-2 (AN/FO Shot), South, North, and Northeast Sites	46
27	P-Wave Particle Velocity, Pre-Dice Throw II-2 (AN/FO Shot), Vertical Component, North Sites and East Sites	47
28	P-Wave Particle Displacement, Pre-Dice Throw II-2 (AN/FO Shot), Vertical Component, North and East Sites	48
29	P-Wave Particle Velocity, Pre-Dice Throw II-2 (AN/FO Shot), Longitudinal Component, North and East Sites	49
30	P-Wave Particle Displacement, Pre-Dice Throw II-2 (AN/ FO Shot) Longitudinal Component, North and East Sites	50
31	P-Wave Particle Velocity, Pre-Dice Throw II-2 (AN/FO Shot), Vertical Component, South Sites	51



<u>FIGURE</u>	<u>TITLE</u>	<u>PAGE</u>
32	P-Wave Particle Displacement, Pre-Dice Throw II-2 (AN/FO Shot), Vertical Component, South Sites	52
33	P-Wave Particle Velocity, Pre-Dice Throw II-2 (AN/FO Shot), Longitudinal Component, South Sites	53
34	P-Wave Particle Displacement, Pre-Dice Throw II-2 (AN/FO Shot), Longitudinal Component, South Sites	54
35	Particle Velocity for Rayleigh Wave, Pre-Dice Throw II-2 (AN/FO Shot), South Sites	55
36	Particle Displacement for Rayleigh Wave, Pre-Dice Throw II-2 (AN/FO Shot), South Sites	56
37	Particle Velocity for Rayleigh Wave, Pre-Dice Throw II-2 (AN/FO Shot), North and Northeast Sites	57
38	Particle Displacement for Rayleigh Wave, Pre-Dice Throw II-2 (AN/FO Shot), North and Northeast Sites	58
39	Particle Velocity for Fundamental Mode Rayleigh Wave, Pre-Dice Throw II-2 (AN/FO Shot), South Sites	59
40	Particle Displacement for Fundamental Mode Rayleigh Wave, Pre-Dice Throw II-2 (AN/FO Shot), South Sites	60
41	Particle Velocity for Fundamental Mode Rayleigh Wave, Pre-Dice Throw II-2 (AN/FO Shot), North and Northeast Sites	61
42	Particle Displacement for Fundamental Mode Rayleigh Wave, Pre-Dice Throw II-2 (AN/FO Shcc), North and Northeast Sites	62
43	Seismograph Stations for Dice Throw Event	63
44	P-Wave Travel Times, Dice Throw, East Sites	64
45	P-Wave Travel Times, Dice Throw, South Sites	65
46	P-Wave Particle Velocity, Dice Throw, Vertical Component, South Sites	66
47	P-Wave Particle Displacement, Dice Throw, Vertical Component, South Sites	67

<u>FIGURE</u>	<u>TITLE</u>	<u>PAGE</u>
48	P-Wave Particle Velocity, Dice Throw, Longitudinal Component, South Sites.	68
49	P-Wave Particle Displacement, Dice Throw, Longitudinal Component, South Sites	69
50	P-Wave Particle Velocity, Dice Throw, Vertical Component, East Sites.	70
51	P-Wave Particle Displacement, Dice Throw, Vertical Component, East Sites	71
52	P-Wave Particle Velocity, Dice Throw, Longitudinal Component, East Sites	72
53	P-Wave Particle Displacement, Dice Throw, Longitudinal Component, East Sites	73
54	Particle Velocity for Rayleigh Wave, Dice Throw, South Sites.	74
55	Particle Displacement for Rayleigh Wave, Dice Throw, South Sites.	75
56	Particle Velocity for Rayleigh Wave, Dice Throw, East Sites.	76
57	Particle Displacement for Rayleigh Wave, Dice Throw, East Sites.	77
58	Particle Velocity for Fundamental Mode Rayleigh Wave, Dice Throw, South Sites.	78
59	Particle Displacement for Fundamental Mode Rayleigh Wave, Dice Throw, South Sites.	79
60	Particle Velocity for Fundamental Mode Rayleigh Wave, Dice Throw, East Sites.	80
61	Particle Displacement for Fundamental Mode Rayleigh Wave, Dice Throw, East Sites	81
62	Plan View of Position of All P and SH Refraction Profiles in the Queen 15 Area.	82

<u>FIGURE</u>	<u>TITLE</u>	<u>PAGE</u>
63	SH Wave Data from the Long Refraction Profile in Figure 62.	83
64	P-Wave Travel Times for Long Line (4 Segments) Shown in Figure 62.	84
65	P ( $\alpha$ ) and SH Wave ( $\beta$ ) Structure Along the Long Refraction Profile Shown in Figure 62.	85
66	SH Travel Time Curve for Long Refraction Profile in Figure 62.	86
67	SH Velocity ( $\beta$ ) Structure Near Queen 15 Area White Sands Missile Range.	87
68	Position of Short P and SH Refraction Profiles at GZ-5 (Queen 15 Area).	88
69	Calibration Lines: P-Waves	89
70	Calibration Lines: SH-Waves	90
71	Crater Line I: P-Waves	91
72	Crater Line I: SH-Waves	92
73	Crater Line II: P-Waves	93
74	Crater Line II: SH-Waves	94
75	Plan View of Three Short P and SH Refraction Profiles Near Ground Zero Area (GZ-5) of Pre-Dice Throw I Area.	95
76	3-D Model of Data Given in Figure 75.	96
77	Ray Tracing Attempt to Determine Crater Size Along Crater Line II	97
78	Ray Tracing Attempt to Determine Crater Size Along Crater Line II	98
APPENDIX FIGURES A-1 THROUGH A-13		101-113

LIST OF TABLES

<u>TABLE</u>	<u>TITLE</u>	<u>PAGE</u>
1	P-Wave Data, Pre-Dice Throw II-1 (TNT Shot), August 1974	15
2	P-Wave Data, Pre-Dice Throw II-2 (AN/FO Shot), September 1975	17
3	P-Wave Data, Dice Throw, 1976	19

Abstract  
↓

INTRODUCTION

During 1975 and 1976 three large chemical explosions of the Pre-Dice Throw and Dice Throw series were detonated on the surface at the White Sands Missile Range, New Mexico. The data for these explosions are ~~as follows:~~ <sup>given in this report.</sup>

Pre-Dice Throw II-1 (TNT Shot)  
12 August 1975  
16:59:59.801 Z  
100 tons of TNT  
32° 22' 43.8536" N  
106° 21' 52.4406" W

Pre-Dice Throw II-2 (AN/FO Shot)  
22 September 1975  
20:00:00.0 Z  
120 tons of ANFO  
33° 22' 51.2754" N  
106° 21' 47.8485" W

Dice Throw  
6 October 1976  
15:00:00.0 Z  
620 tons of ANFO  
33° 40' 48." N  
106° 31' 06." W

also

This report, <sup>also</sup> presents the results of some seismic field measurements over the distance range of 0.91 km (3,000 ft) to 17.7 km (58,000 ft). The P waves and Rayleigh waves from these events are described (travel times and amplitudes) in this report. One of the predominant features of the seismograms was the presence of a very large amplitude, low velocity, fundamental mode Rayleigh wave. This wave had a velocity only slightly greater than the speed of sound in air. The implications of this low phase velocity for the local structure is given by Reinke (1977) and <sup>is</sup> will not be treated here. The maximum amplitudes observed

Cont. → for this phase, as well as the amplitudes of the higher mode Rayleigh waves are given here. Austen

A different, but related, study is also described in this work. A series of P and SH refraction profiles were performed near the ground zero area (GZ-5) for the Pre-Dice Throw II-1 event. These data were collected to address two different problems.

First, the nature of the dispersion curve of the large amplitude fundamental mode Rayleigh wave needed considerable study. Reinke needed S wave velocities in order to conduct that study and the Environmental Research Institute of Michigan (ERIM) provided those velocities by means of a long (1.52 km) double-ended SH refraction profile. For completeness P wave data was also collected. One leg of the profile extends further to a range of 1.83 km. Good SH velocities were obtained to a depth of approximately 0.43 km (1,400 ft), while the P wave data reaches a depth of approximately 0.12 km.

Three short P and SH profiles were deployed in the GZ-5 area to study the feasibility of using P and SH refraction data to determine the size of the altered region around a large explosion.

## SEISMIC STATIONS

## 2.1 PRE-DICE THROW II-1 (TNT Shot)

Figure 1 shows the position of the seismometers for Pre-Dice Throw II-1 within the Queen 15 area of the White Sands Missile Range. The distances from ground zero (GZ-5) to the seismometers are given in Table 1. The array of seismometers tends "along the axis" of the Tularosa Basin. The north end of the array covers some of the "nose" of the Basin where the sedimentary layers form a monocline up towards Mockingbird Gap.

The types of seismometers and their response curves are given in a previous report (Turpening, 1976). For the purposes of this report it is sufficient to say that the four seismometers nearest the event (N3000 and S3000; N5000 and S5000) are special low sensitivity three-component seismometers (0.11 volts/cm/sec) whereas the remaining three component seismometers have a high sensitivity of 22.05 volts/cm/sec. The data from the sites (N5000, N3000, S3000, S5000, S8700) closest to the event were recorded on a single digital tape recorder at a sample rate of 300 samples/second. The data from the other sites were recorded on analog tape recorders.

## 2.2 PRE-DICE THROW II-2 (AN/FO Shot)

Figure 22 shows the position of the seismometers for the Pre-Dice Throw II-2 event. Again the closest five (5) sites were hardwired to the digital tape recorder. The position of these five sets were unchanged from the previous event. The orientation of each three-component seismometer was changed to "point" the longitudinal toward the new ground zero area (GZ-6). Three new stations were occupied along Highway 8. The two stations at NW 70 and Ben Site were placed there in anticipation of the 620 ton event (Dice Throw) in 1976. The type of seismometers used were the same as for Pre-Dice Throw II-1. Table 2 gives the distances from each site to the event.

### 2.3 DICE THROW

Figure 43 displays the position of the seismic stations used for the Dice Throw event. Here the low sensitivity (Mark Products L10-B) seismometers were placed at 6000 East, 8500 East, 6000 South and 8500 South. All other sites used the high sensitivity (Hall Sears HS-10-2) seismometers. The Ben Site was reoccupied.



## STRUCTURE FROM BODY WAVE TRAVEL TIMES

## 3.1 TRAVEL TIMES FROM PRE-DICE THROW II-1 (TNT Shot)

The travel times for the P wave for this event are given in Table 1 and Figure 2. The travel time curve shown in Figure 2 has been fit by eye to the data. The data point at 35,000 feet appears to be a late pick but Figure 26 shows that it is merely on the next branch of the travel time curve.

## 3.2 TRAVEL TIMES FROM PRE-DICE THROW II-2 (AN/FO Shot)

The travel times for Pre-Dice Throw II-2 are given in Table 2 and Figures 23, 24, and 25. In Figure 26 we display the P wave travel time data from both events.

## 3.3 TRAVEL TIMES FROM DICE THROW

The travel times for the Dice Throw event are given in Table 3 and Figures 44 and 45.

## 3.4 STRUCTURE

The travel times from Dice Throw II-1 and II-2 provide a coarse look at the structure of the Tularosa Basin. Near surface details are provided in two steps, by the refraction profiles around the ground zero area (GZ-5) for Pre-Dice Throw II-1. These shorter profiles are also of two wave types (P and SH).

The travel times from the Pre-Dice Throw II-1 and II-2 events do not yield the first layer velocities because of the coarse station spacing, therefore, the structures shown in Figure 3 use the average of the near surface P wave velocities from the three short profiles around GZ-5. This velocity (1.78 km/sec) is the velocity observed for the alluvium below the water table. We observed very few data points for the dry

alluvium since the water table is very close to the surface in the Queen 15 area. Adding a thin layer of dry alluvium to the structures in Figure 3 would make no measureable difference in the deep structure.

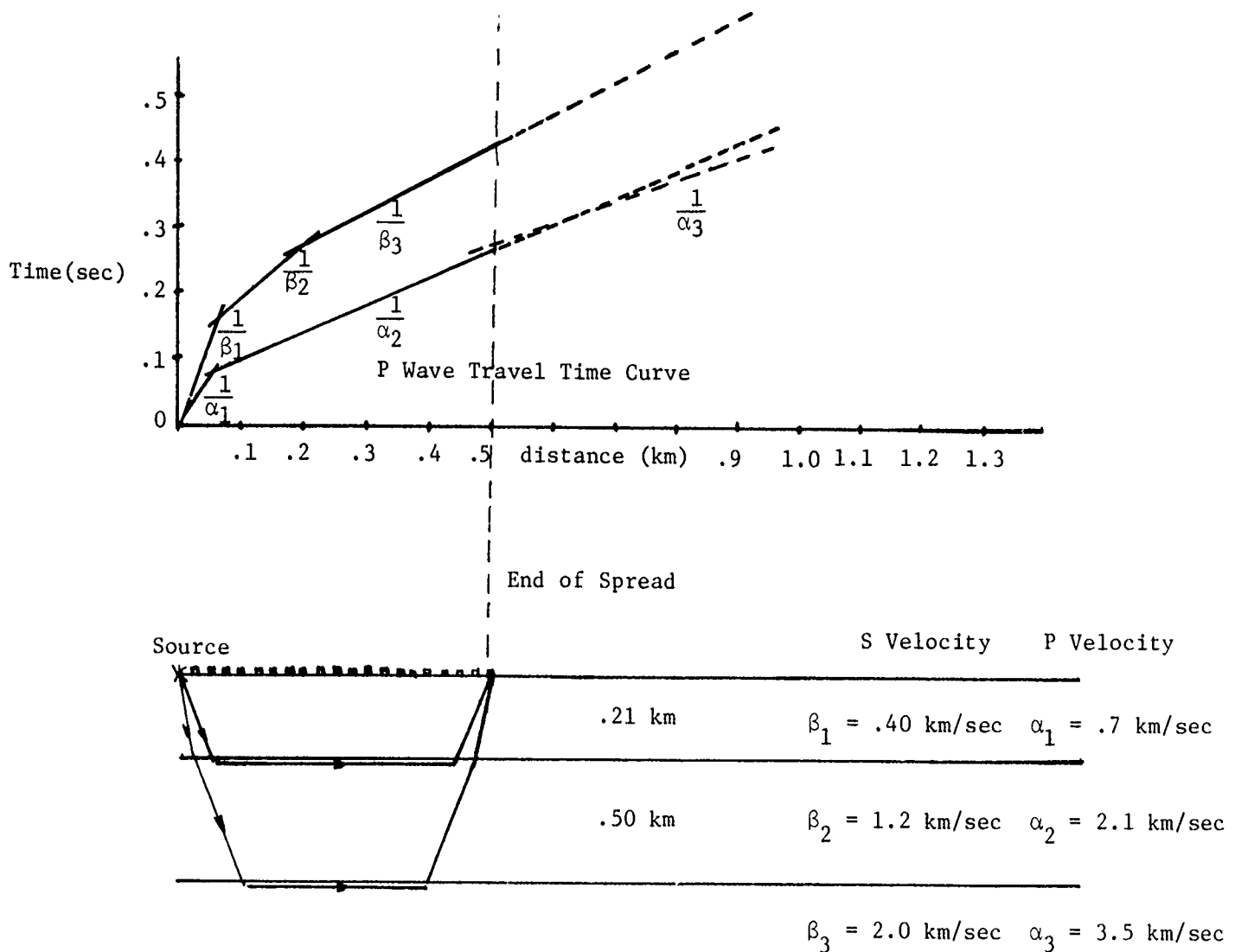
We show in Figure 3 two structures which are very similar; the only difference being the velocity of the third layer. One structure represents the region south of the shot points while the other depicts the structure to the northeast of the Queen 15 area. The P wave velocity ( $\alpha$ ) of the third layer, the top of which is at a depth of approximately one kilometer is 4.88 km/sec to the south while 4.4 km/sec to the northeast. This probably is not a major difference, but rather reflects some local dip to that layer.

The second layer ( $\alpha = 2.56$  km/sec) in both models obviously does not show the detail obtained on the double ended profiles shown in Figure 65 and 67. The depth to the top of the second layer is consistent among the three P wave measurements since the P wave double ended profile shows a dip to the northwest and since the position of this profile is between (see Figure 62) the seismic stations to the south of GZ-5 and those stations to the northeast of GZ-6.

The more shallow structure in the Queen 15 area is given in Figures 63 through 67. There we see the SH data (Figure 63), SH travel time curve (Figure 66) and SH structure (Figure 67). The SH structure has been derived by Reinke (1977). An additional interpretation of the second layer is given in the dashed lines. These indicate the faulted structure seen in the P wave data. The deeper SH structure, the low velocity zone, and higher SH velocity (1.38 km/sec) under it is not seen on the P wave data because the profile was not long enough. Stated differently this means that our profile of 1.52 km in length was able to "penetrate" to a depth greater than one half a kilometer for the SH structure but only about one tenth of a kilometer for P waves. The reason is simply the difference in velocities. Not only are the

velocity ratios involved but also the absolute value of the velocities.

In the example shown below one can see that the P wave break point between the second layer and the half space occurs outside the geophone spread. Therefore, we never see the  $\alpha_3$  arrivals as first arrivals. However, because  $\beta_1$  and  $\beta_2$  are small,  $\frac{1}{\beta_1}$  and  $\frac{1}{\beta_2}$  are large (slopes are steep) therefore we see the  $\beta_3$  arrivals as first arrivals.



This observation is clearly shown in the three very shallow profiles done in and near GZ-5. Here the object was to see if the P and SH data could delineate the region of material altered by the explosion.

In the vicinity of the Pre-Dice Throw II-1 ground zero area (GZ-5) special seismic studies were conducted in October 1976. They involved a close look at the P and SH structure in the area. The work was divided into two parts. First the work of Reinke and Herrin at SMU required knowledge of the S wave structure in the area to a depth of approximately 0.4 km (3000 ft). To achieve that goal a double-ended refraction profile was deployed east, southeast of GZ-5 (Figure 62). The profile was 1.521 km (5000 ft) long with an extension of 0.3 km (1000 ft) by adding data beyond the north shot point and into the GZ-5 area. Good SH data was obtained along the entire profile (Figure 63) from ERIM's gun type shear wave generator. P wave data was also gathered with routine use of buried explosives. The P and SH data are displayed in Figure 64 and Figure 66. The SH data was used by Reinke (1976) (unpublished PhD Thesis) to determine the structural control (Figure 67) for the fundamental mode Rayleigh wave. The P wave data is studied with the SH data because of the current need to understand the full use of such data in rubbleization work. More specifically, recent work (Toksoz, Cheng, and Timur, 1976; O'Connell and Budiansky, 1974) have shown that given "before" and "after" P and S wave data one can determine something about the porosity or crack density and degree of saturation of an altered portion of rock.

Using the same shear wave generator three short profiles (P and SH) were done very near GZ-5 (Figure 68). These profiles are shown in Figures 69-74, and a statement of the results shown in Figure 75 and 76. It is clear that the altered rock or sediments in the vicinity of GZ-5 are seen by means of the low SH velocities. Even though there is scatter in the calibration line data (this would be eliminated in any future work by means of a strict before and after deployment), it is clear that nowhere are the SH velocities as low as they are near GZ-5.

## AMPLITUDES

## 4.1 MEASUREMENT TECHNIQUE

Three different seismic wave amplitude measurements were made on the explosion data (see Appendix for the wave forms of the explosion events). P wave measurements were made, "normal" Rayleigh wave amplitudes were taken and the amplitude of the late, large arrival was taken. This arrival was determined by Herrin and Reinke (1976, personal communication) to be the fundamental mode Rayleigh wave. In the data that follows it is labelled as such. The "normal" Rayleigh wave consists of the higher mode components. This is labelled here simply as Rayleigh wave data. We present both particle velocity and displacement data.

The P wave data were read as indicated in Figure 4 by measurements (A) and (B). This convention was adopted by many investigators during the early years of nuclear explosion seismology. It is used here as a convenient standard. For the (A) measurement the period associated with that is four times the time seen from the first break to the first peak. The frequency quoted is the reciprocal of that period. This measurement is obviously less certain than the (B) measurement since one must make a judgement of the first break time. The period associated with a (B) measurement is twice the time between the two measurement points (the plus peak to the minus peak). For the Rayleigh waves the maximum peak to peak measurement was taken on the seismogram. The displacement for that measurement was then calculated. The frequency for the calculation was obtained just as in the (B) data for P waves. We duplicated all of these measurements for the longitudinal and the transverse seismograms for the surface waves.

To aid in the understanding of the data certain arbitrary functions of amplitude and distance are placed on the graphs. The choice of these curves is arbitrary and is intended to aid the eye

in drawing out differences. For P wave data we display a  $\frac{1}{r^3}$  function for comparison. Only the slope of the curve should be observed, the position of the curve has been arbitrarily chosen. The Rayleigh wave data is displayed with curves derived from Zbur's (personal communication) displacement curves for a 100 ton surface explosion. As shown in Figure 5 several curves are used. A particle velocity curve was derived from a displacement curve by selecting a frequency (f) common to most of the data on the graph and multiplying the displacement values for all distances by  $2\pi f$  (i.e., the curve is moved upward).

When scaling from the 100 ton surface explosion to the 620 ton surface explosion (Dice Throw) we chose a displacement amplitude scaling exponent of  $1/2$ . Much literature exists on the scaling of underground amplitudes as a function of charge weight (e.g., Rodean, 1971), but little exists on surface blasts. Thus the value of  $1/2$  is tested here.

Figures 6 through 21 display the P wave and Rayleigh wave amplitude data from Pre-Dice Throw II-1. The Pre-Dice Throw II-2 amplitude data is given in Figures 27 through 42 and the Dice Throw amplitudes are shown in Figures 46 through 61.

## 4.2 DISCUSSION OF AMPLITUDES

### 4.2.1 Pre-Dice Throw II-1 (TNT Shot)

The P wave particle velocity measurements are merely a direct conversion of A and B measurements from the seismograms since they (the seismograms) do, in fact present particle velocity. The displacement data are calculated from the particle velocity data. The particle velocity data follow a  $\frac{1}{r^3}$  relationship very nicely whereas the displacement data do not. The close-in displacement data are generally low. This would lead one to state that the close-in data were clipped at the seismometer, however, no indication of that exists in any of the waveforms. It is clear that the particle velocity of the close-in stations are high because the frequency of those P waves is high.

If one examines only the (B) measurement one finds that the attenuation to the south is much less than that to the north. This observation holds true for the overall particle velocity level of the higher mode Rayleigh waves also. Compare Figure 14 with Figure 16, note that we had to use curve D to "fit" the data to the south whereas curve C fits quite well to the north. Curve D differs from curve C by a factor of approximately 3. The fundamental mode Rayleigh data do not show this difference. The data to the north and to the south seem equally distributed about curve C.

#### 4.2.2 Pre-Dice Throw II-2 (AN/FO Shot)

The P wave particle velocity data do indicate that the close-in measurements are clipped. With those data in quotes we see that again the attenuation to the south is less than that to the north and east. With the higher mode Rayleigh waves we see that the particle velocities at the north and northeast sites exceed the C curve and the displacements exceed Zbur's curve. The fundamental mode is also greater in displacement amplitude and particle velocity but not as great a departure as that of the higher modes. One can see that Pre-Dice Throw II-1 exceeded II-2 by approximately a factor of 1.11 (P wave displacement ratio). This represents a ratio of explosive charge of 1.22 if an exponent of  $1/2$  is used or 1.37 if an exponent of  $1/3$  is used.

#### 4.2.3 Dice Throw

The P wave amplitude data are very well behaved for the Dice Throw event. The observation can be made that at approximately 9 km from the source (to the south) we see a grouping of amplitudes that could arise from the junction of two branches of the travel time curve. These stations are also the ones leading up to and in Mockingbird Gap. Therefore, one would expect much less attenuation in this area and resulting grouping of data. The limited amount of data to the east is nonetheless very well represented by the  $\frac{1}{r^3}$  decay rate. If we assume

that spherical spreading holds for the P wave here then the remaining attenuation can be described by an absorption coefficient  $\alpha = 0.000083/\text{km}$  where  $\alpha$  enters as:

$$A_i = A_o \left(\frac{1}{r}\right)^n e^{-i\omega\alpha r}$$

$n = 1$ , for spherical spreading

$$\omega = 2\pi f$$

For the problem of weight scaling the surface waves, the higher modes seem best scaled as

$$\left(\frac{w_1}{w_2}\right)^{1/2}$$

where  $w_1$  and  $w_2$  are the weights of the explosives

for the sites east of the event, but a coefficient of  $1/3$  is better for the data to the south. On the fundamental mode Rayleigh we must alter the rate of decay from Zbur's  $r^{-1.9}$  to  $r^{-4.9}$  and then we see that a weight scaling coefficient of  $1/2$  is good.



## SUMMARY

The key observations in this report are:

- 1) The travel time data from the three events yields a simple three-layer structure for the Tularosa Basin. The long P wave refraction profile adds knowledge of local dip and two faults to the southeast of GZ-5 and GZ-6. The SH profile, however, shows not only these faults and dip but also gives support to the idea of a low velocity zone in the area. At this time we cannot say whether that low velocity zone affects both the P and SH velocities or the SH velocity alone since the detailed long P wave refraction profile did not go deep enough.
- 2) Shear wave (SH) wave refraction work is now routine for spread lengths up to 1.5 km in length. It must be made clear that SH not SV profiles are routine. This is unfortunate since the SV velocities are required for Rayleigh wave velocity computations. Jolly (1956) has shown that the shear wave velocity in a layered medium is a function of polarization. The SH wave, as seen in this report, is easier to observe because it can be recorded on transverse horizontal geophones with little P wave contamination. The SV wave must be recorded on either longitudinal geophones or vertical geophones both of which easily record the P wave and, therefore contaminate the SV arrival time.
- 3) As a seismic source function Pre-Dice Throw II-1 was slightly (weight ratio of 1.22) larger than Pre-Dice Throw II-2.
- 4) The Dice Throw event data support a weight scaling coefficient of  $1/2$  for sites to the east but a coefficient of  $1/3$  to the south.

- 5) When viewed in graphical form the fundamental mode Rayleigh wave is not strikingly greater than the peak-to-peak measurement of the higher mode Rayleigh wave seen in seismograms.
- 6) The P wave data from the Dice Throw event show an overall rate of decay very close to the  $\frac{1}{r^3}$  and, therefore, an absorption coefficient of  $\alpha = 0.000083/\text{km}$  is appropriate for the second layer in the Trinity area.
- 7) The very short P and SH profiles in the vicinity of GZ-5, Queen 15 area show the value of SH measurements. Over the 0.3 km spread lengths the P wave data gives no indication whatsoever (probably due to the high water table) of an altered area of alluvium. The SH data show a distinctly lower velocity in the region around GZ-5. Furthermore, the SH data show a great deal of scatter in travel times that is related to the detailed earth structure and not the usual difficulty in reading S wave arrival times.

PRE DICE THROW II-1 - AUGUST 1975

[illegible]

V = Vertical Seismometers

R = Radial Seismometers

TABLE 1.

P-Wave Data  
PRE-DICE THROW II-1- August 1975

[illegible]

V = Vertical Seismometers

R = Radial Seismometers

TABLE 1. (Continued)

PRE-DICE THROW P-Wave Data  
II-2 - September 1975

[illegible]

V = Vertical Seismometers

R = Radial Seismometers

TABLE 2

PRE-DICE THROW II-2 - September 1975

[illegible]

V = Vertical Seismometers

R = Radial Seismometers

TABLE 2. (Continued)

[illegible]

R = Radial Seismometers

19

## DICE THROW-Analog-1976

V = Vertical Seismometers

R = Radial Seismometers

TABLE 3. (Continued)



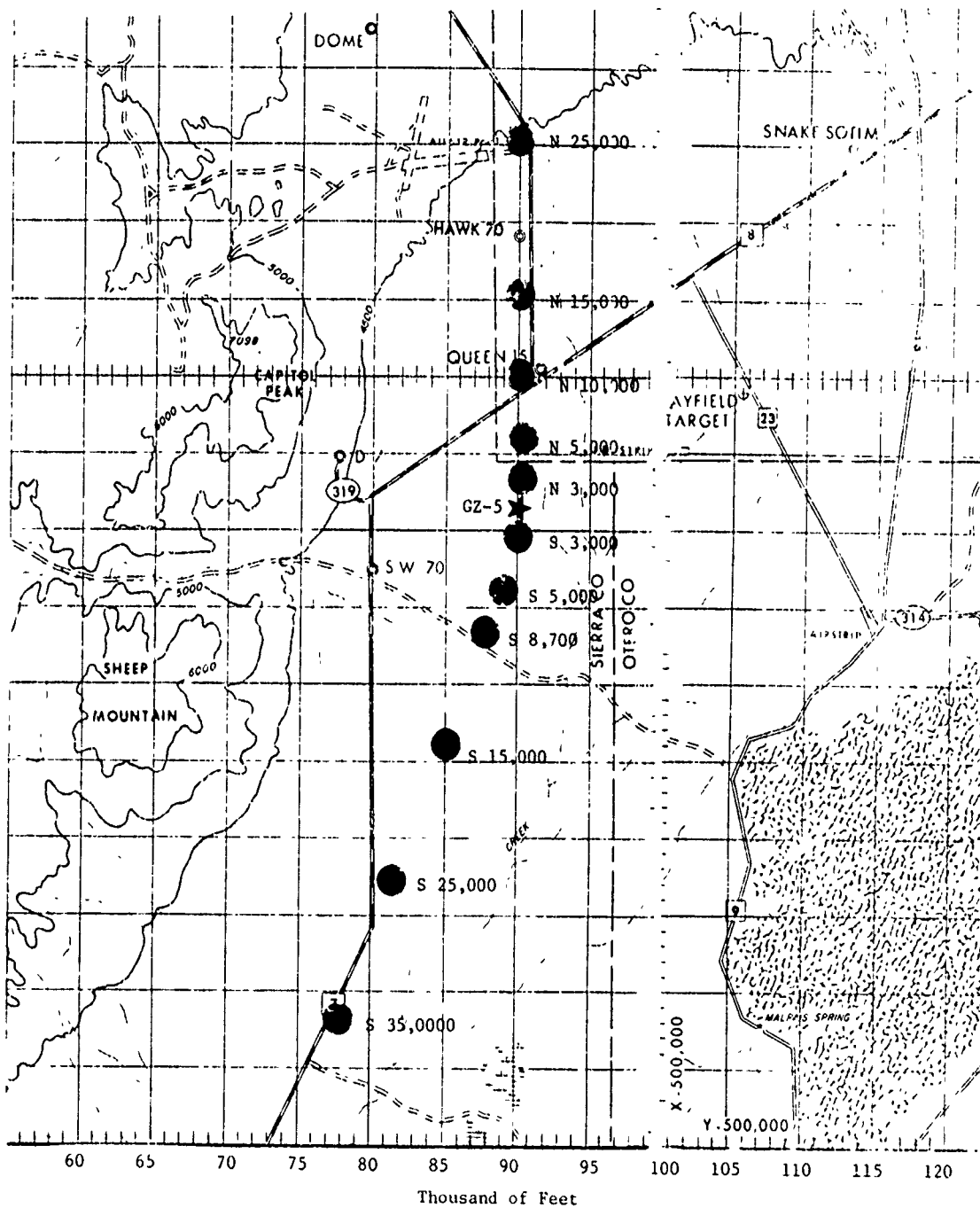


FIGURE 1. SEISMOGRAPH STATIONS FOR PRE-DICE THROW II-1 (TNT Shot)

ERIM

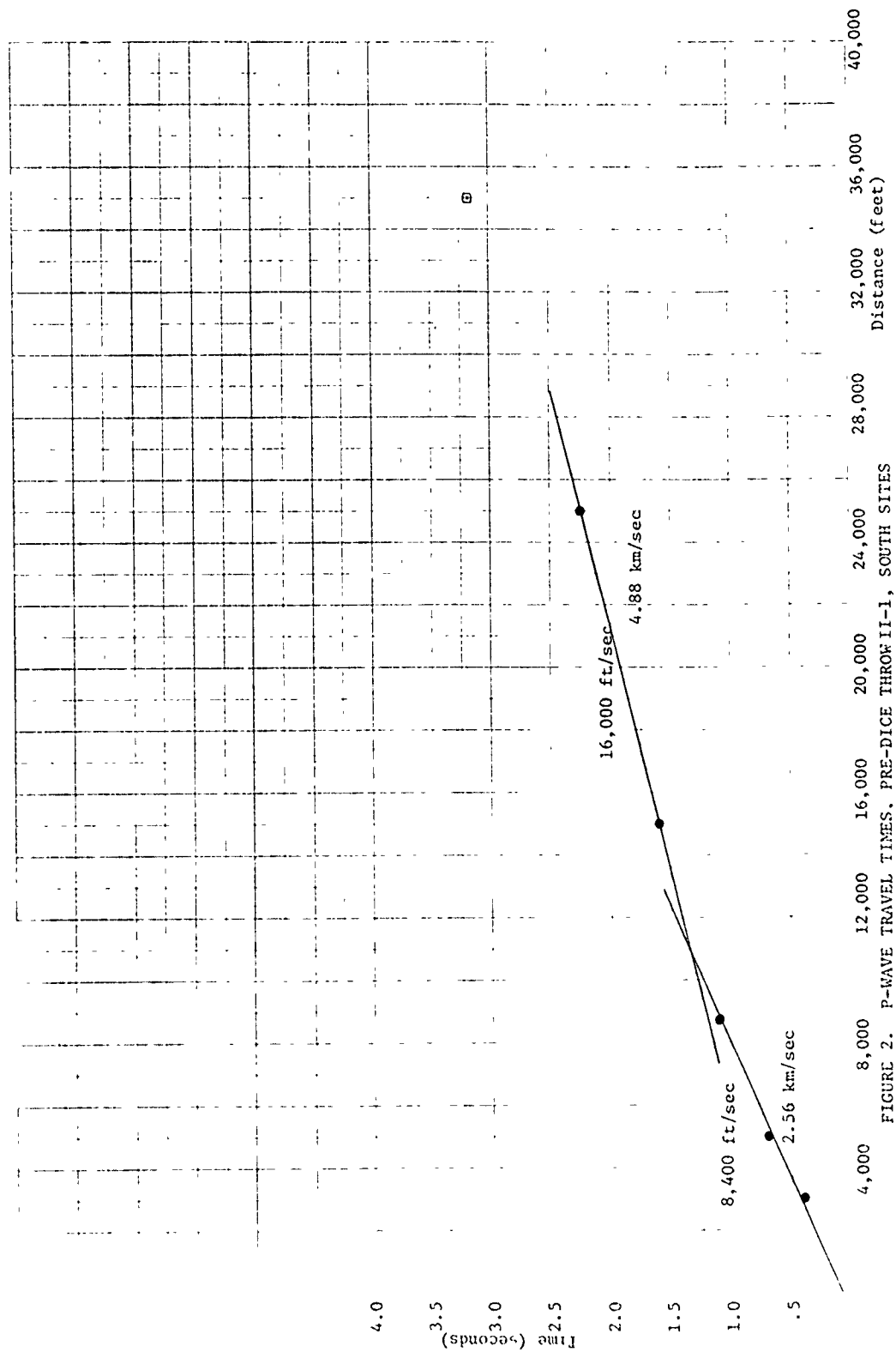


FIGURE 2. P-WAVE TRAVEL TIMES. PRE-DICE THROW II-1, SOUTH SITES

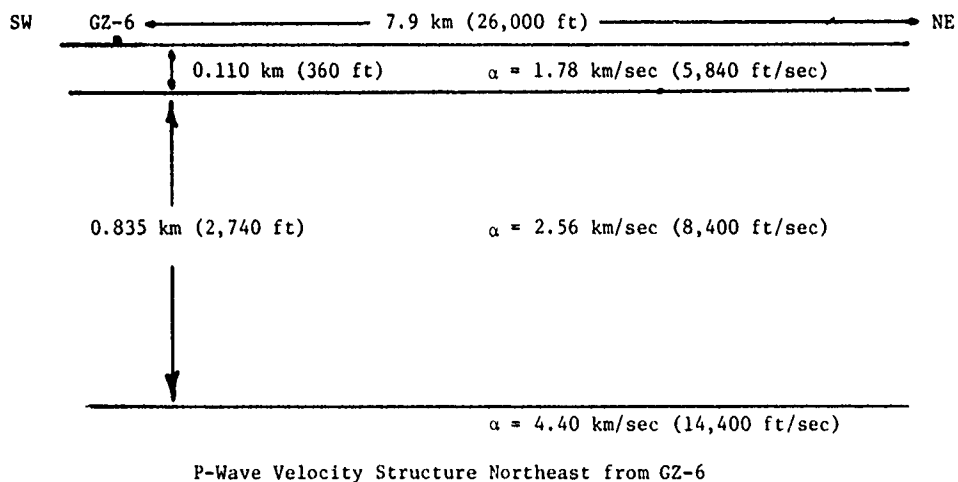
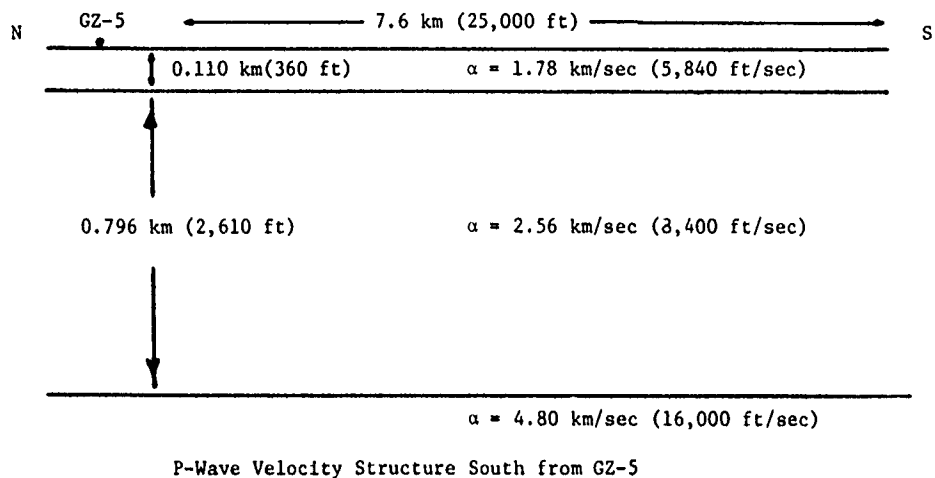


FIGURE 3. P-WAVE STRUCTURE IN THE QUEEN 15 AREA OF WHITE SANDS MISSILE RANGE, DERIVED FROM THE FIRST ARRIVALS FROM THE PRE-DICE THROW II-1 and II-2 EVENTS.

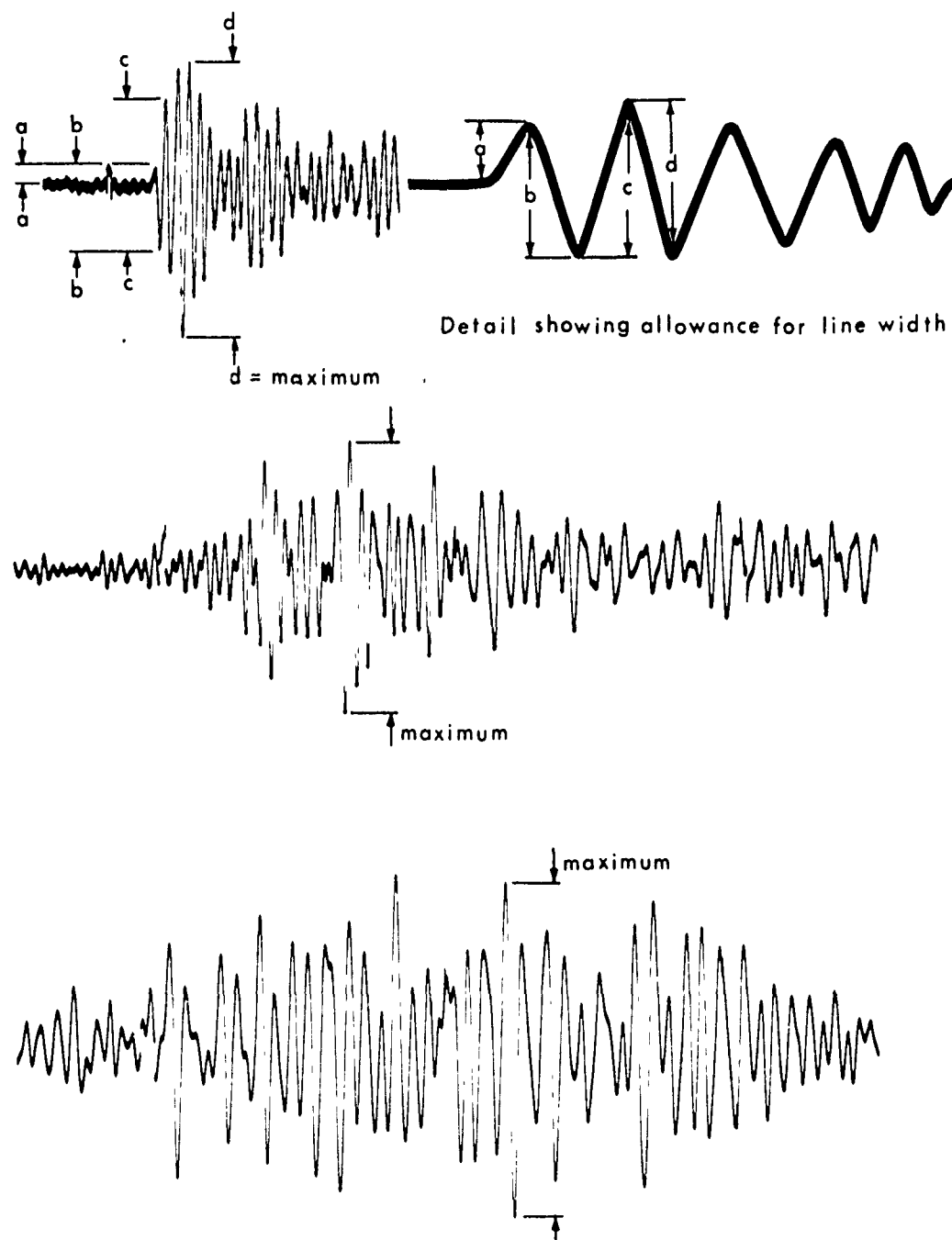


FIGURE 4. DESCRIPTION OF MEASUREMENT CRITERIA. In this report measurements a, b and the maximum were used.

- A. Zbur's maximum displacement curve for a 100 ton surface explosion (Slope  $\approx \frac{1}{r^{1.9}}$ )
- B. Zbur's maximum displacement curve scaled by  $\sqrt{6.3}$  for a 630 ton surface explosion (Slope  $\approx \frac{1}{r^{1.9}}$ )
- C. Particle velocity curve for 100 ton surface explosion with  $f = 3$  Hz. (scaled by  $2\pi \cdot 3$ )
- D. Maximum particle velocity curve for 630 ton surface explosion with  $f = 3$  Hz also maximum particle velocity curve for 100 ton surface explosion with  $f = 10$  Hz (scaled by  $2\pi \cdot 10$ )
- E. Maximum particle velocity curve for 630 ton surface explosion with  $f = 15$  Hz.

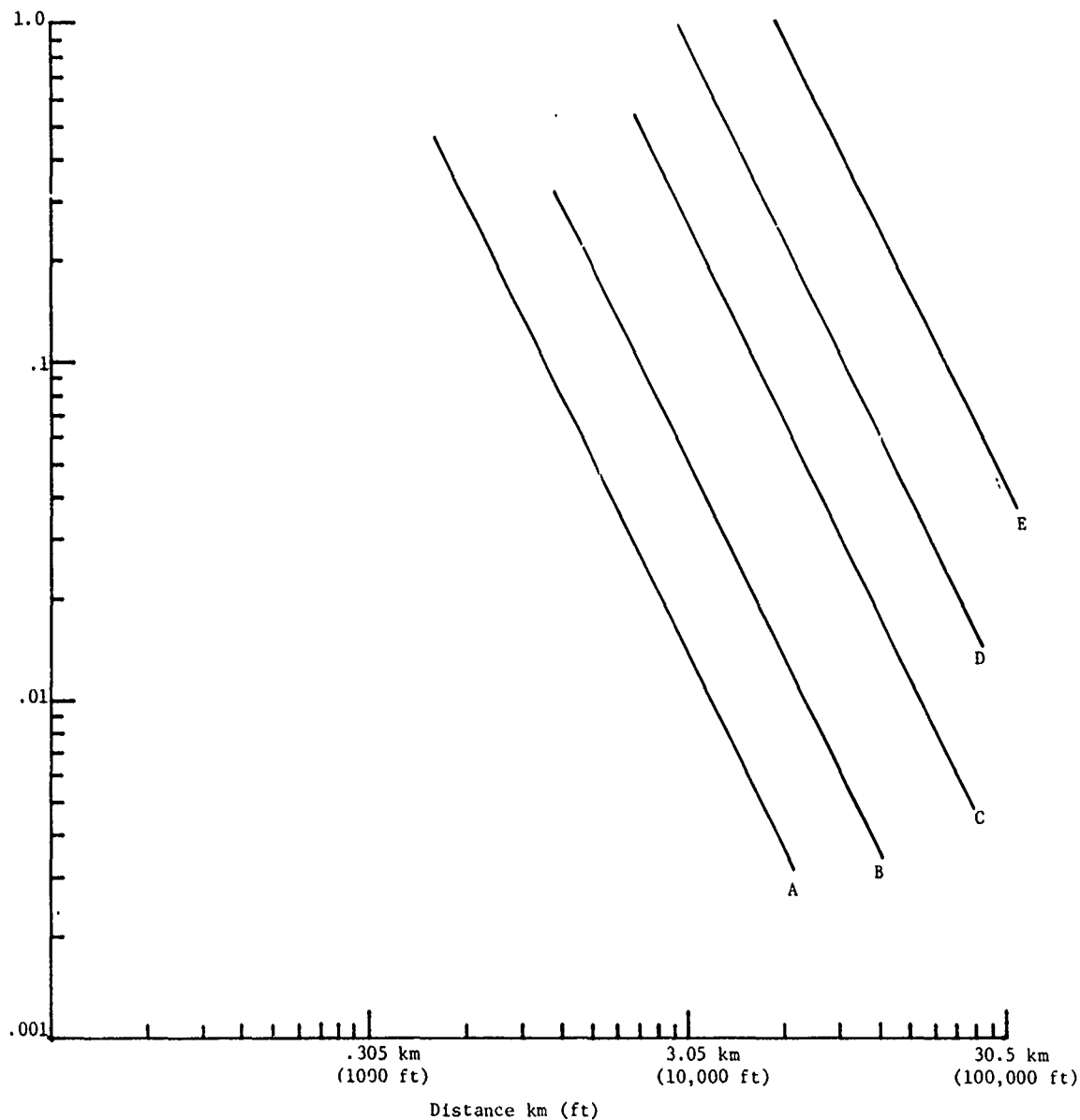


FIGURE 5. VARIOUS DISPLACEMENT AND PARTICLE VELOCITY CURVES USED FOR ASSOCIATION WITH RAYLEIGH WAVE DATA IN THIS REPORT.

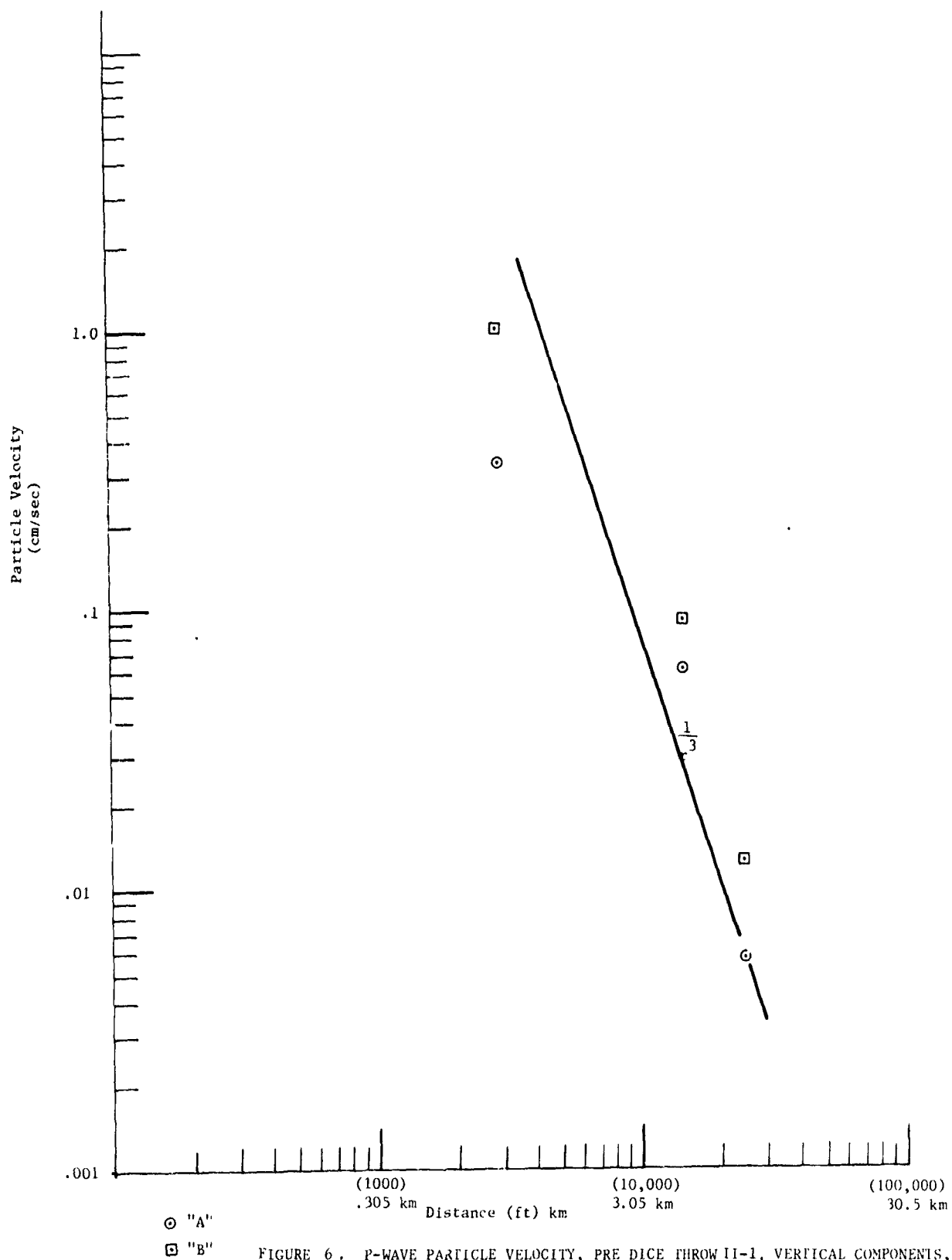


FIGURE 6. P-WAVE PARTICLE VELOCITY, PRE DICE THROW II-1, VERTICAL COMPONENTS, NORTH SITES.

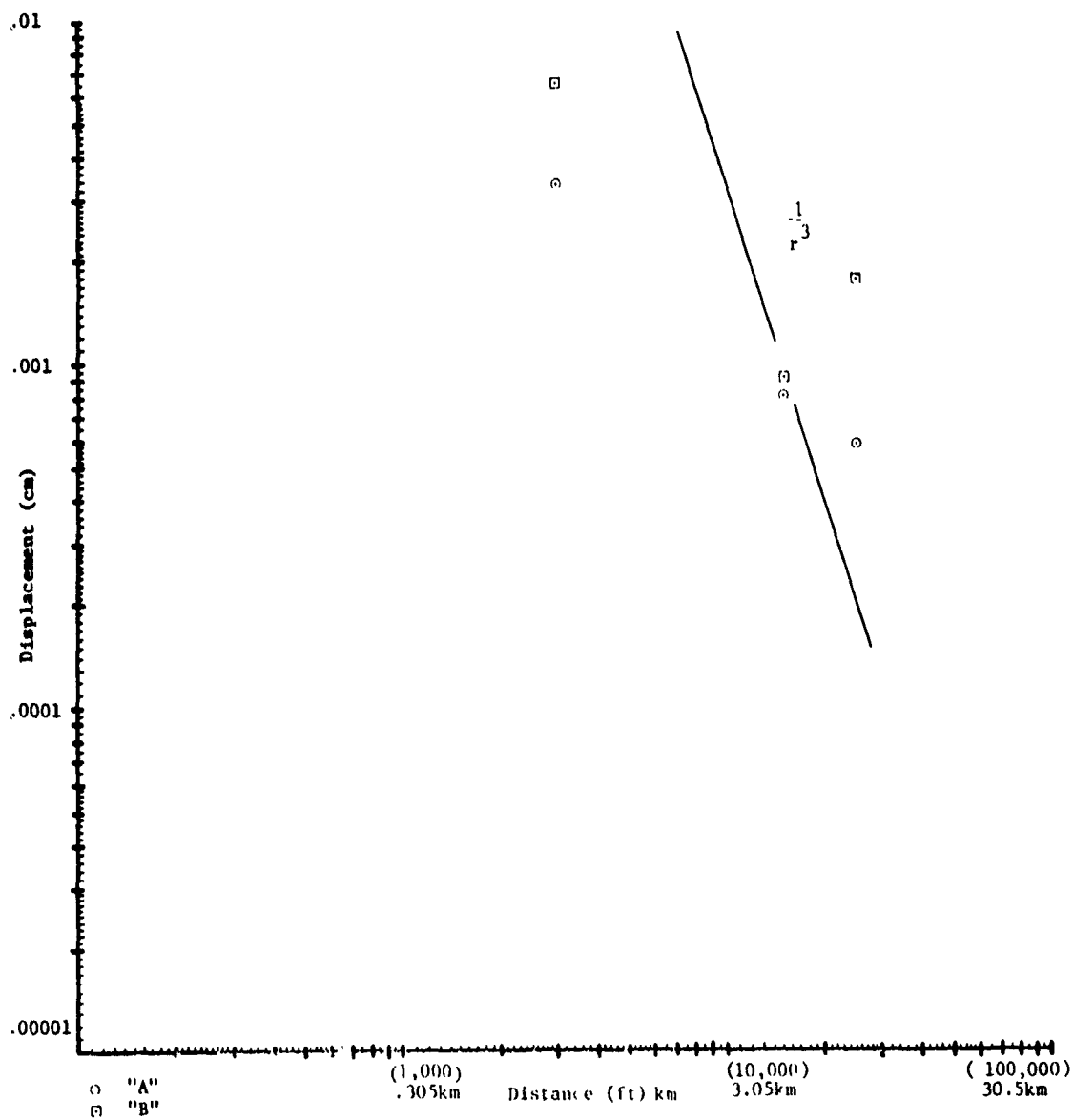


FIGURE 7. P-WAVE PARTICLE DISPLACEMENT, PRE-DICE THROW 11-1, VERTICAL COMPONENT, NORTH SITES.

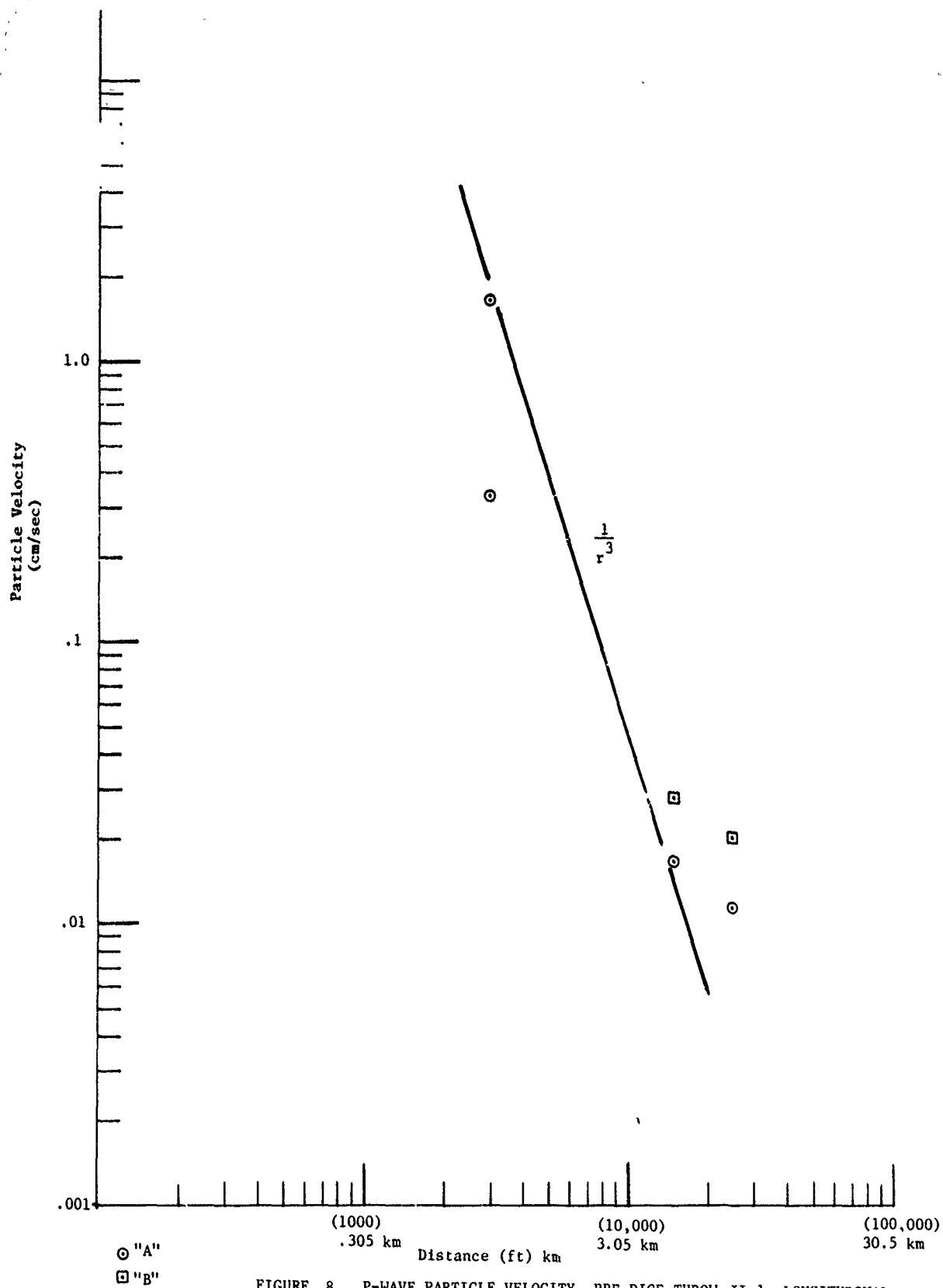


FIGURE 8. P-WAVE PARTICLE VELOCITY, PRE DICE THROW II-1, LONGITUDINAL COMPONENT, NORTH SITES.



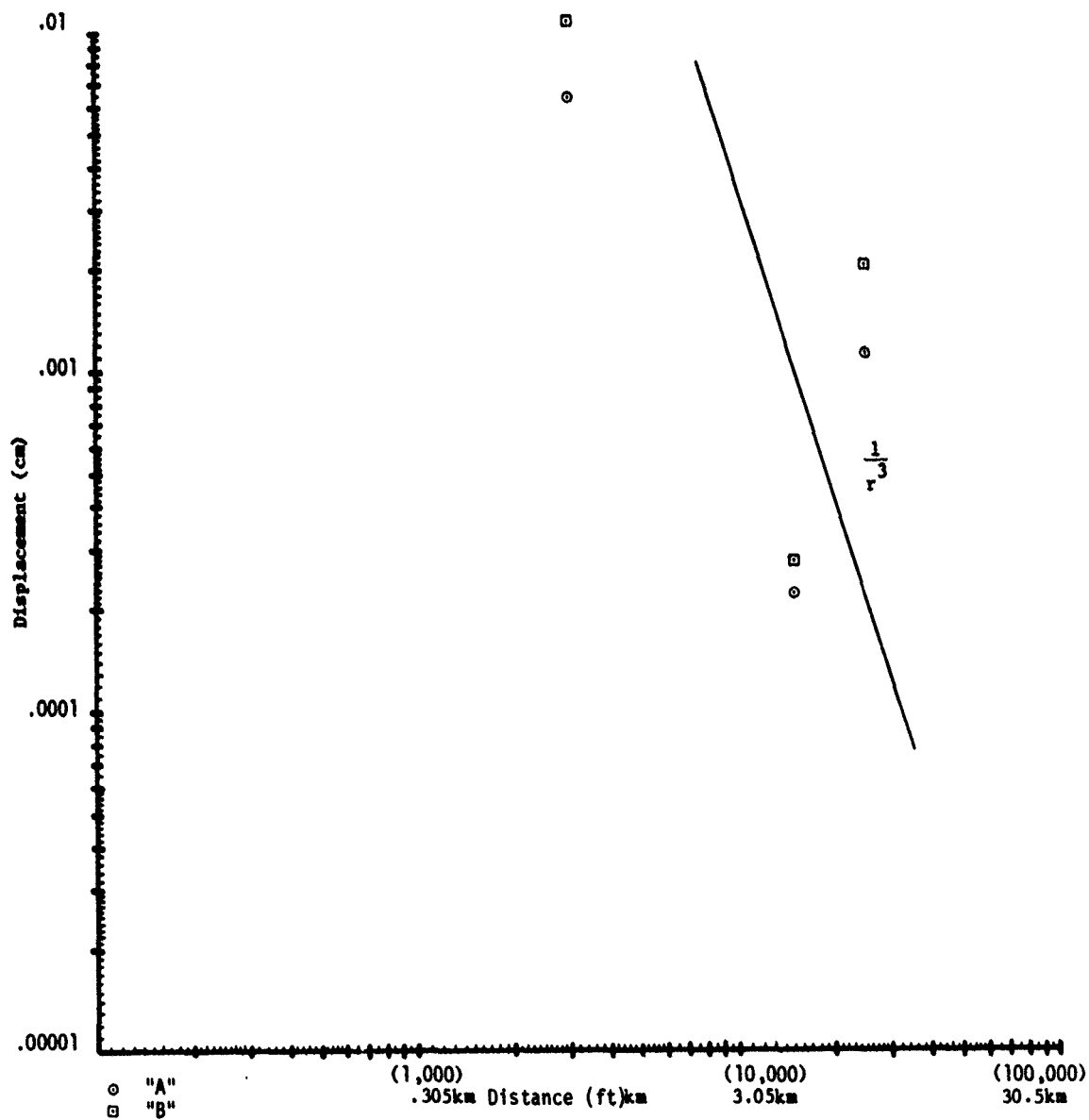
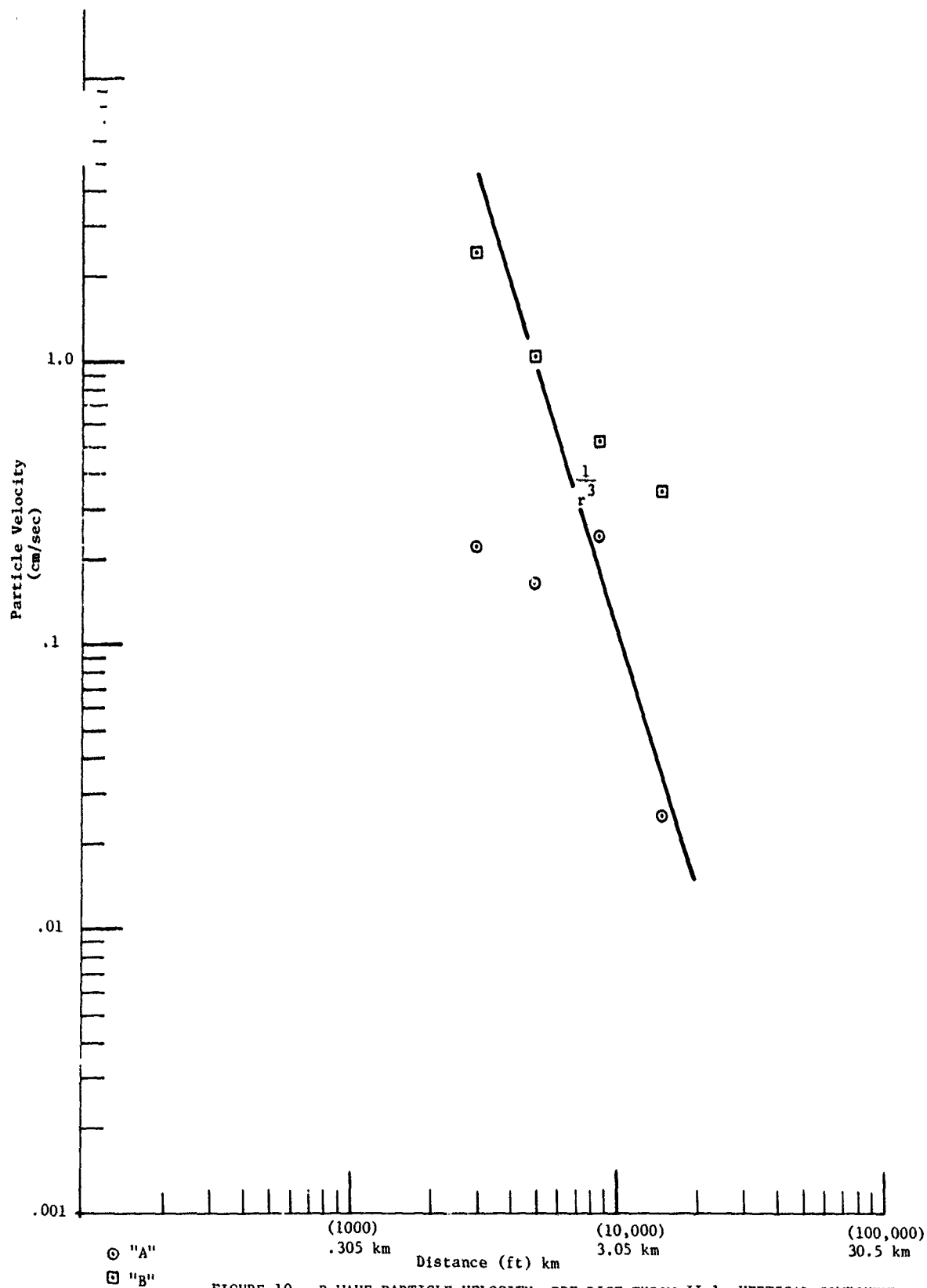


FIGURE 9. P-WAVE PARTICLE DISPLACEMENT, PRE-DICE THROW II-1, LONGITUDINAL COMPONENT, NORTH SITES.



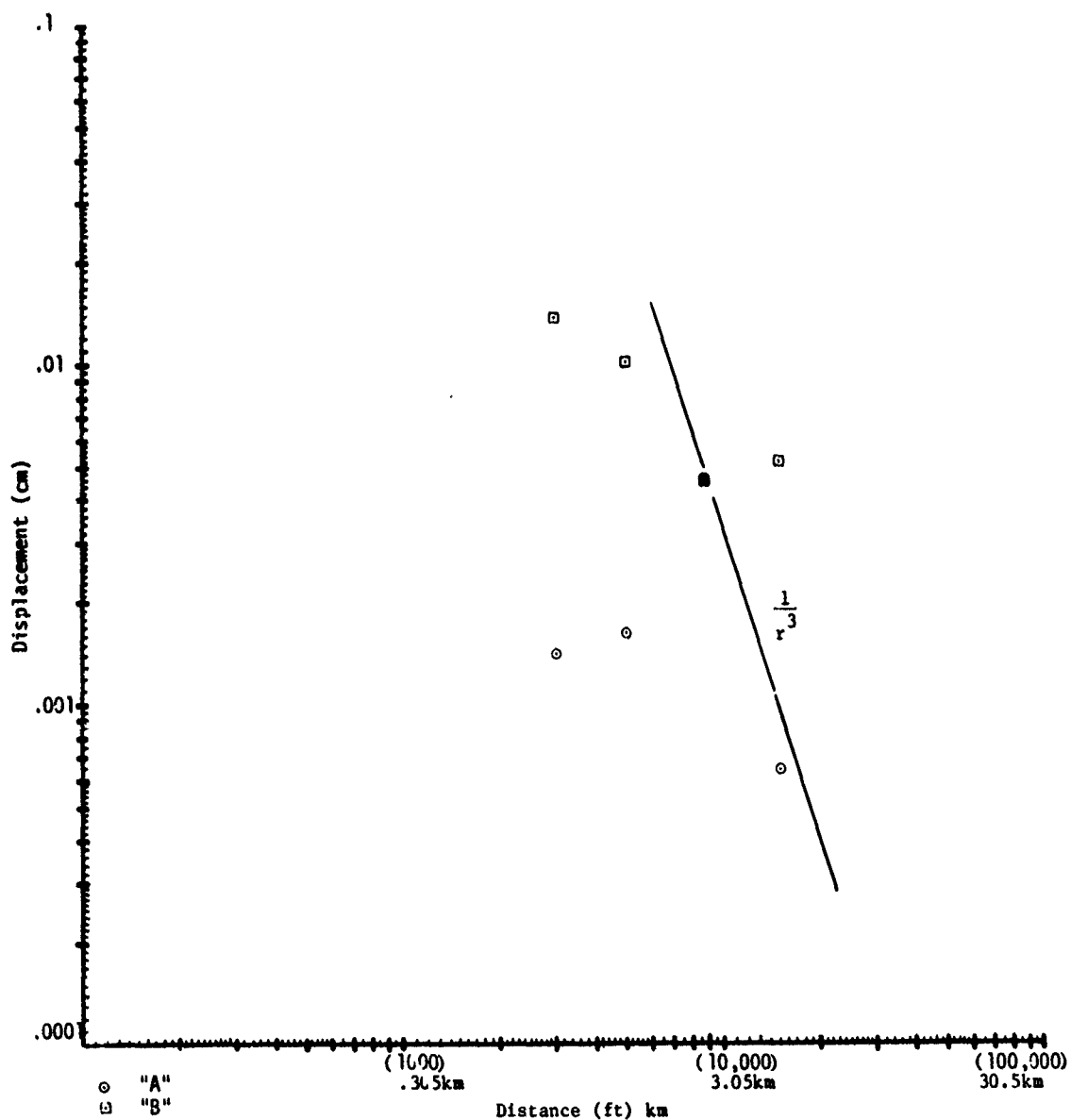


FIGURE 11. P-WAVE PARTICLE DISPLACEMENT, PRE-DICE THROW II-1, VERTICAL COMPONENT, SOUTH SITES.

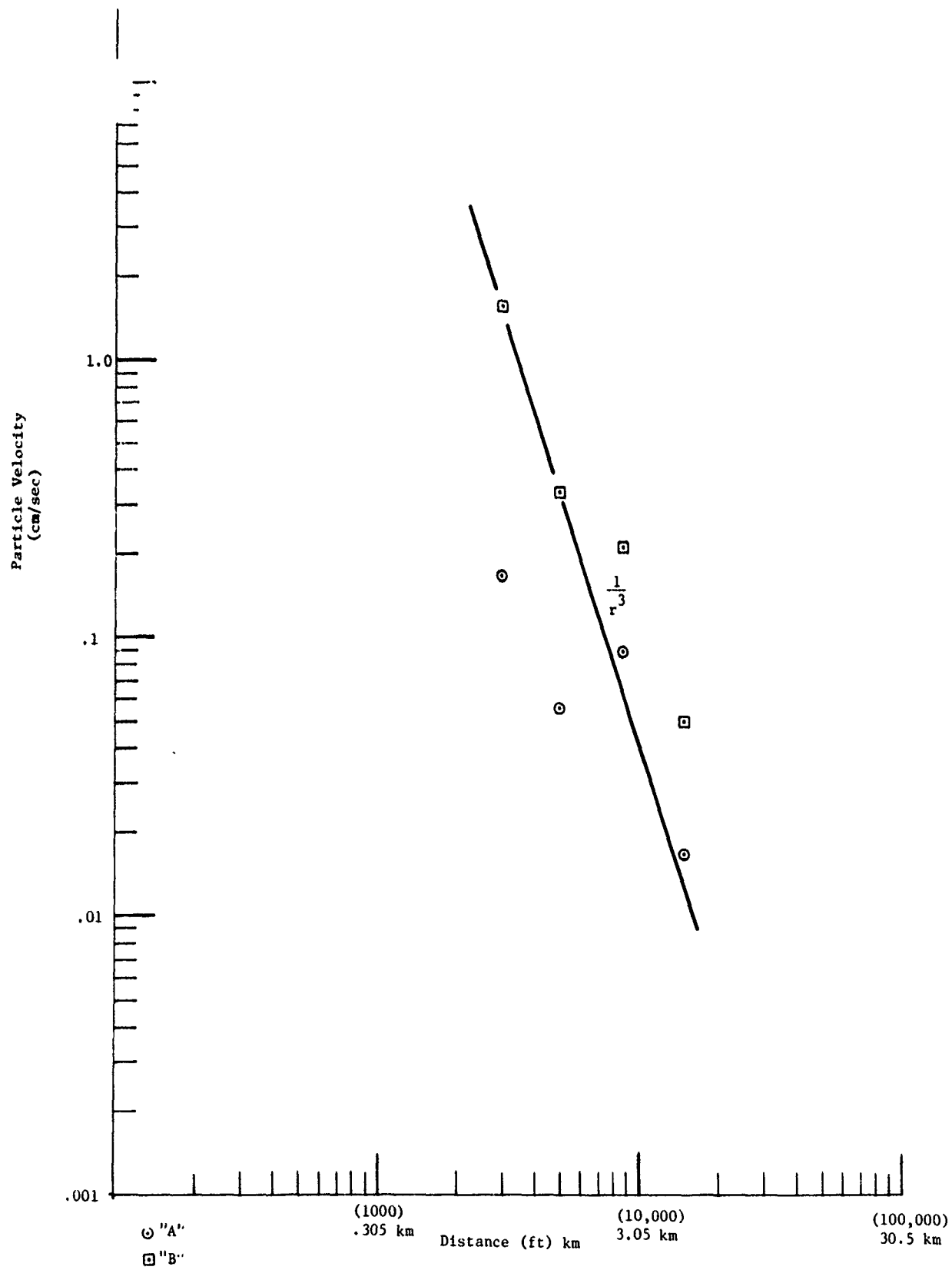


FIGURE 12. P-WAVE PARTICLE VELOCITY, PRE DICE THROW II-1, LONGITUDINAL COMPONENT, SOUTH SITES.

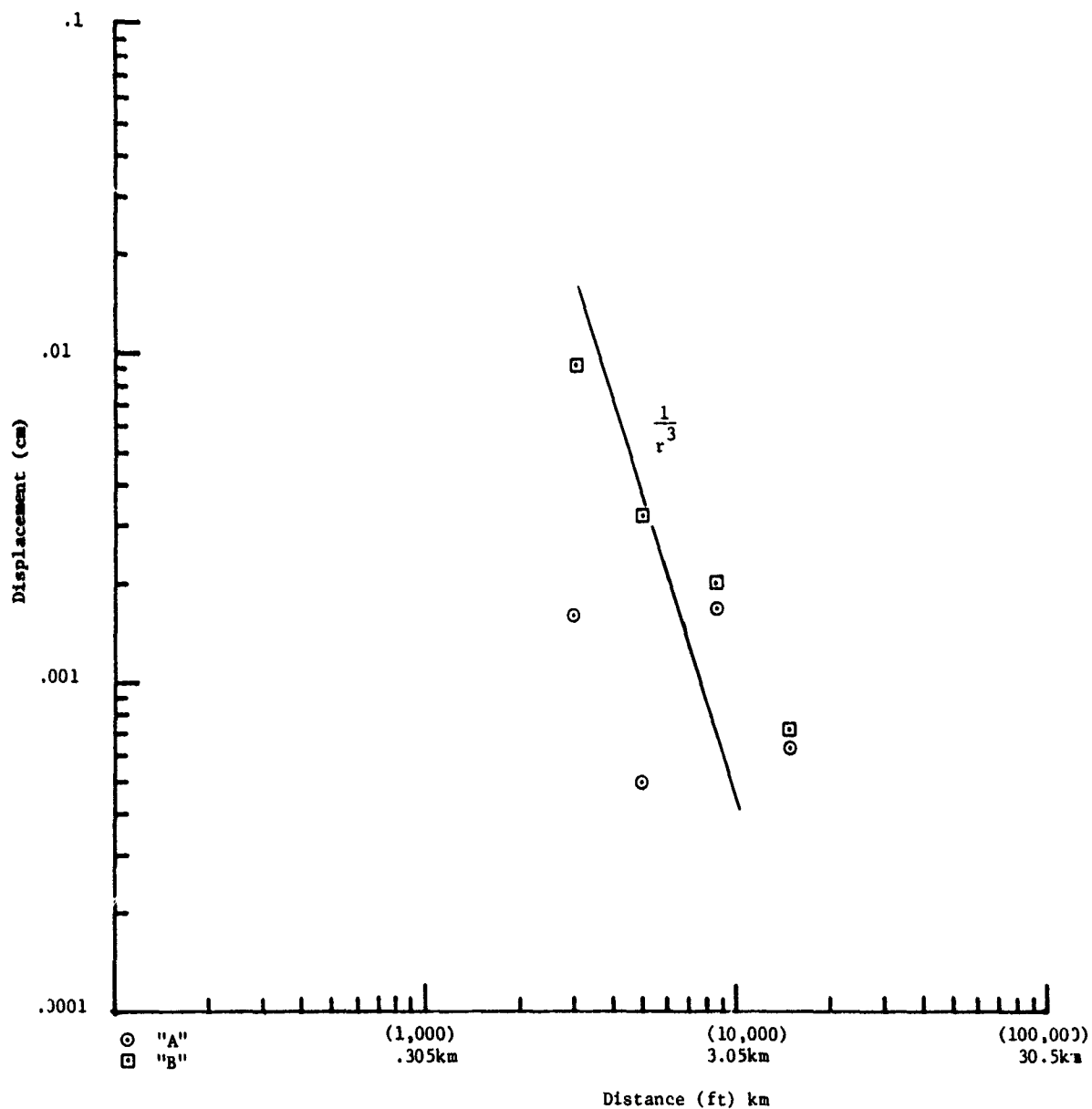


FIGURE 13. P-WAVE PARTICLE DISPLACEMENT, PRE-DICE THROW II-1, LONGITUDINAL COMPONENT, SOUTH SITES.

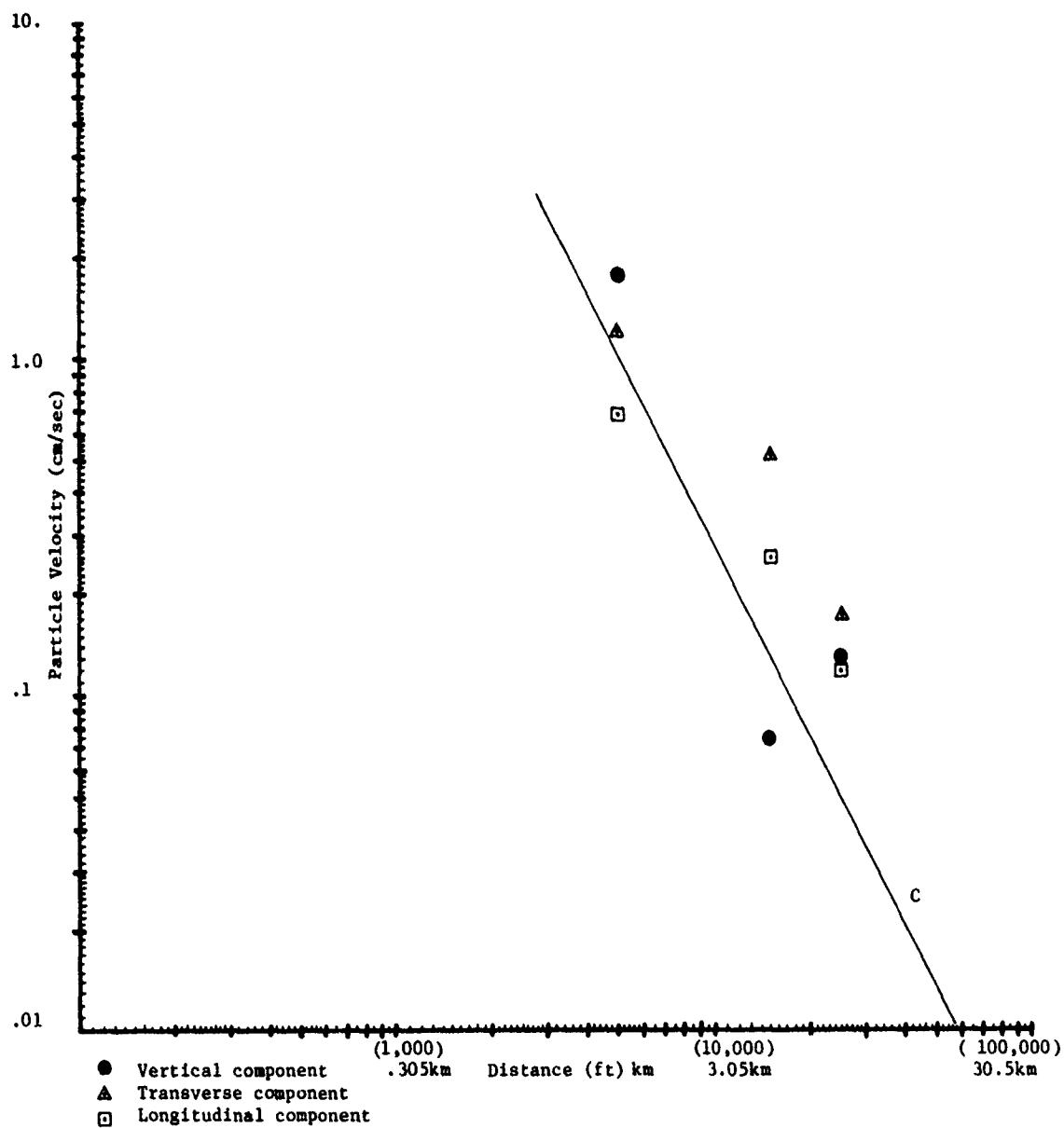


FIGURE 14. RAYLEIGH WAVE PARTICLE VELOCITY, PRE-DICE THROW 11-1 NORTH SITES.

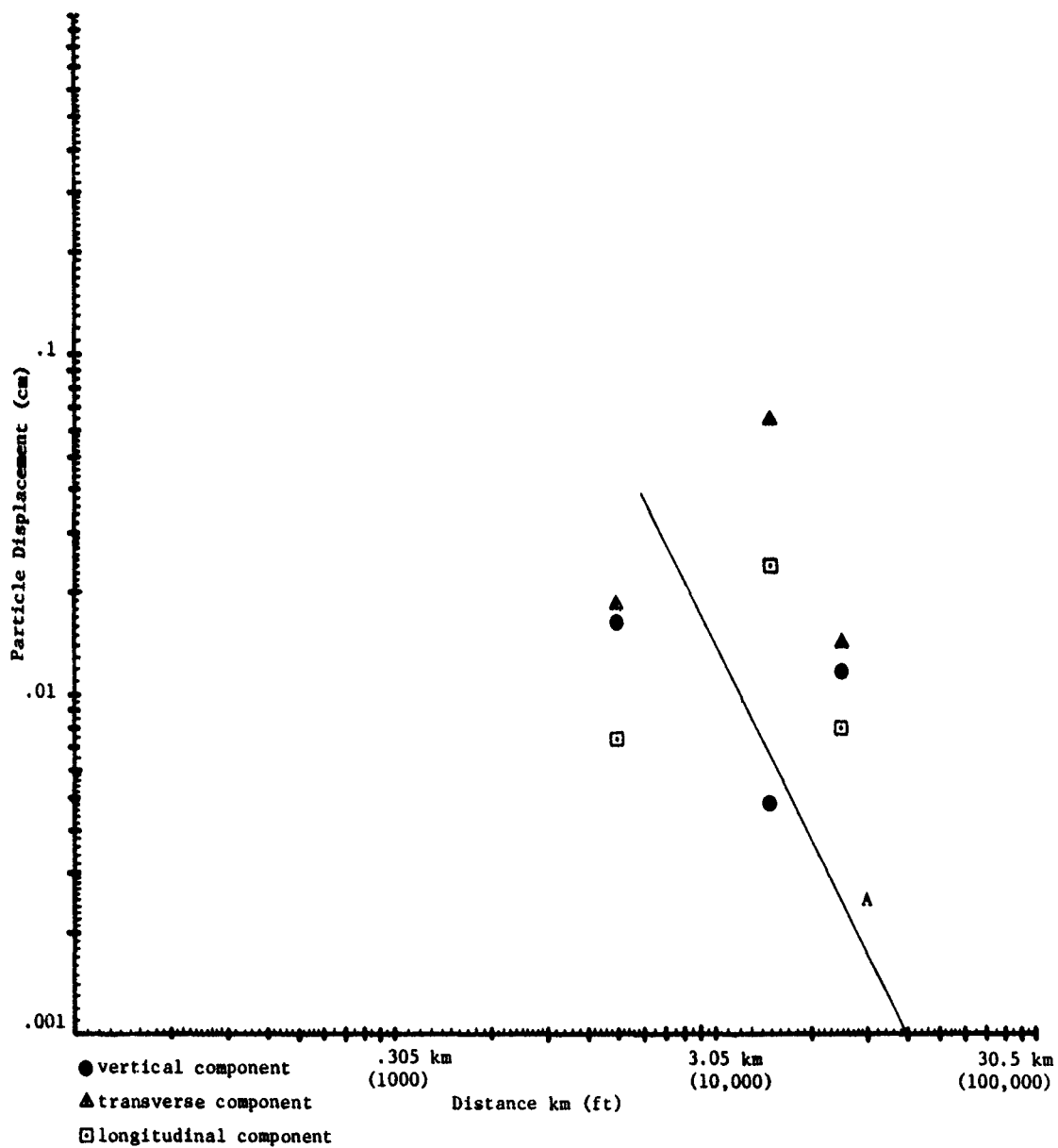


FIGURE 15. RAYLEIGH WAVE PARTICLE DISPLACEMENT, PRE-DICE THROW II-1 NORTH SITES.

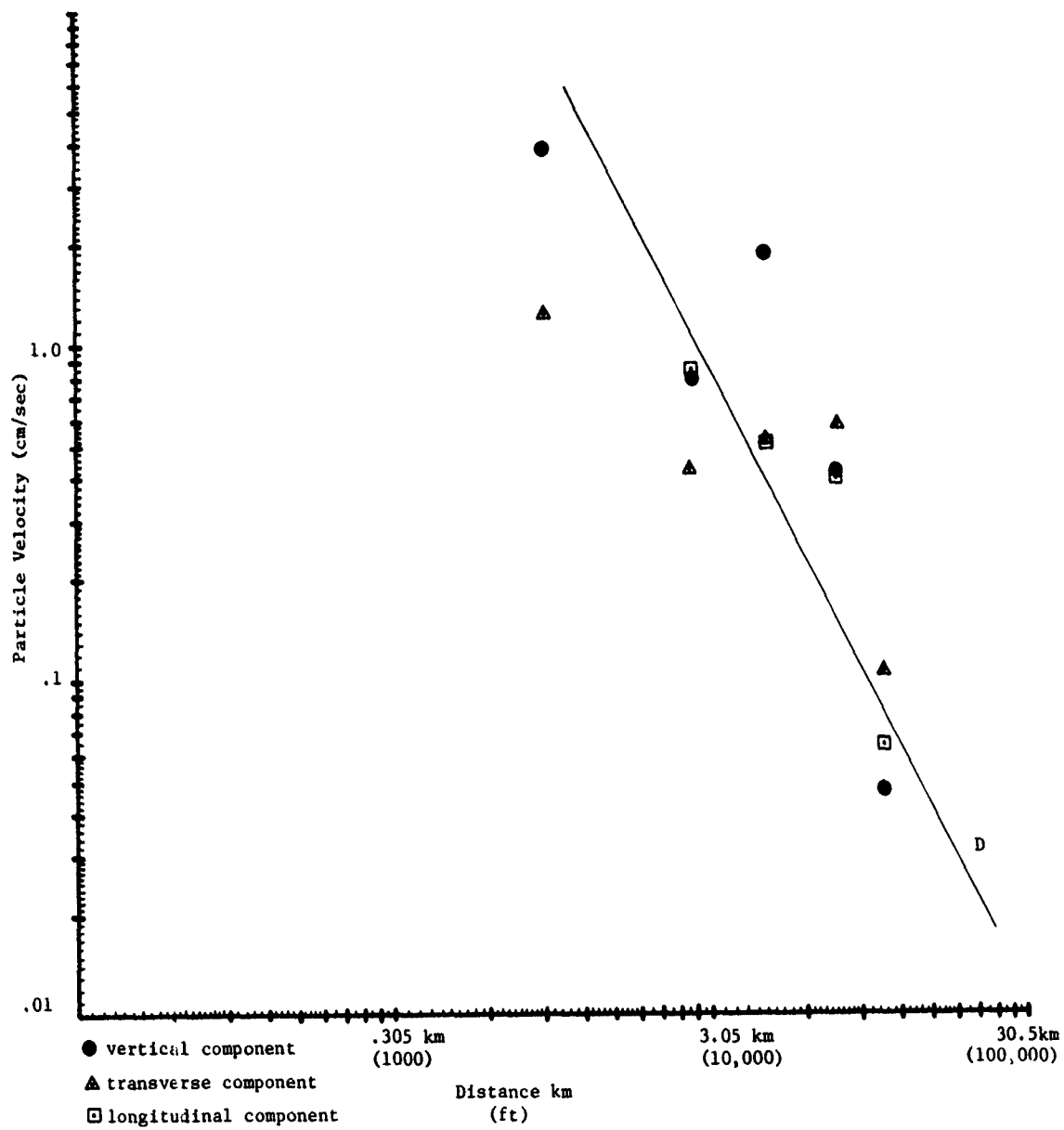


FIGURE 16. PARTICLE VELOCITY, PRE-DICE THROW II-1, RAYLEIGH WAVES SOUTH SITES.



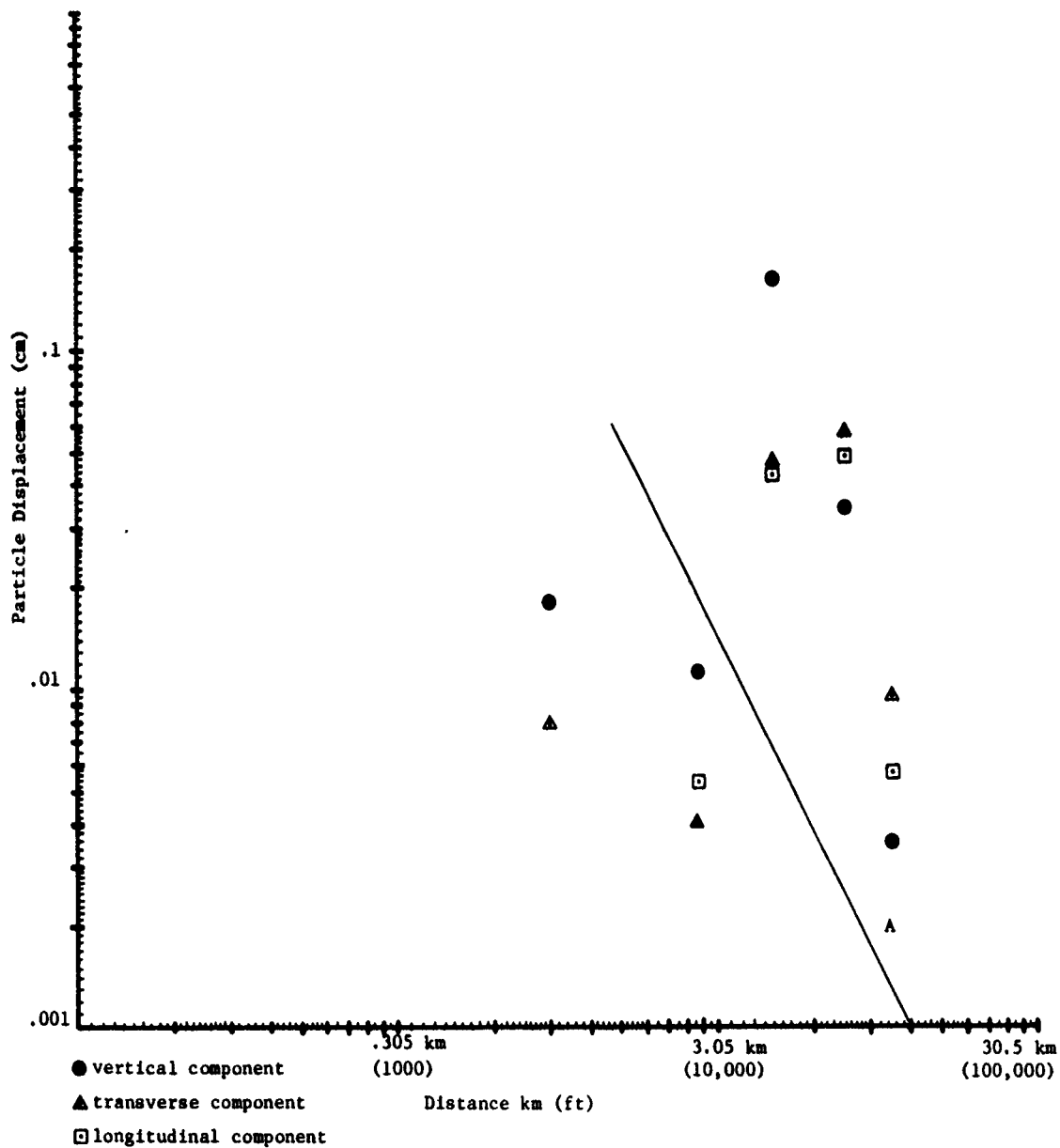


FIGURE 17. RAYLEIGH WAVE PARTICLE DISPLACEMENT, PRE-DICE THROW II-1 SOUTH SITES.

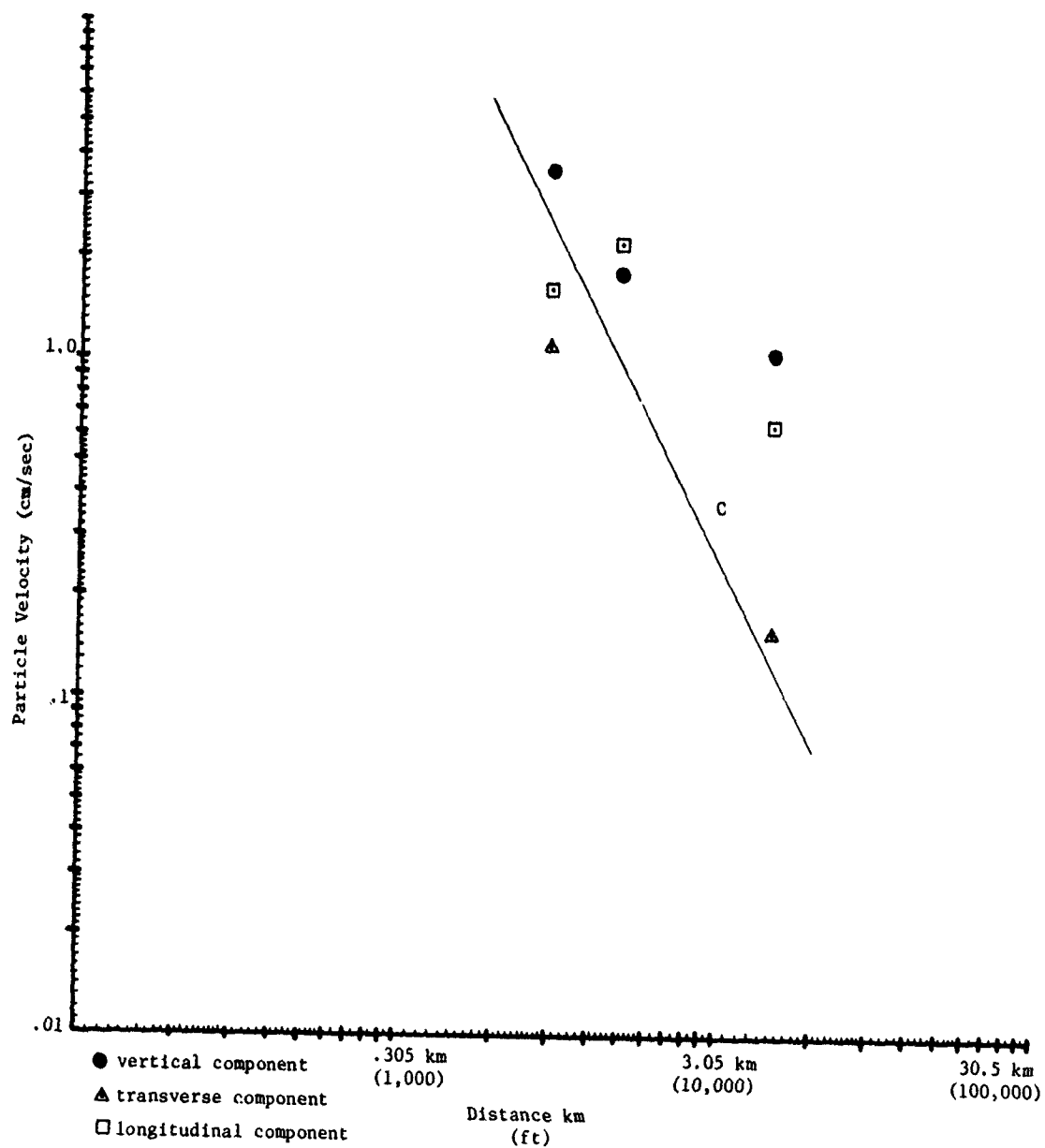


FIGURE 18. PARTICLE VELOCITY FOR FUNDAMENTAL MODE RAYLEIGH WAVE, PRE-DICE THROW II-1, NORTH SITES.

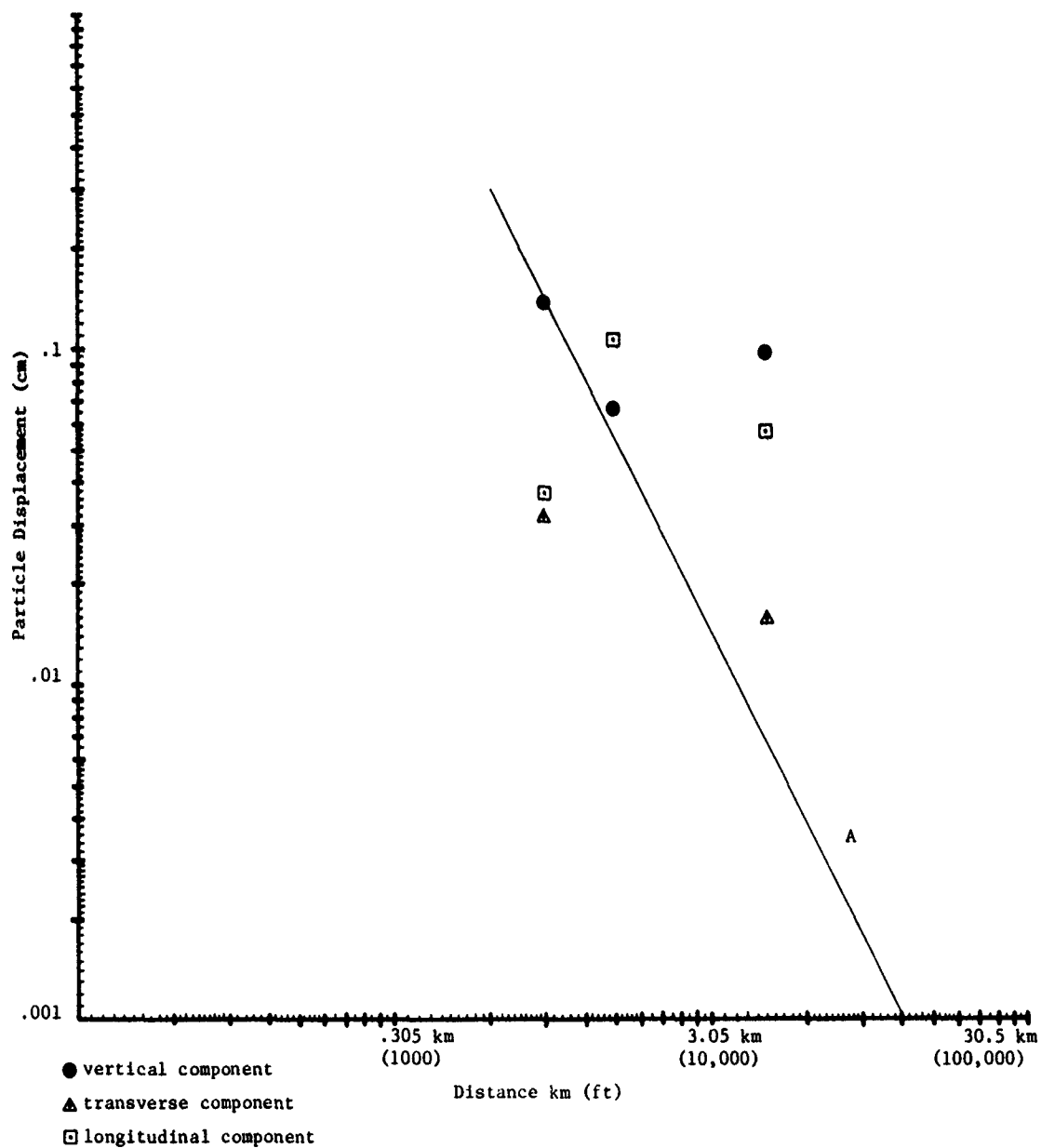


FIGURE 19. PARTICLE DISPLACEMENT FOR FUNDAMENTAL MODE RAYLEIGH WAVE, PRE-DICE II-1, NORTH SITES.

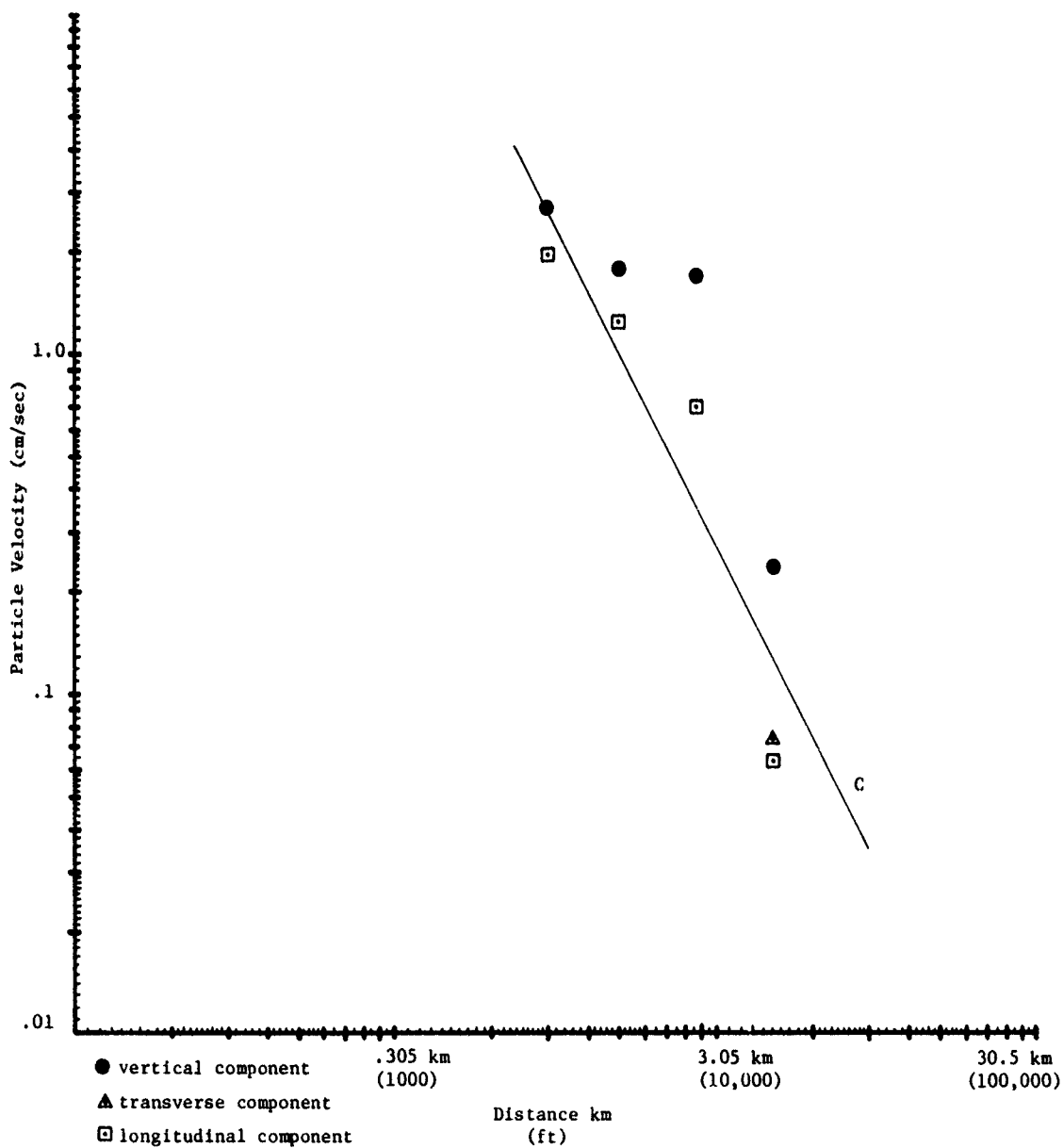


FIGURE 20. PARTICLE VELOCITY FOR FUNDAMENTAL MODE RAYLEIGH WAVE, PRE-DICE THROW II-1, SOUTH SITES

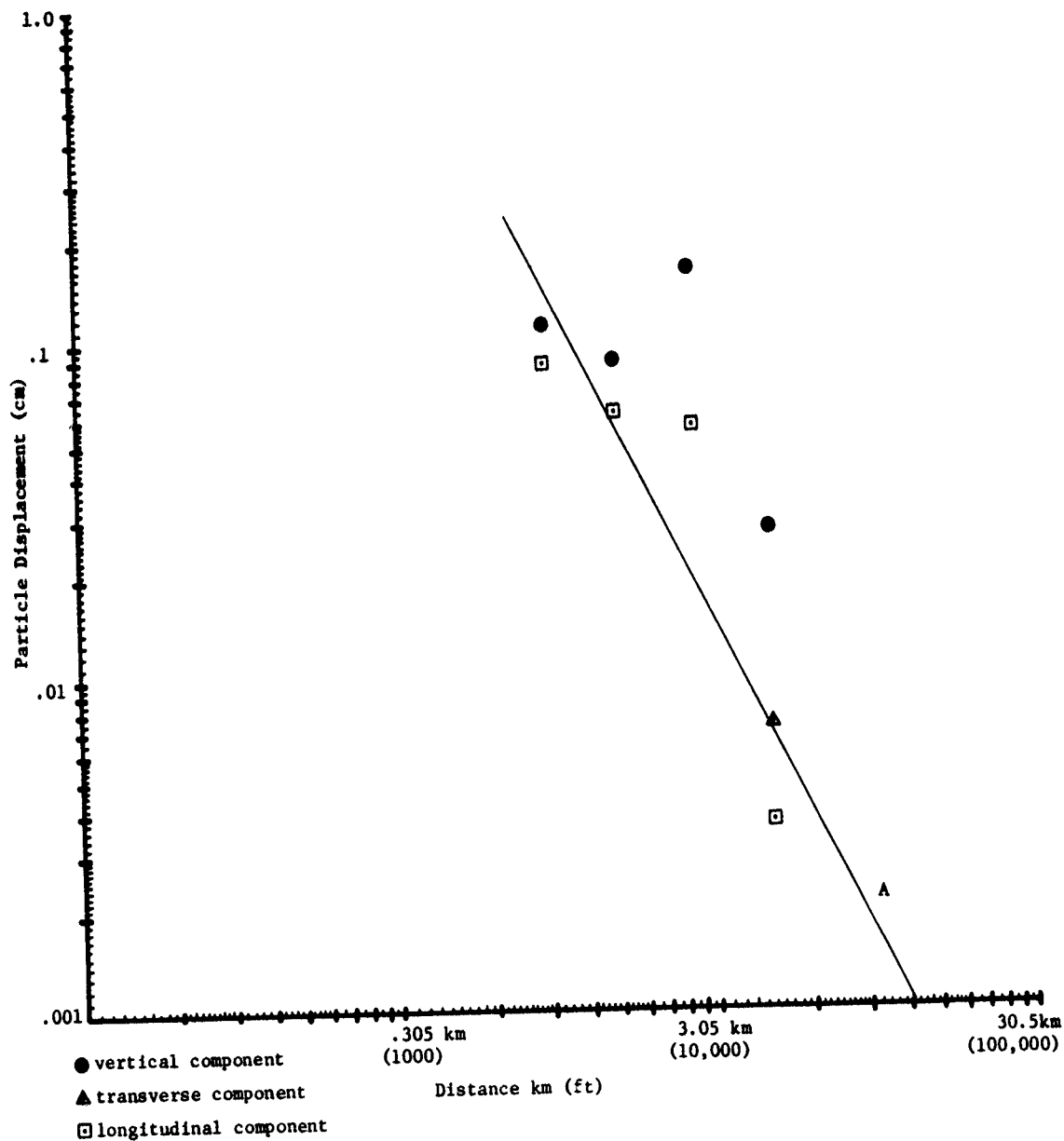


FIGURE 21. PARTICLE DISPLACEMENT FOR FUNDAMENTAL MODE RAYLEIGH WAVE, PRE-DICE THROW II-1 SOUTH SITES.

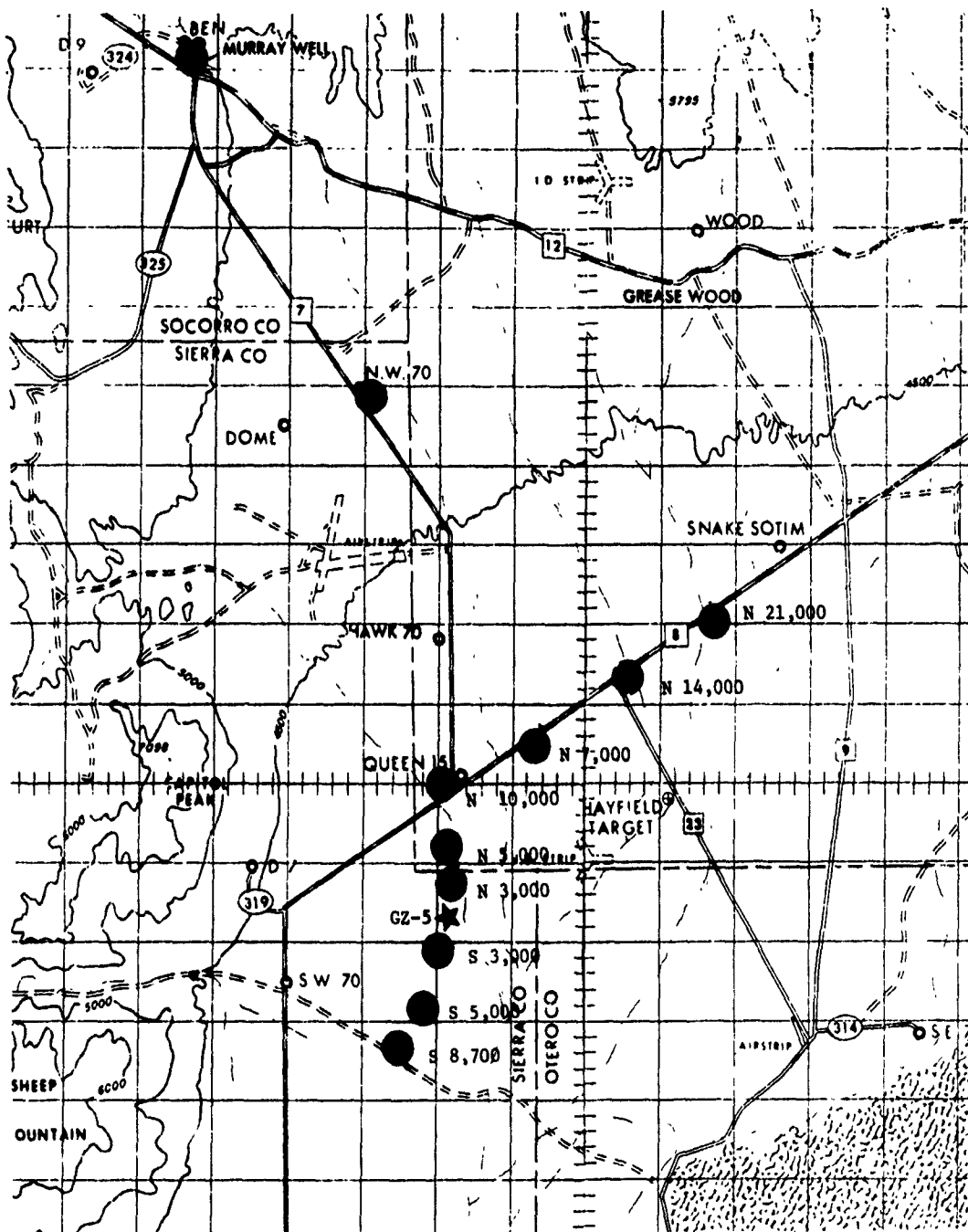


FIGURE 22. SEISMOGRAPH STATIONS FOR PRE-DICE THROW II-2

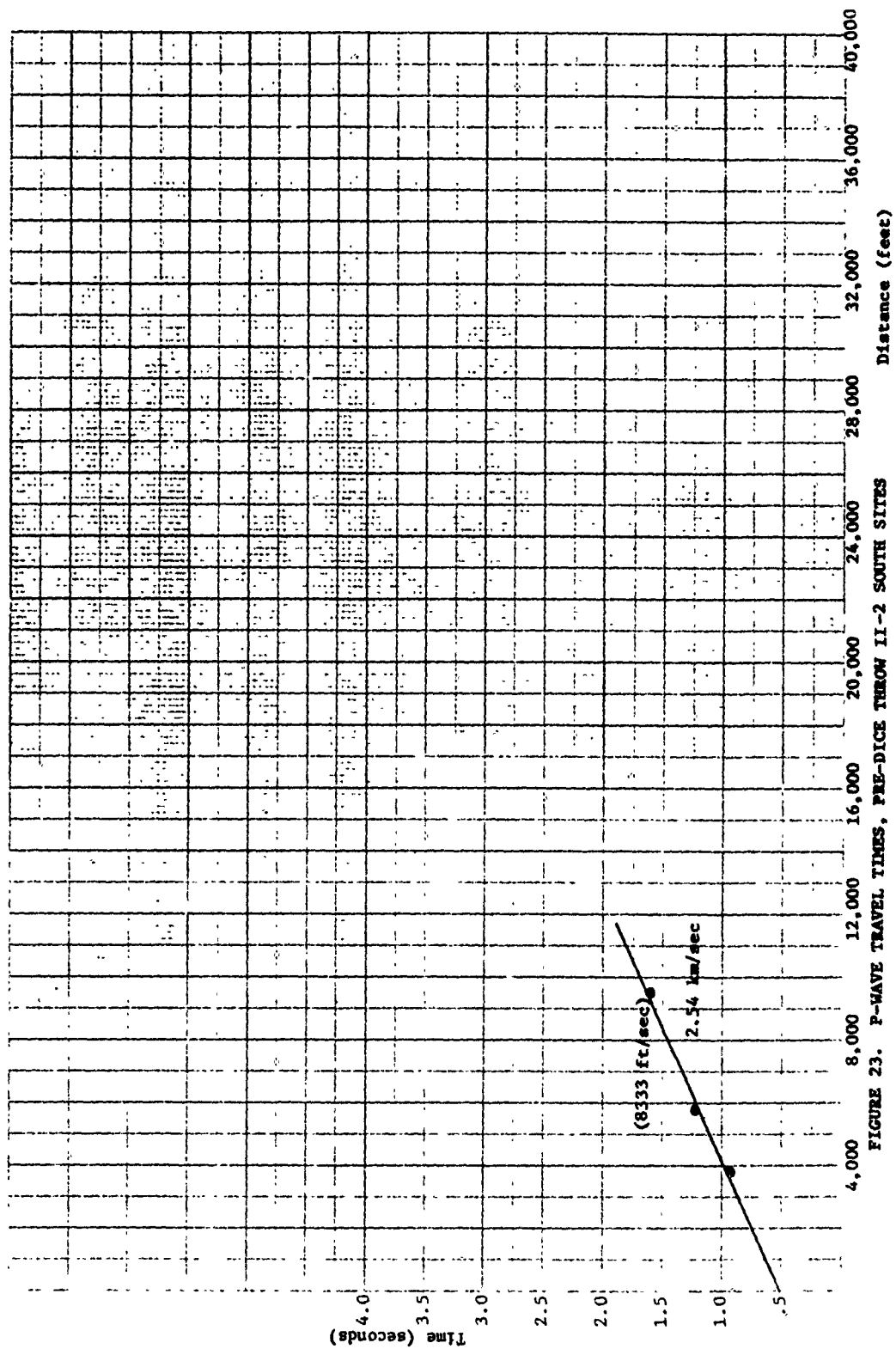
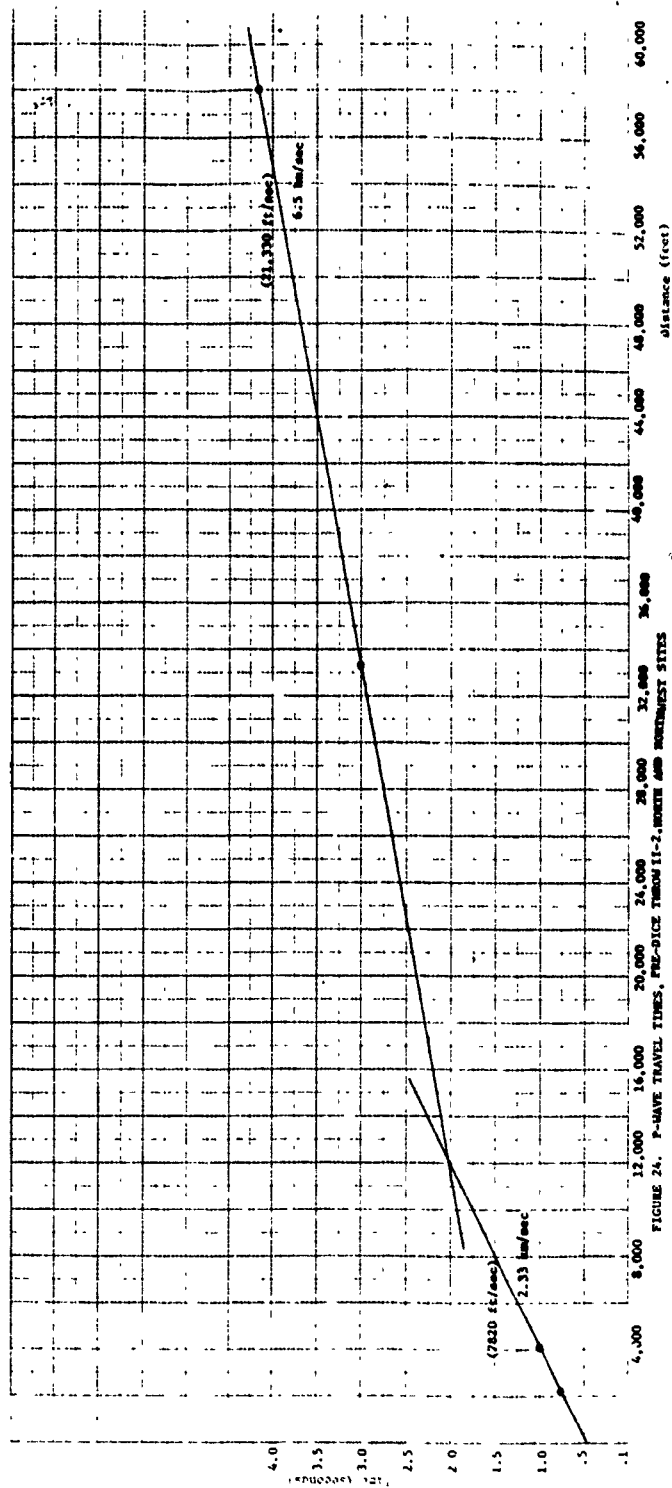


FIGURE 23. P-WAVE TRAVEL TIMES, PRE-DICE THROW II-2 SOUTH SITES





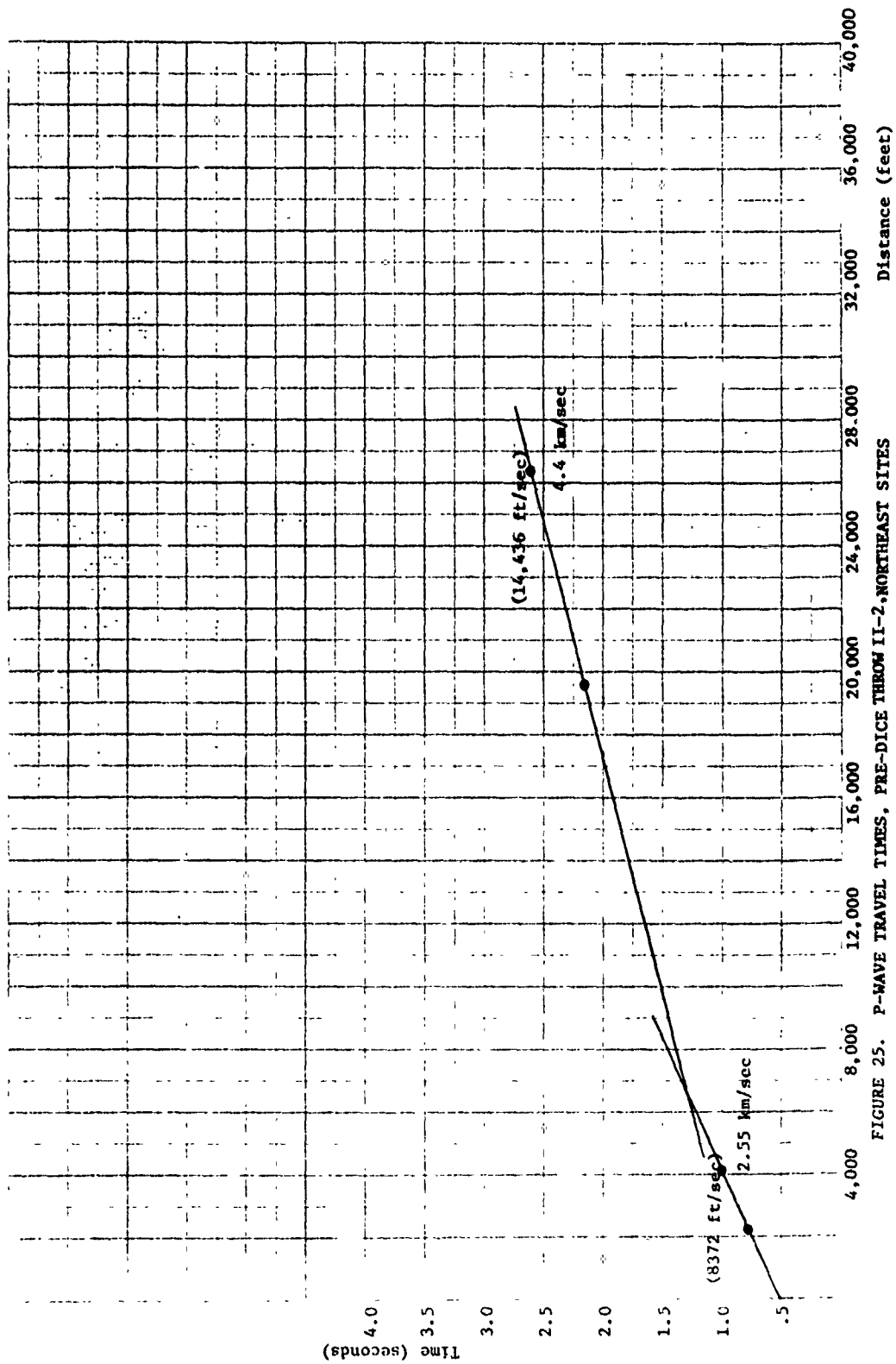
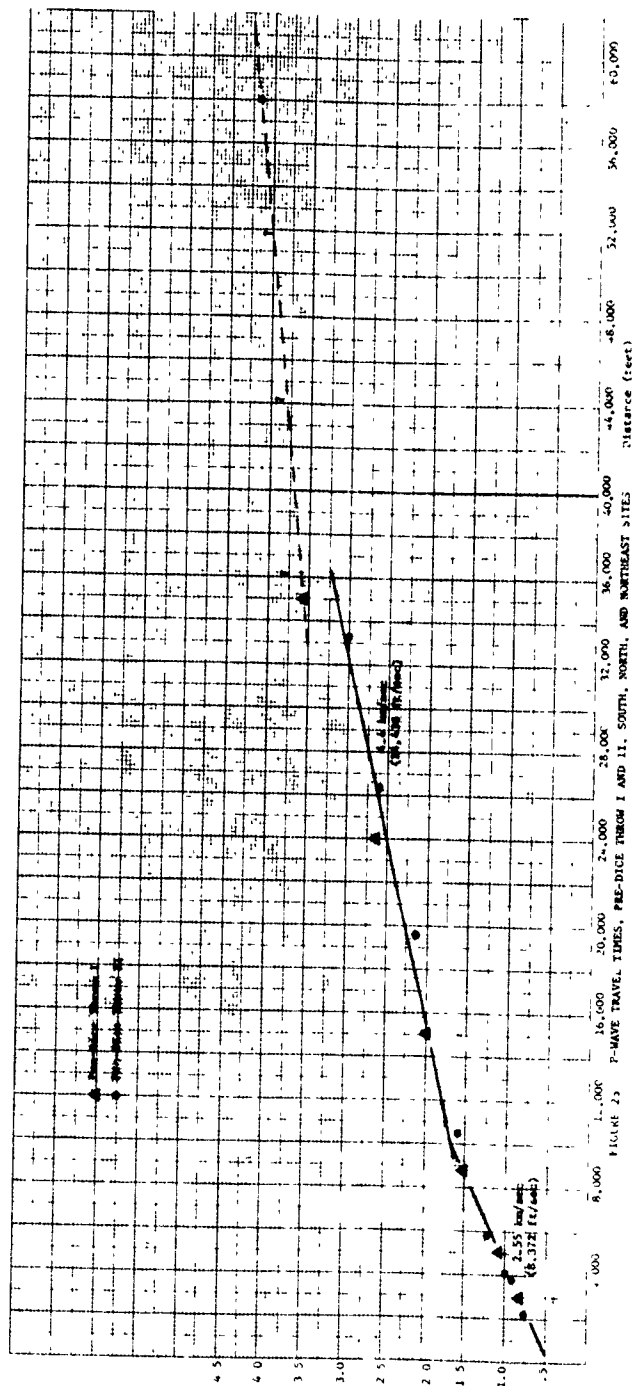
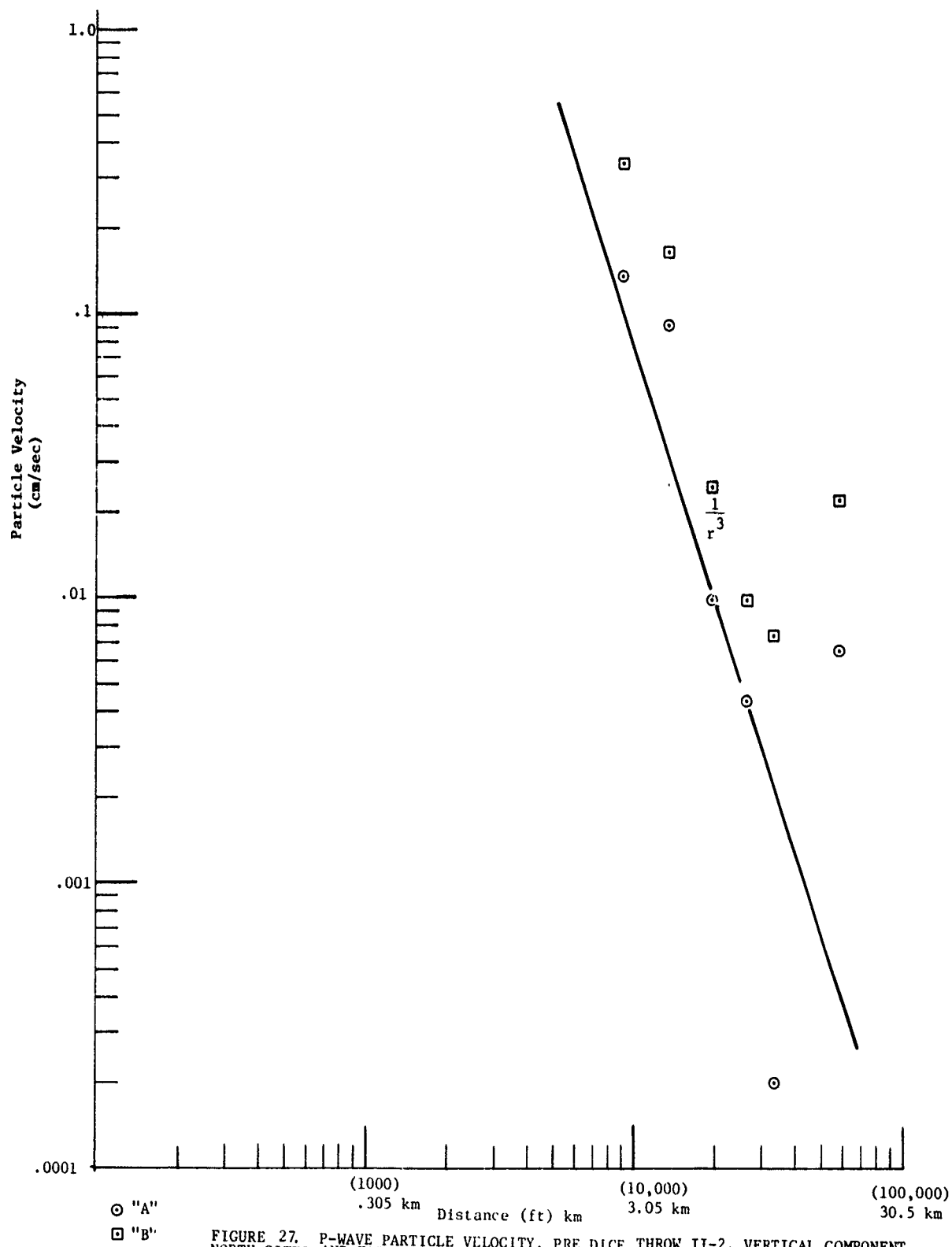


FIGURE 25. P-WAVE TRAVEL TIMES, PRE-DICE THROW II-2, NORTHEAST SITES





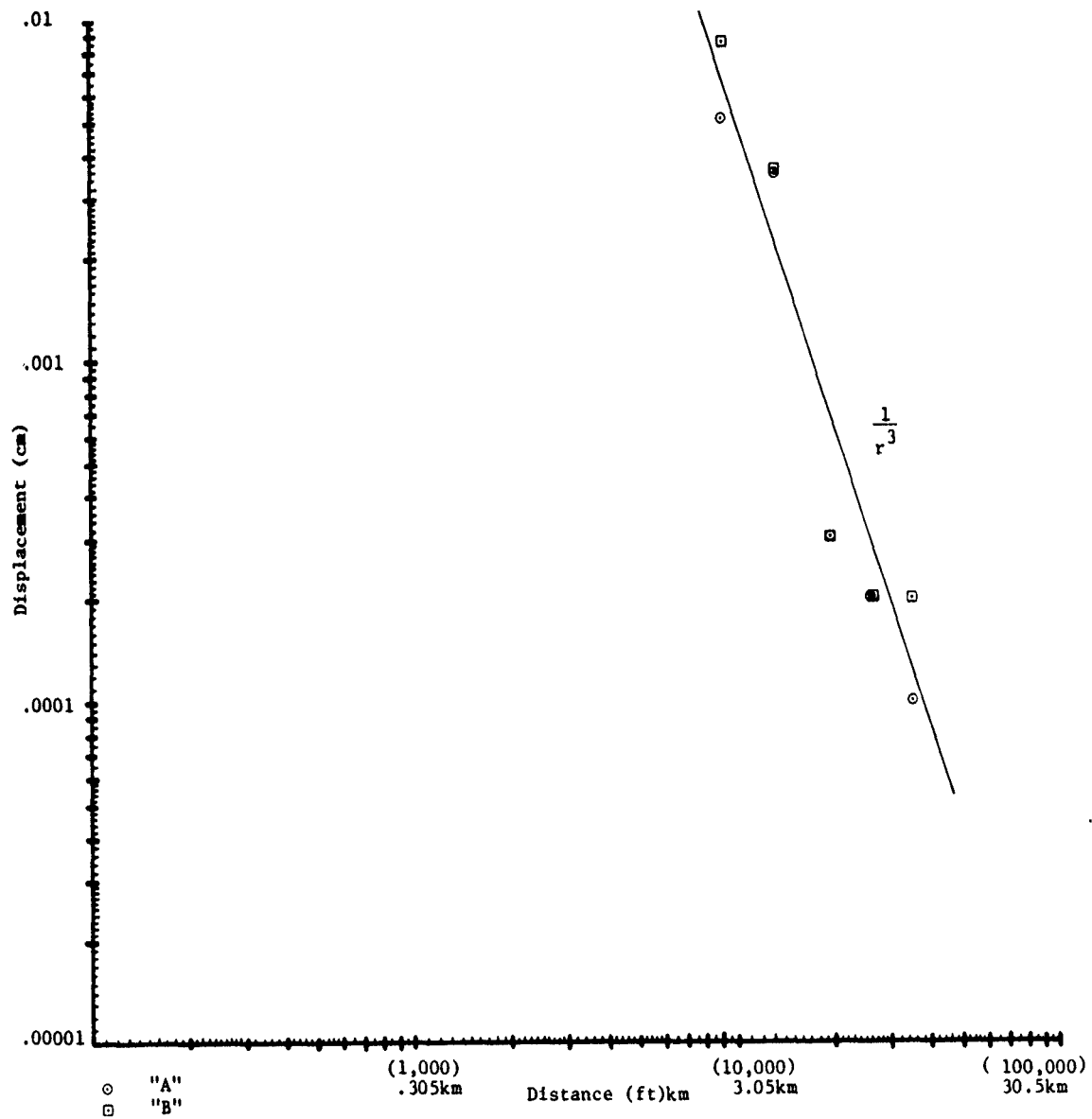


FIGURE 28. P-WAVE PARTICLE DISPLACEMENT, PRE-DICE THROW 1I-2, VERTICAL COMPONENT, NORTH AND EAST SITES.

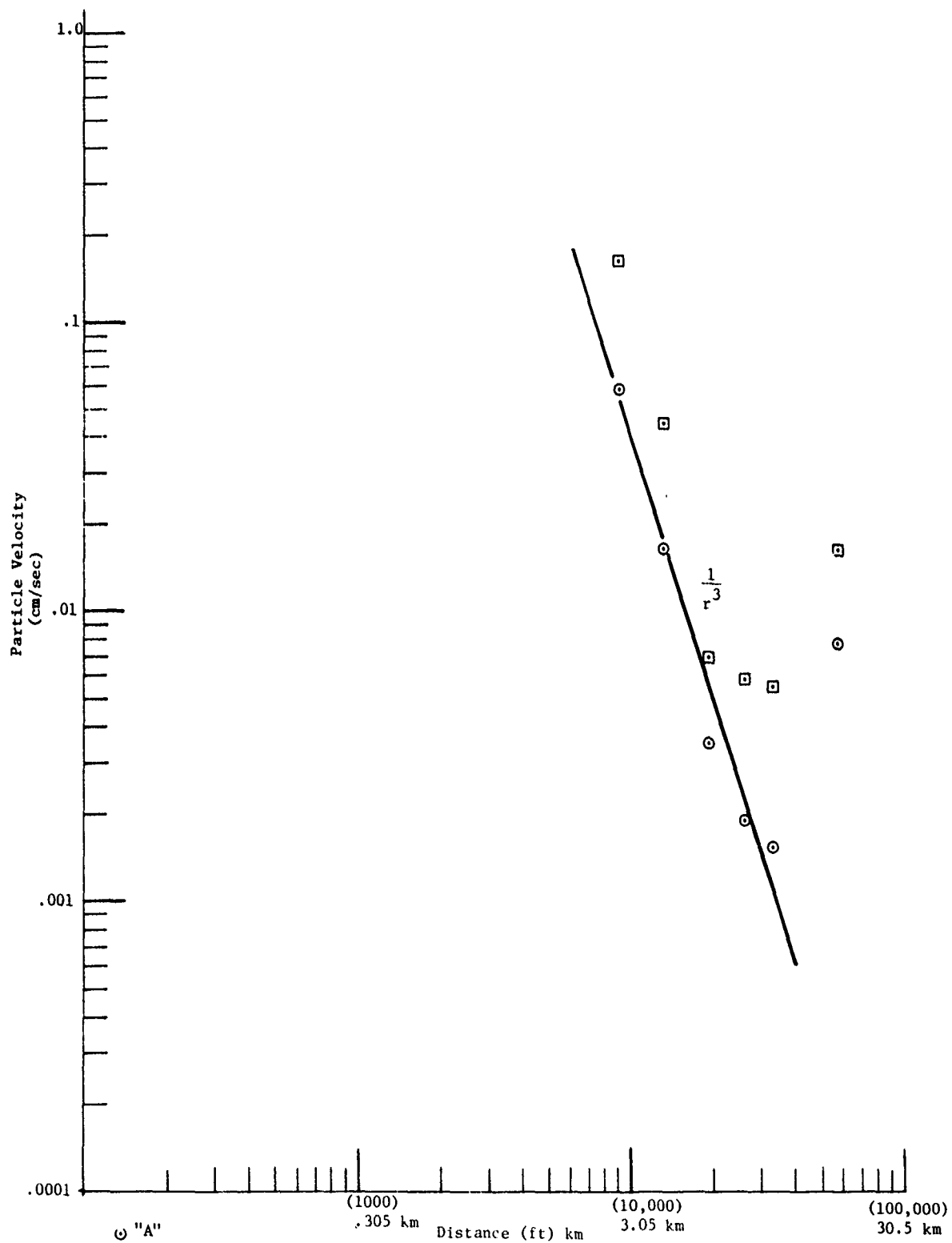


FIGURE 29. P-WAVE PARTICLE VELOCITY, PRE DICE THROW 11-2, LONGITUDINAL COMPONENT NORTH AND EAST SITES.

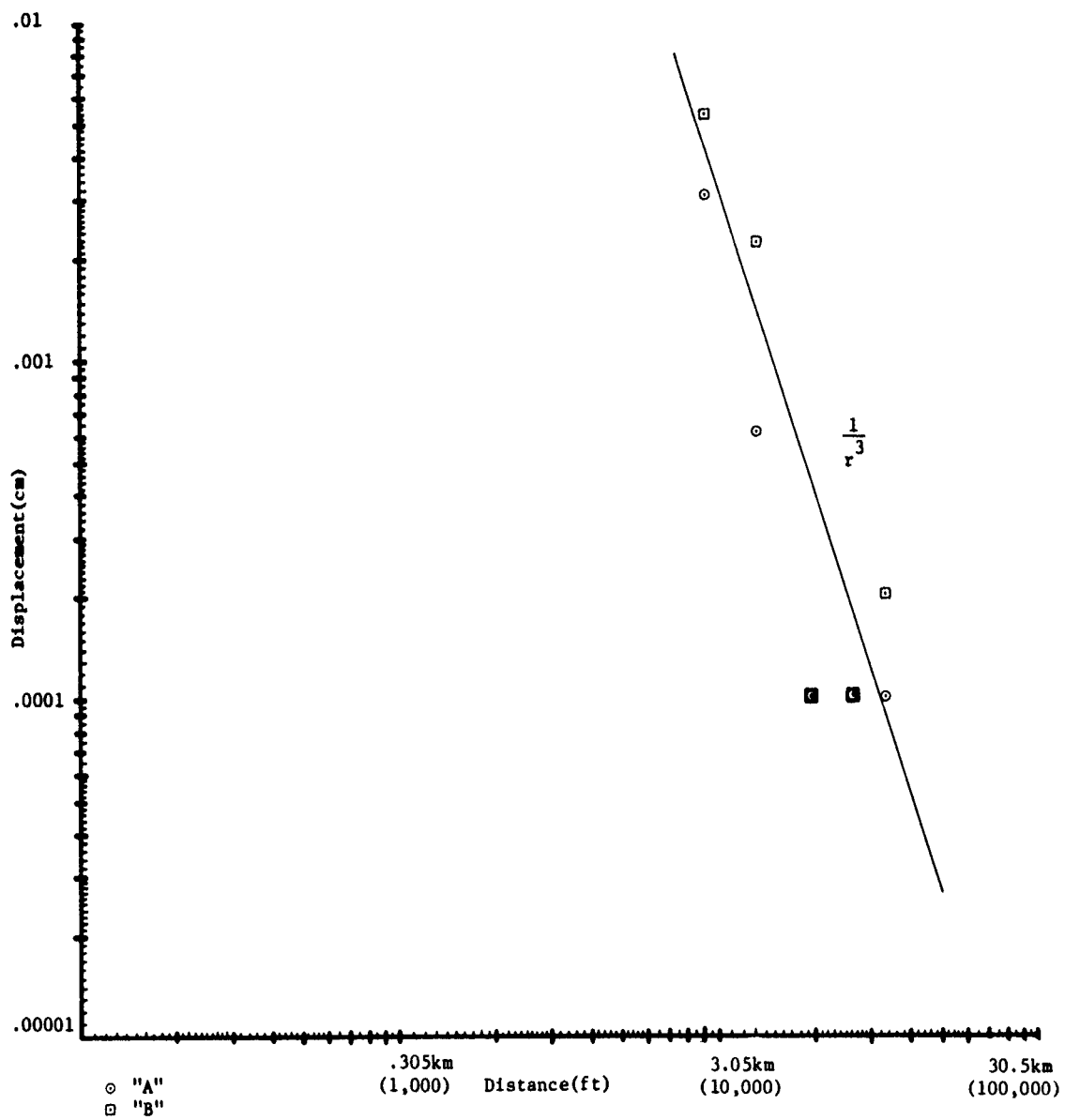


FIGURE 30. P-WAVE PARTICLE DISPLACEMENT, PRE-DICE THROW II-2, LONGITUDINAL COMPONENT, NORTH AND EAST SITES.

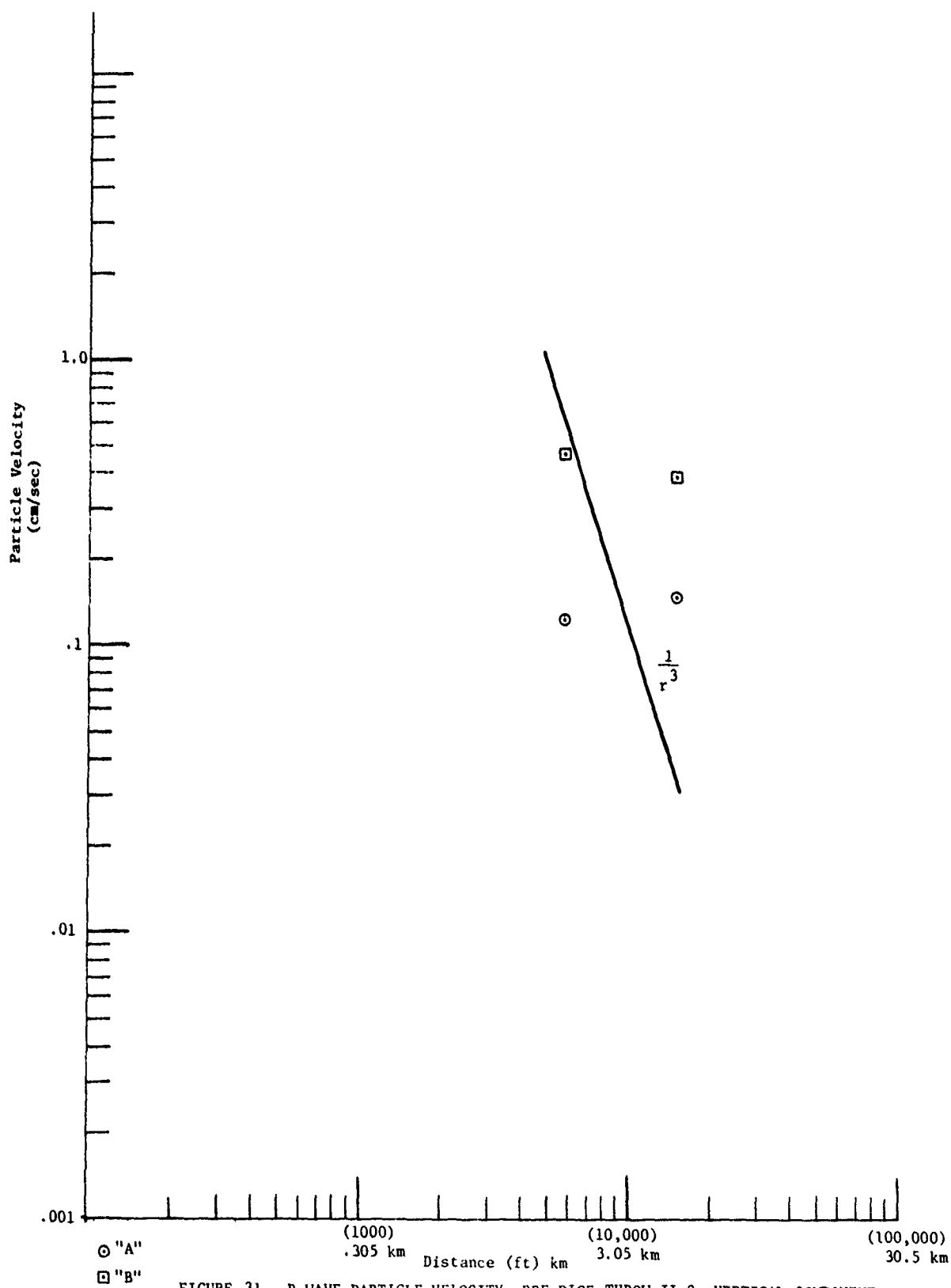


FIGURE 31. P-WAVE PARTICLE VELOCITY, PRE DICE THROW II-2, VERTICAL COMPONENT SOUTH SITES.

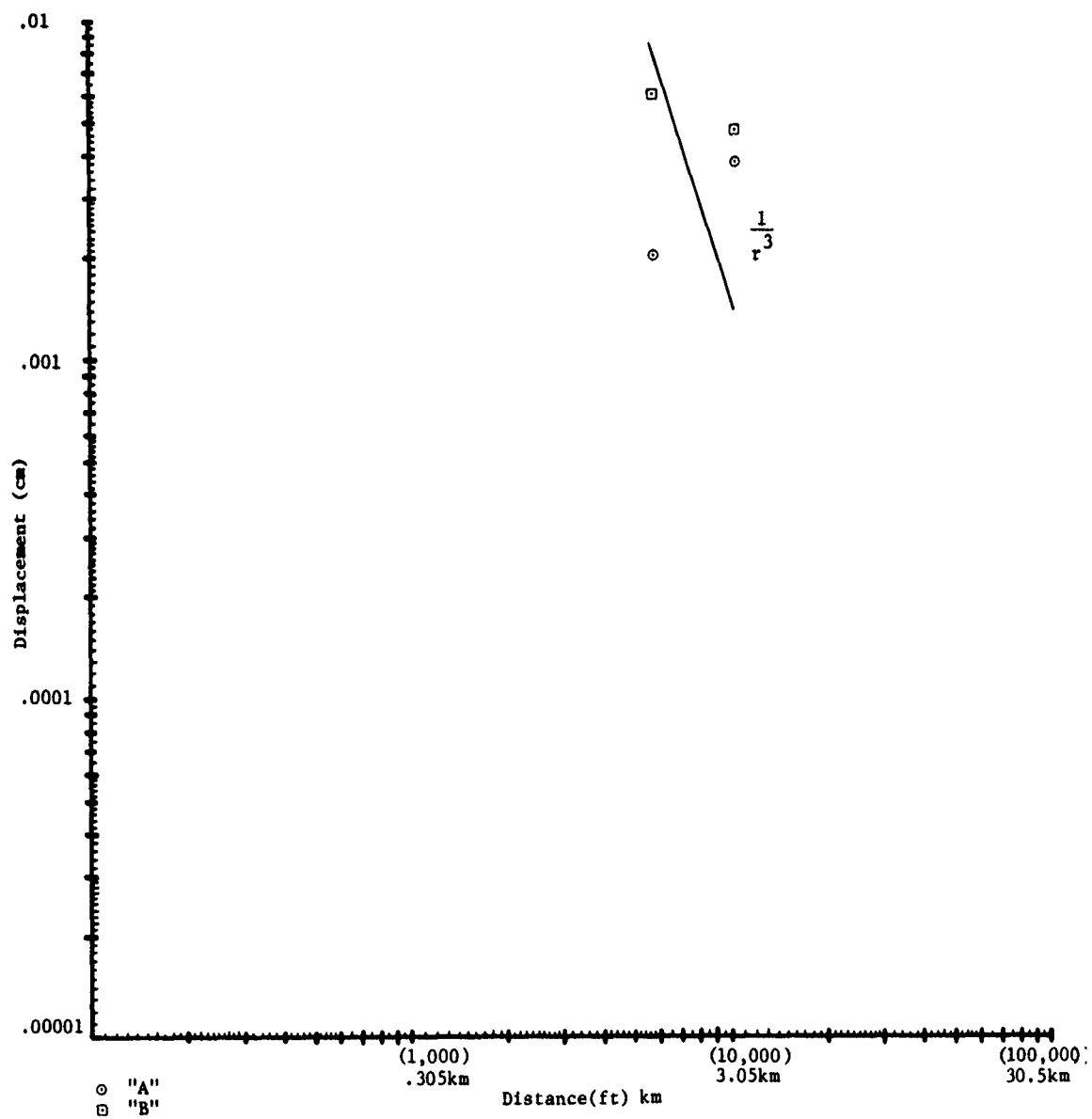


FIGURE 32. P-WAVE PARTICLE DISPLACEMENT, PRE-DICE THROW II-2  
VERTICAL COMPONENT, SOUTH SITES.



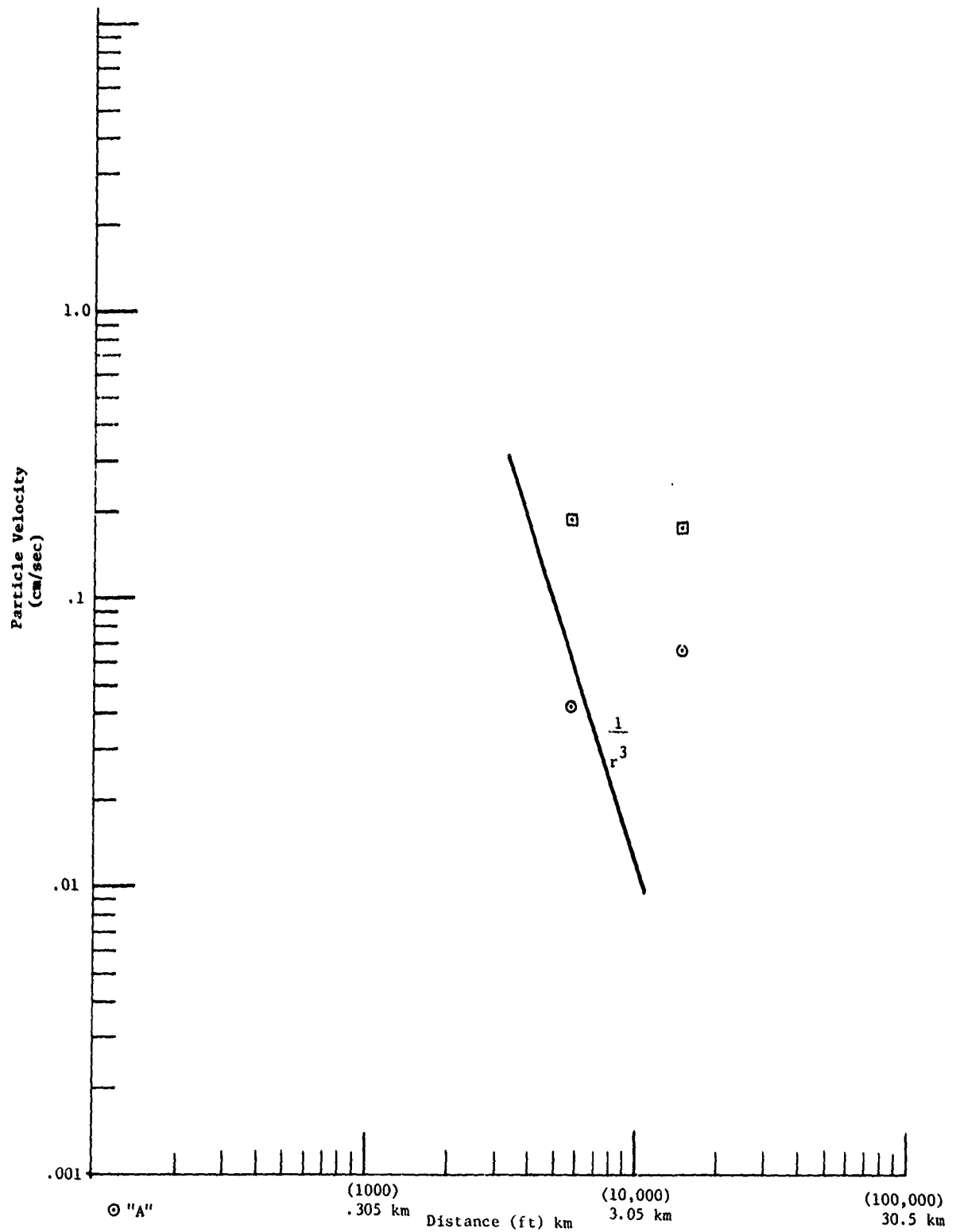


FIGURE 33. P-WAVE PARTICLE VELOCITY, PRE DICE THROW II-2, LONGITUDINAL COMPONENT SOUTH SITES.

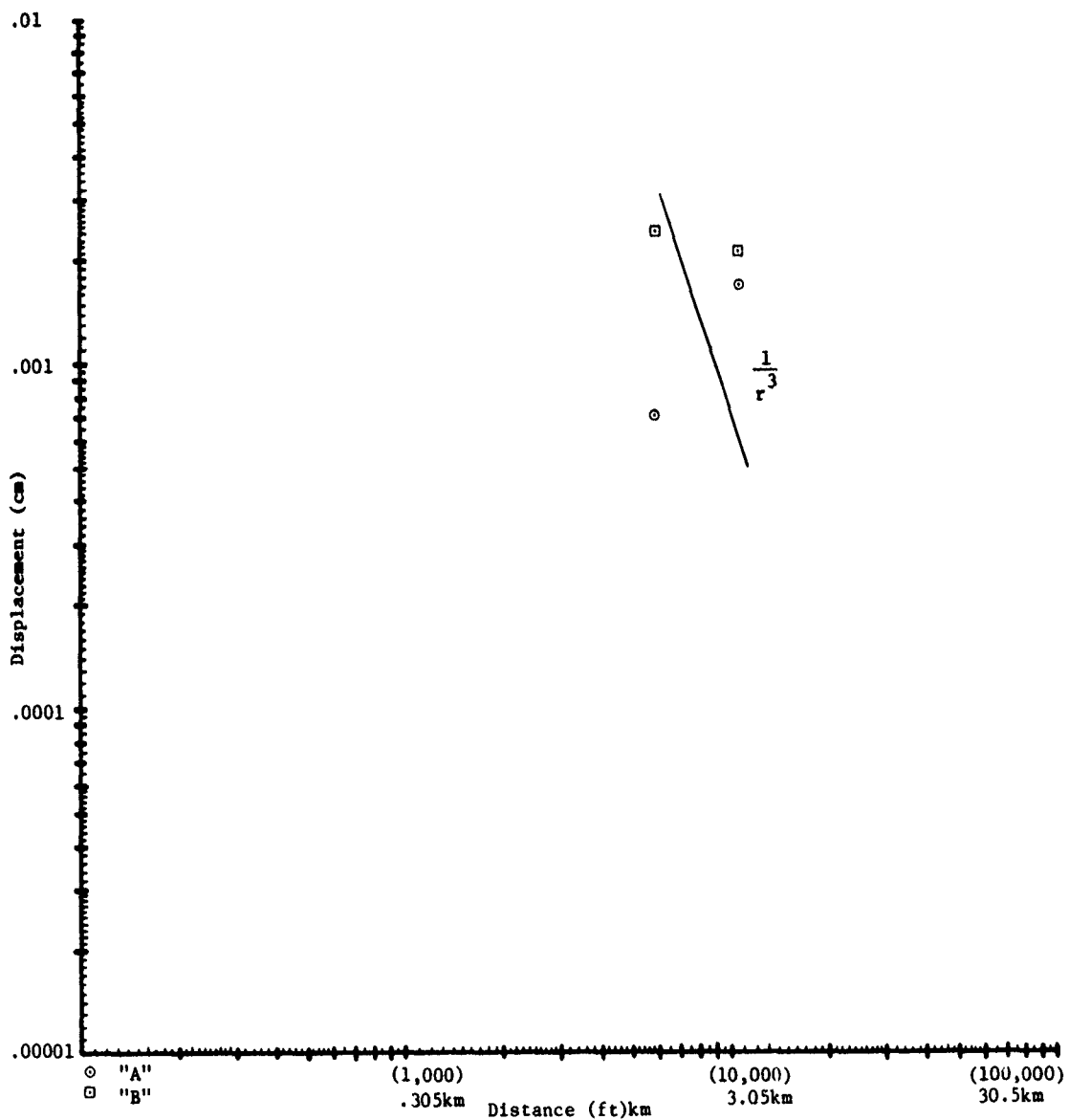


FIGURE 34. P-WAVE PARTICLE DISPLACEMENT, PRE-DICE THROW II-2  
LONGITUDINAL COMPONENT, SOUTH SITES.

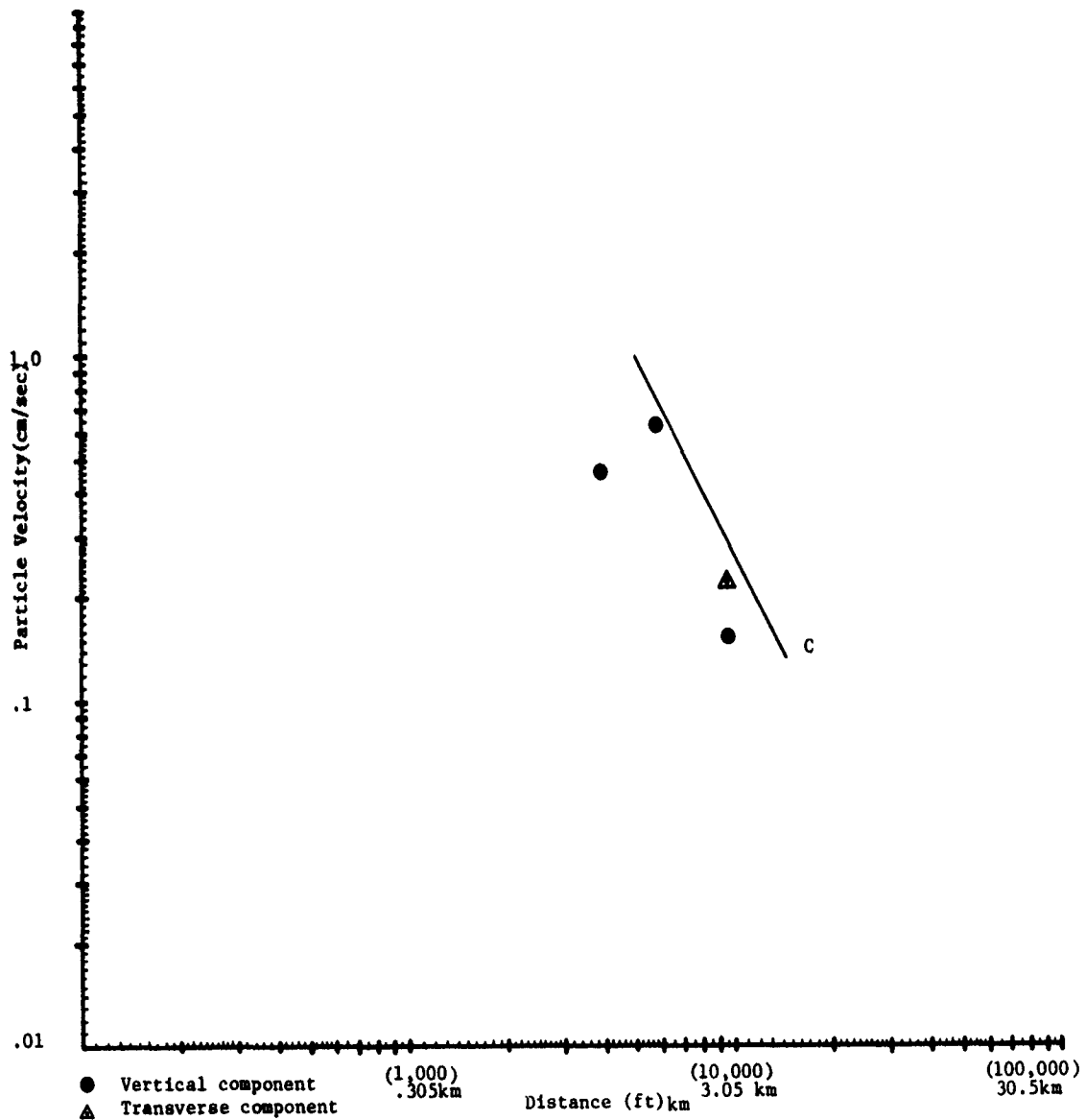


FIGURE 35. PARTICLE VELOCITY FOR RAYLEIGH WAVE, PRE-DICE THROW 11-2 SOUTH SITES.

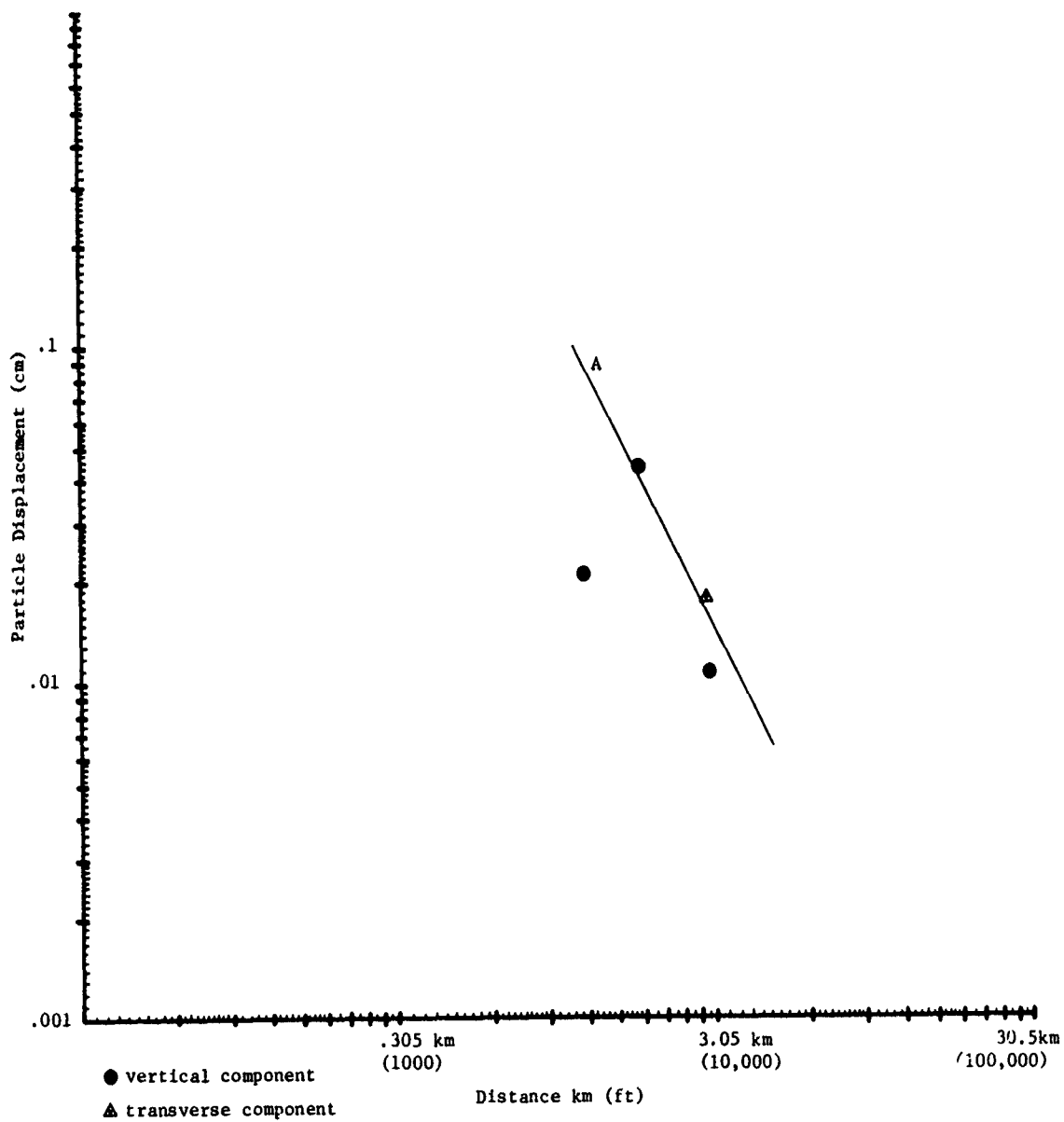


FIGURE 36. PARTICLE DISPLACEMENT FOR RAYLEIGH WAVE, PRE-DICE THROW 11-2 SOUTH SITES.

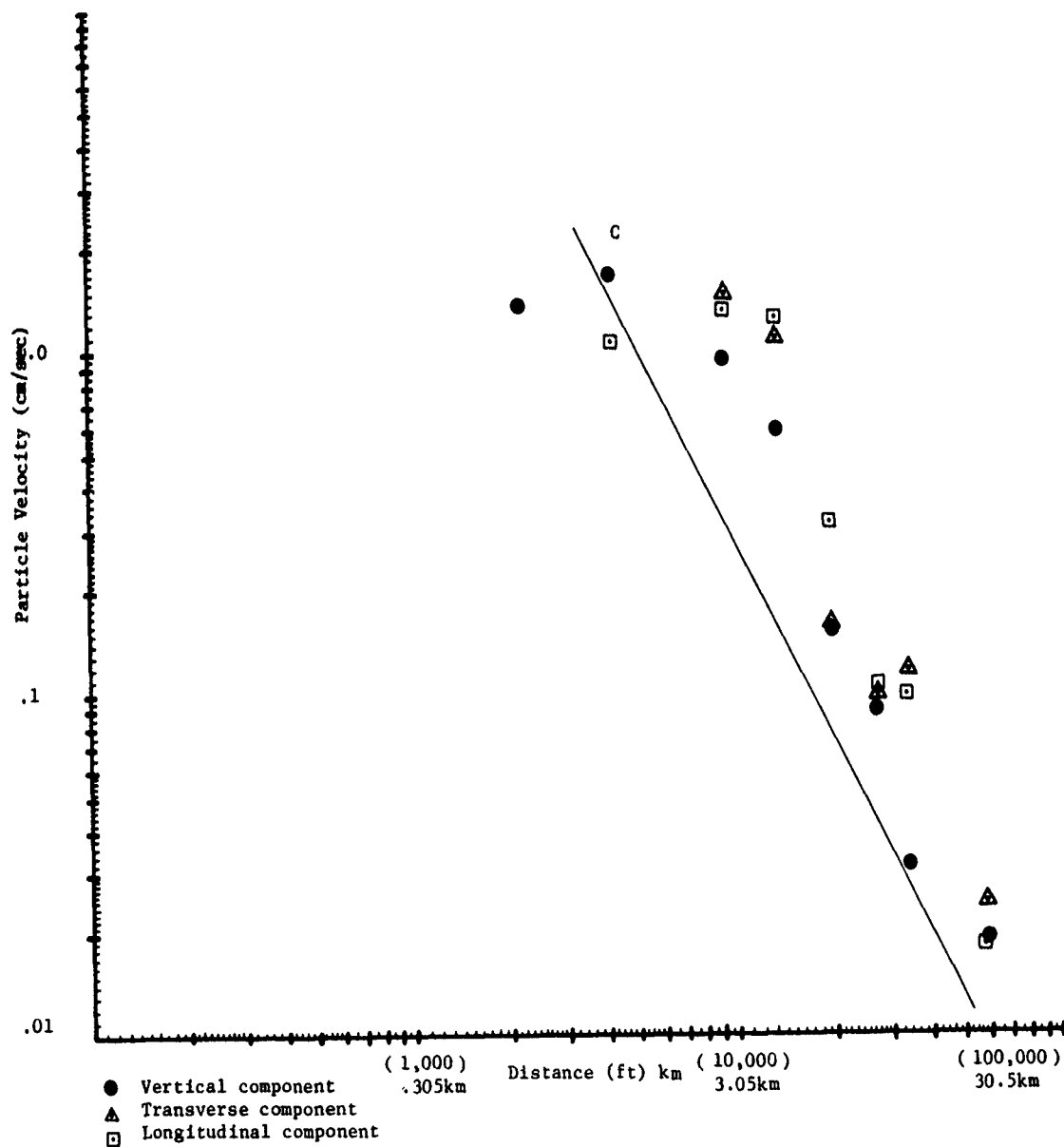


FIGURE 37. PARTICLE VELOCITY FOR RAYLEIGH WAVE, PRE-DICE THROW II-2 NORTH AND NORTHEAST SITES.

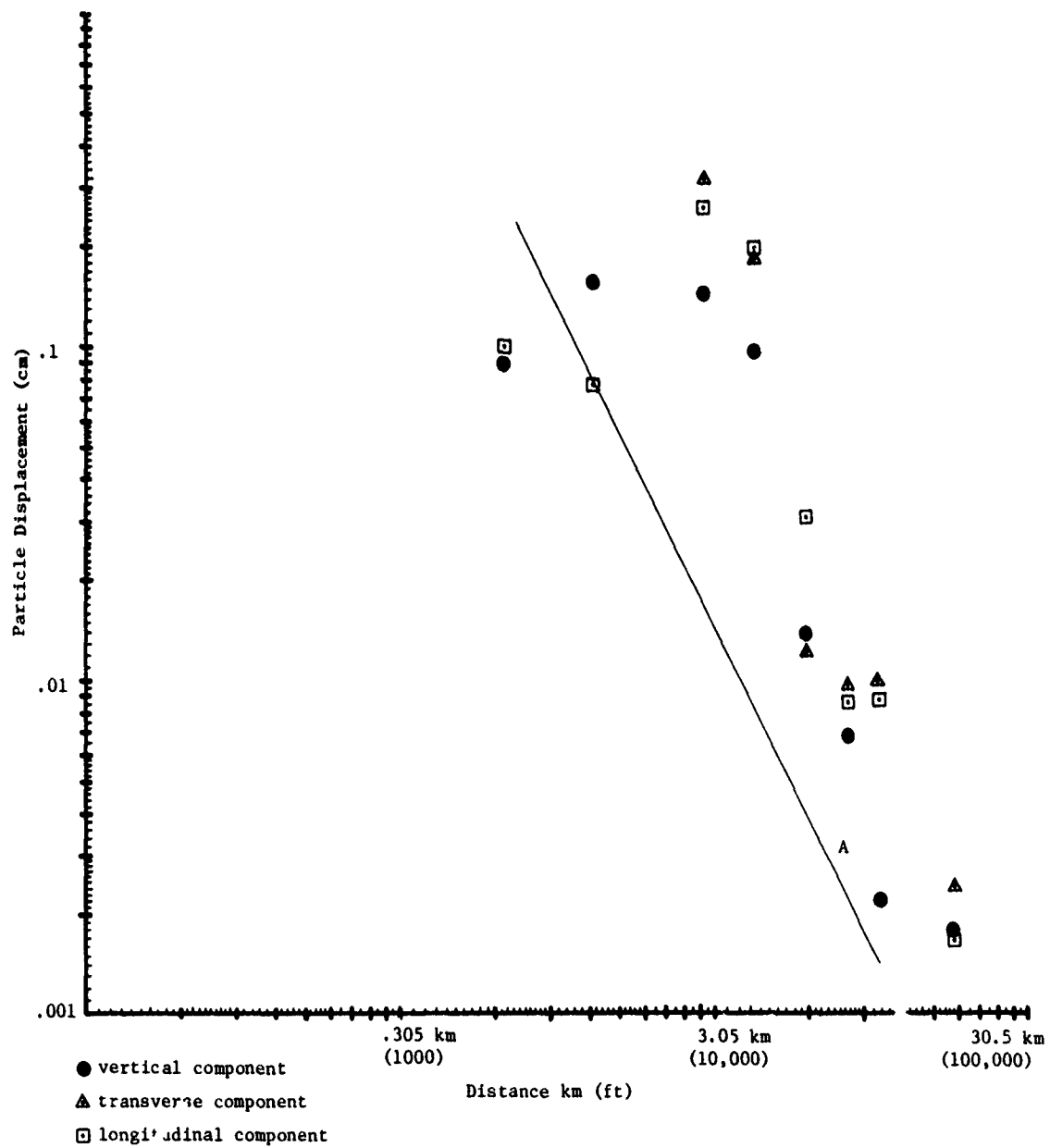


FIGURE 38. PARTICLE DISPLACEMENT FOR RAYLEIGH WAVE, PRE-DICE THROW II-2 NORTH AND NORTHEAST SITES.

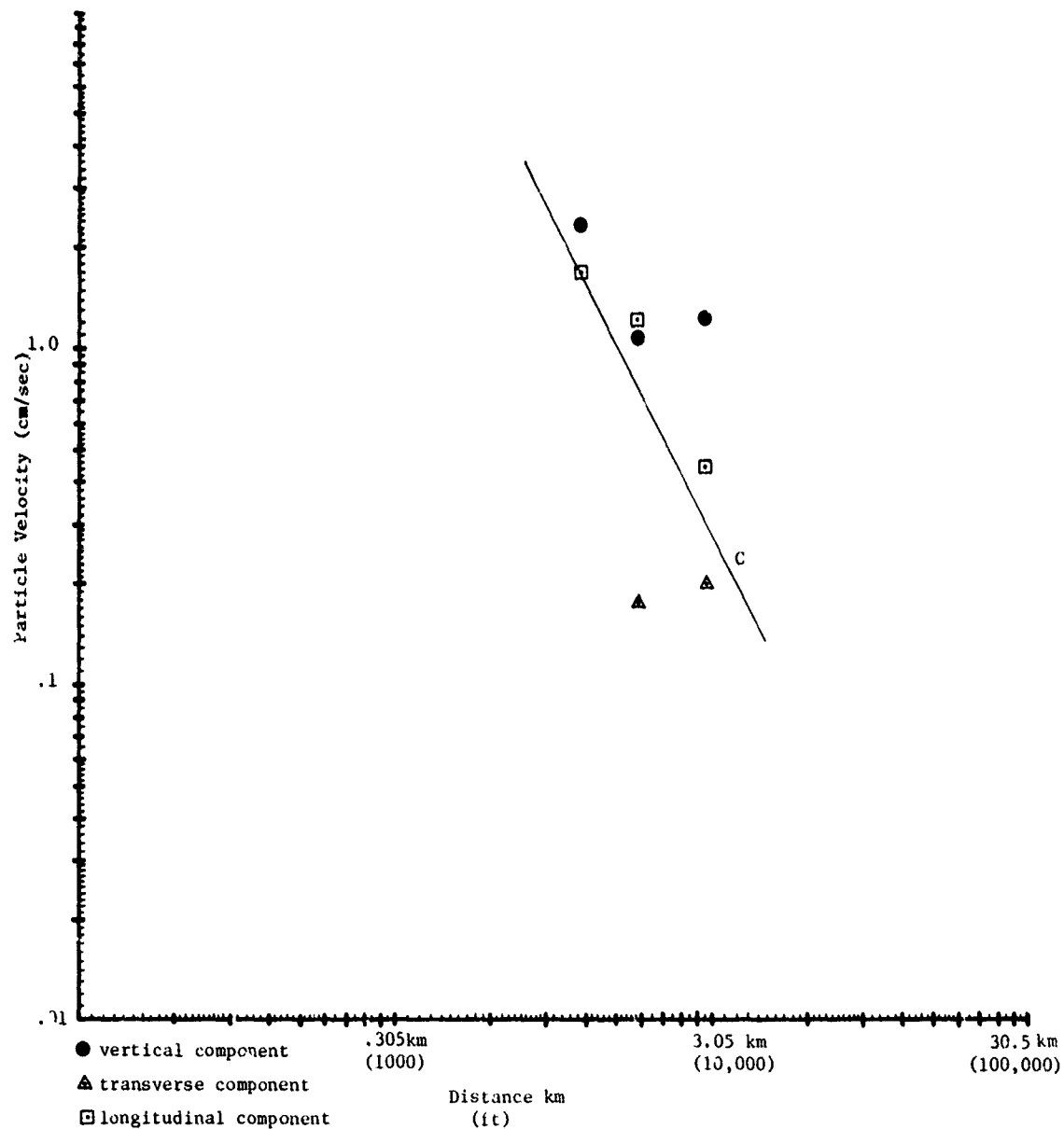


FIGURE 39. PARTICLE VELOCITY FOR FUNDAMENTAL MODE RAYLEIGH WAVE, PRE-DICE THROW 11-2, SOUTH SITES

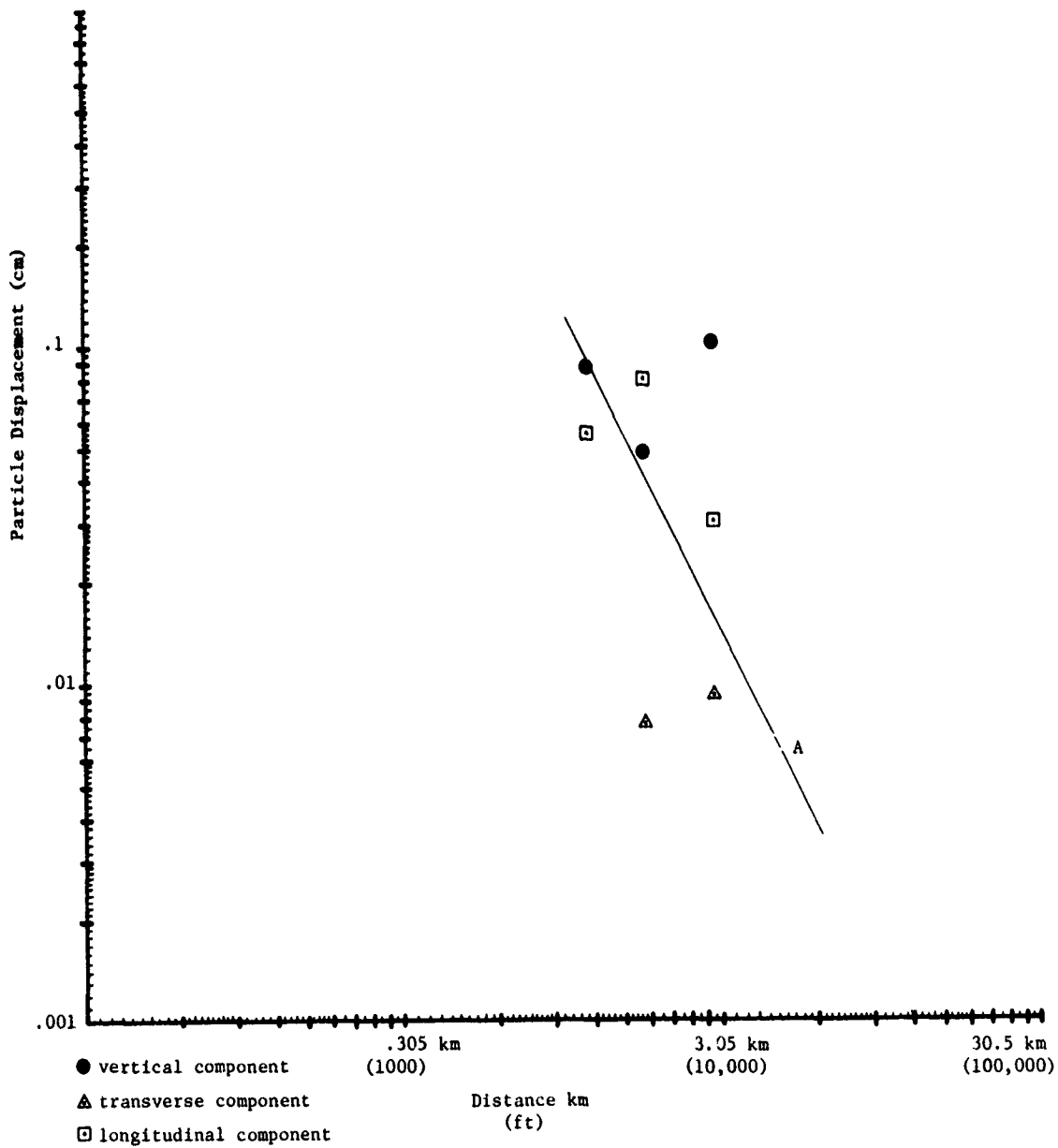


FIGURE 40. PARTICLE DISPLACEMENT FOR FUNDAMENTAL MODE RAYLEIGH WAVE, PRE-DICE THROW 11-2, SOUTH SITES



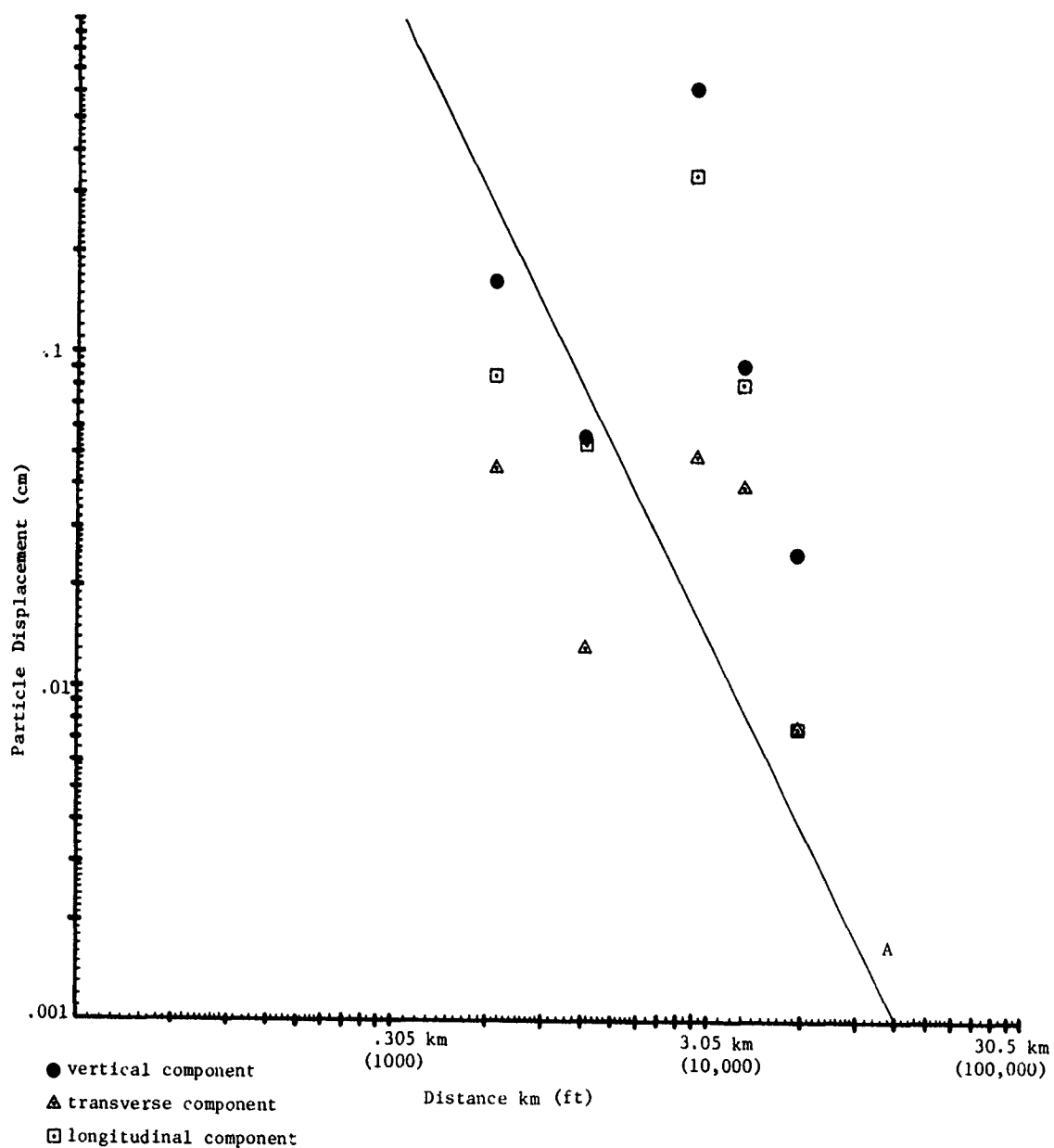


FIGURE 41. PARTICLE VELOCITY FOR FUNDAMENTAL MODE RAYLEIGH WAVE, PRE-DICETHROW 11-2,NORTH AND NORTHEAST SITES.

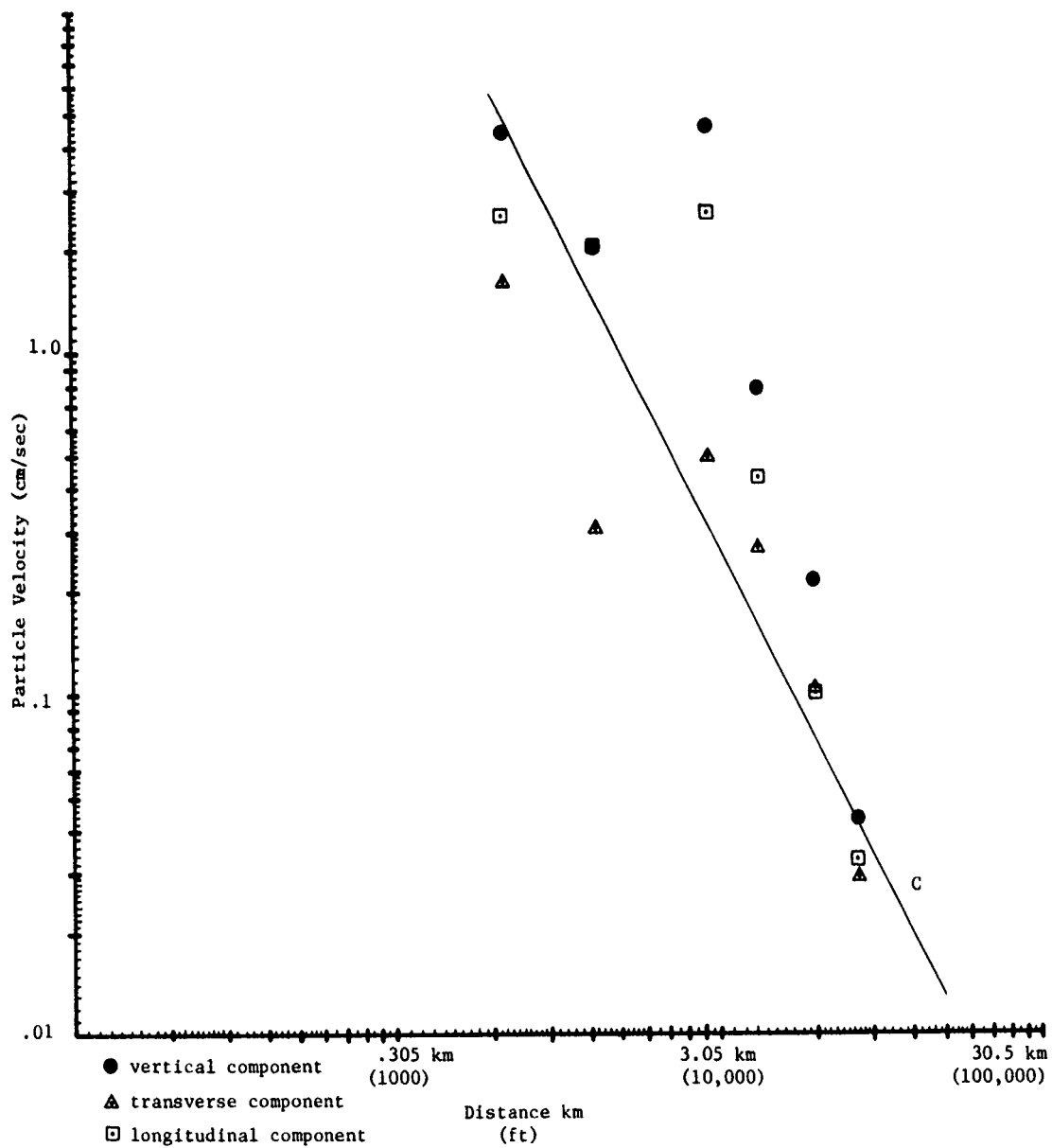


FIGURE 42. PARTICLE DISPLACEMENT FOR FUNDAMENTAL MODE RAYLEIGH WAVE, PRE-DICE THROW II-2, NORTH AND NORTHEAST SITES.

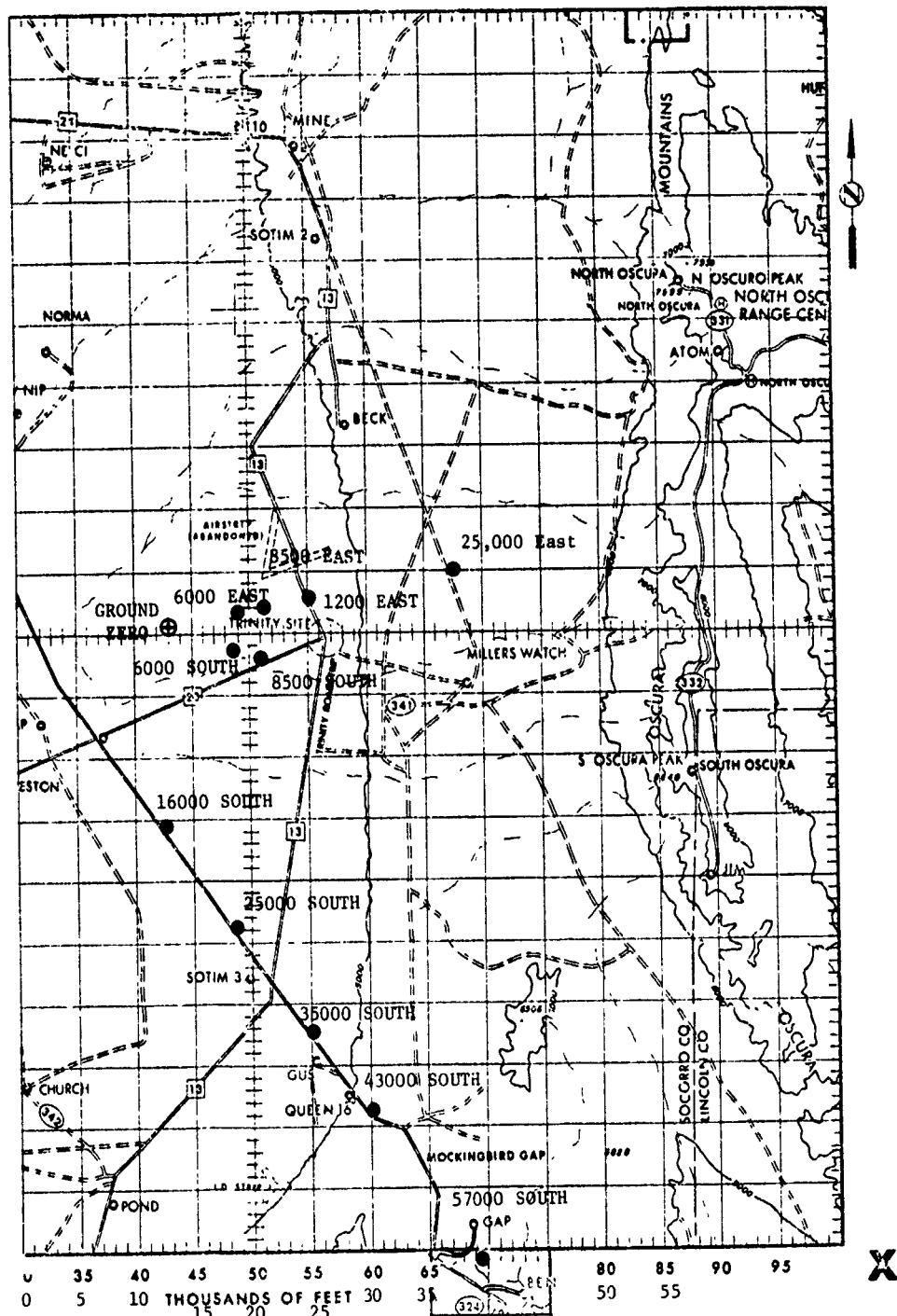


FIGURE 43. SEISMOGRAPH STATIONS FOR DICE THROW EVENT

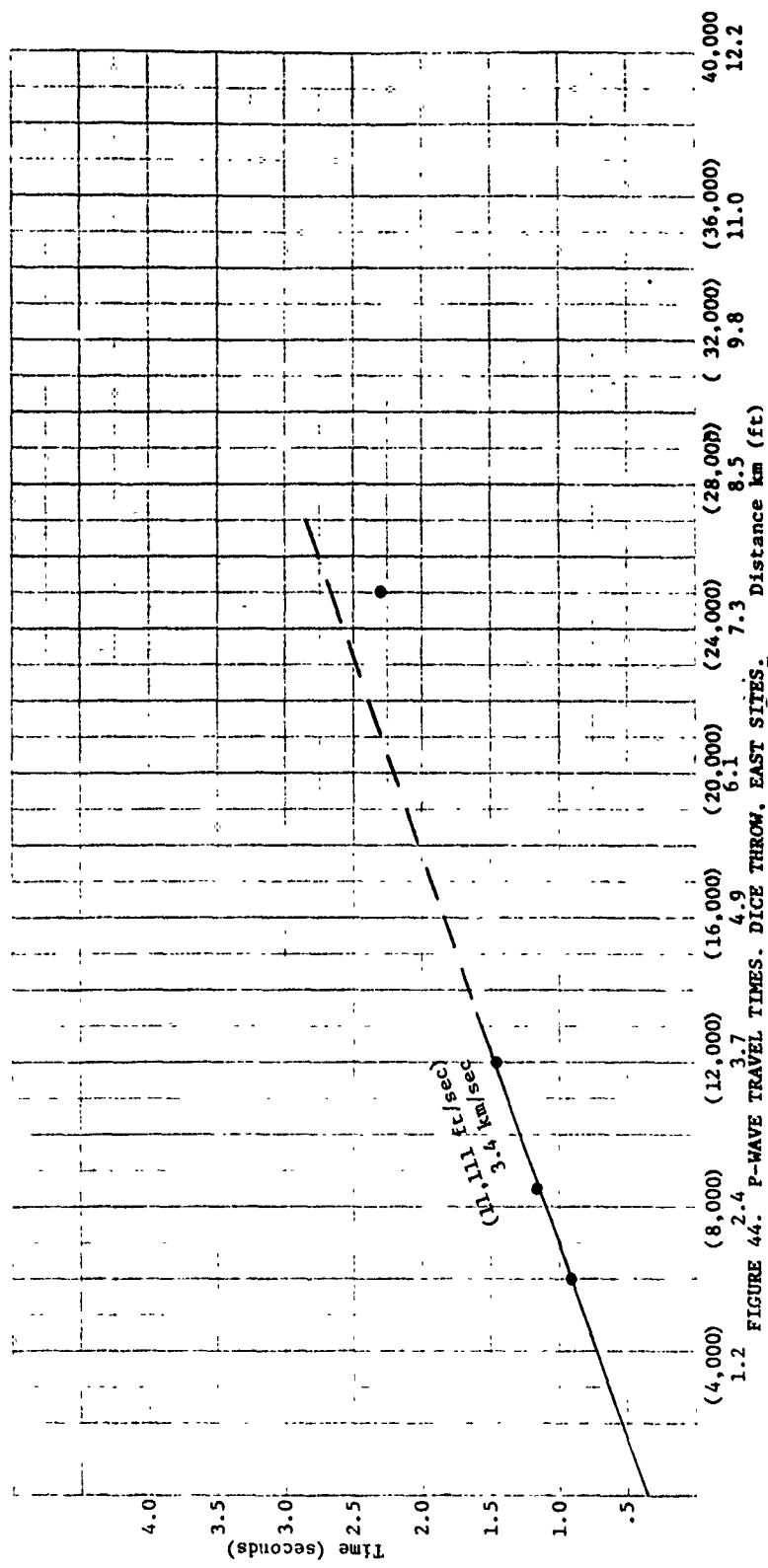
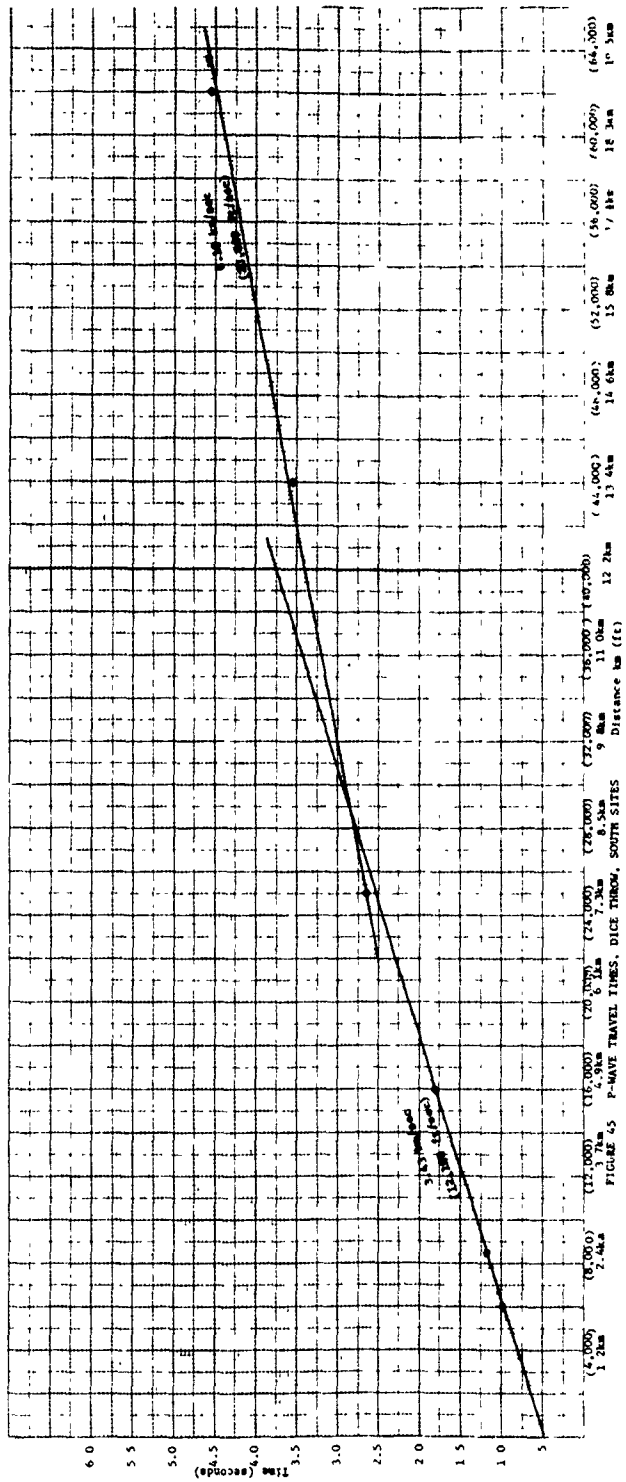


FIGURE 44. P-WAVE TRAVEL TIMES. DICE THROW, EAST SITES.



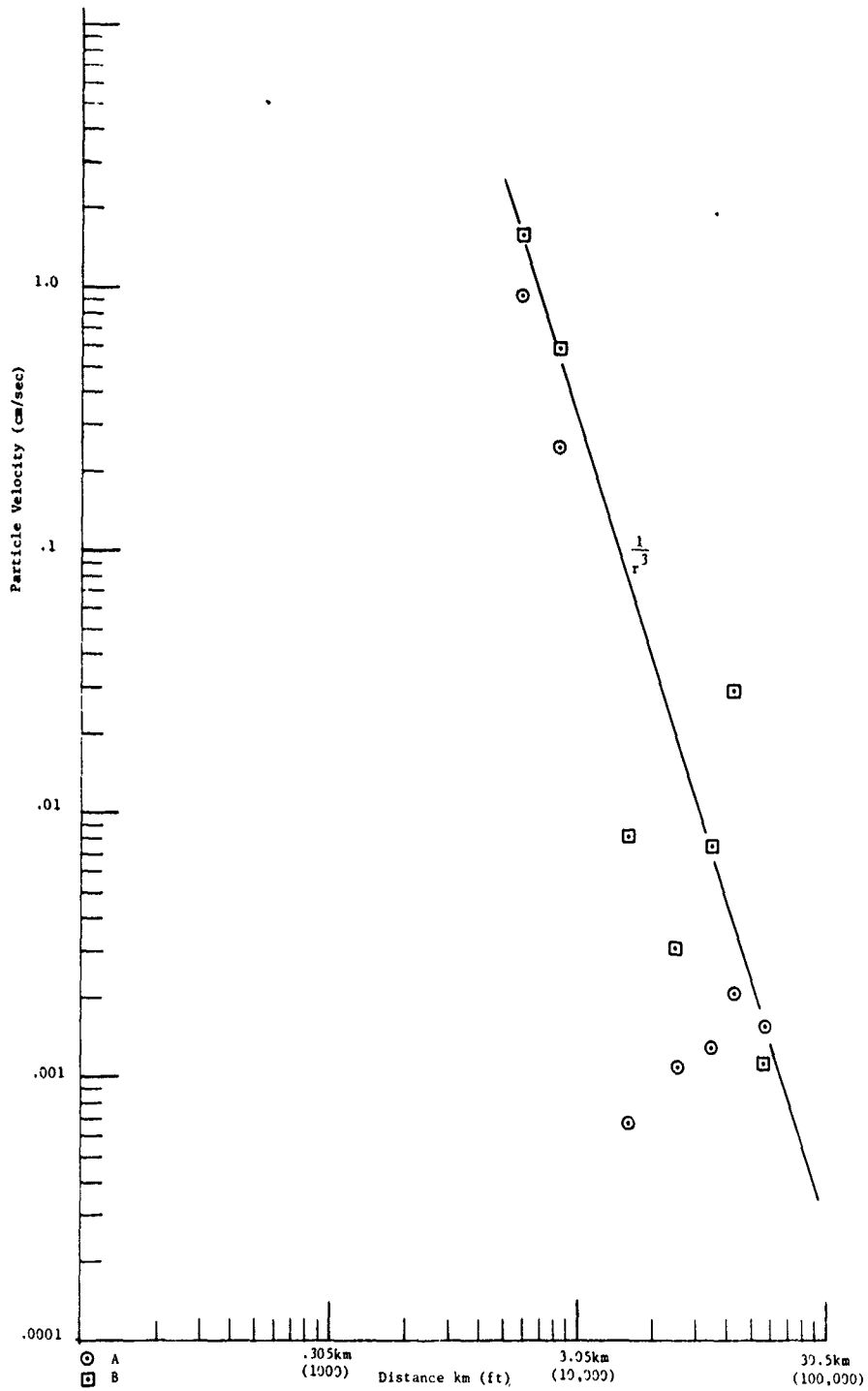


FIGURE 46. P-WAVE PARTICLE VELOCITY, DICE THROW, VERTICAL COMPONENT, SOUTH SITES

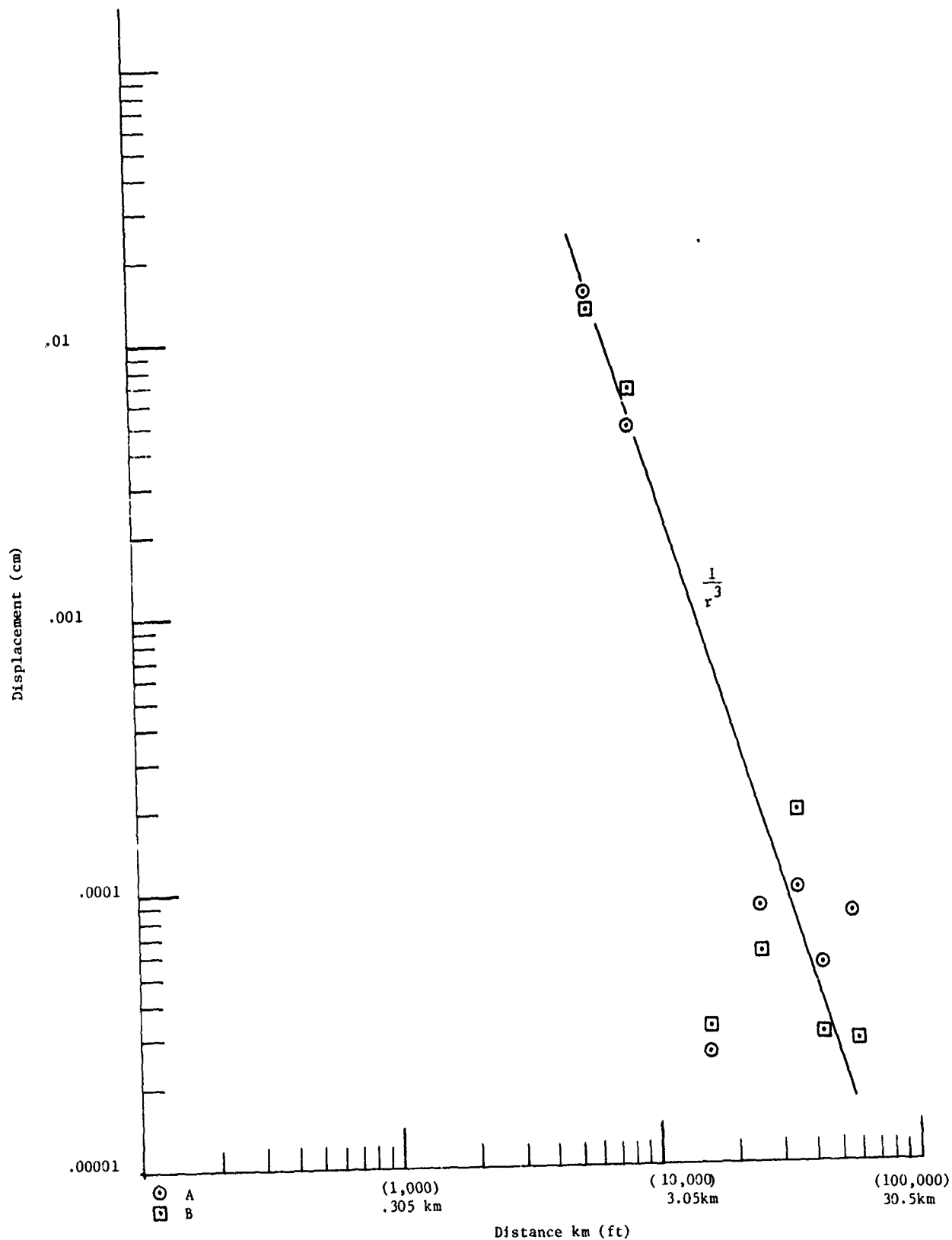


FIGURE 47. P-WAVE PARTICLE DISPLACEMENT, DICE THROW, VERTICAL COMPONENT, SOUTH SITES

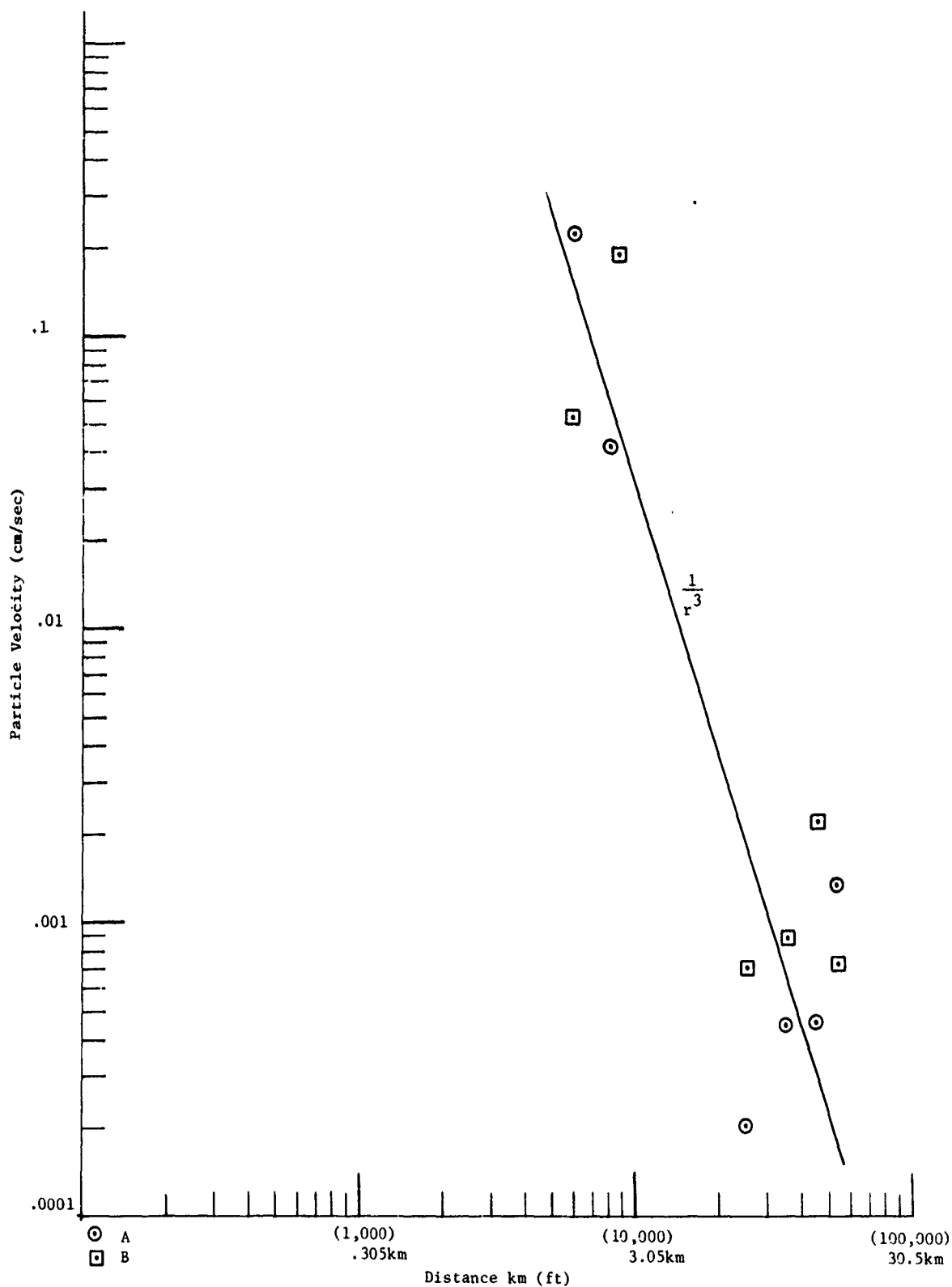


FIGURE 48. P-WAVE PARTICLE VELOCITY, DICE THROW, LONGITUDINAL COMPONENT, SOUTH SITES.



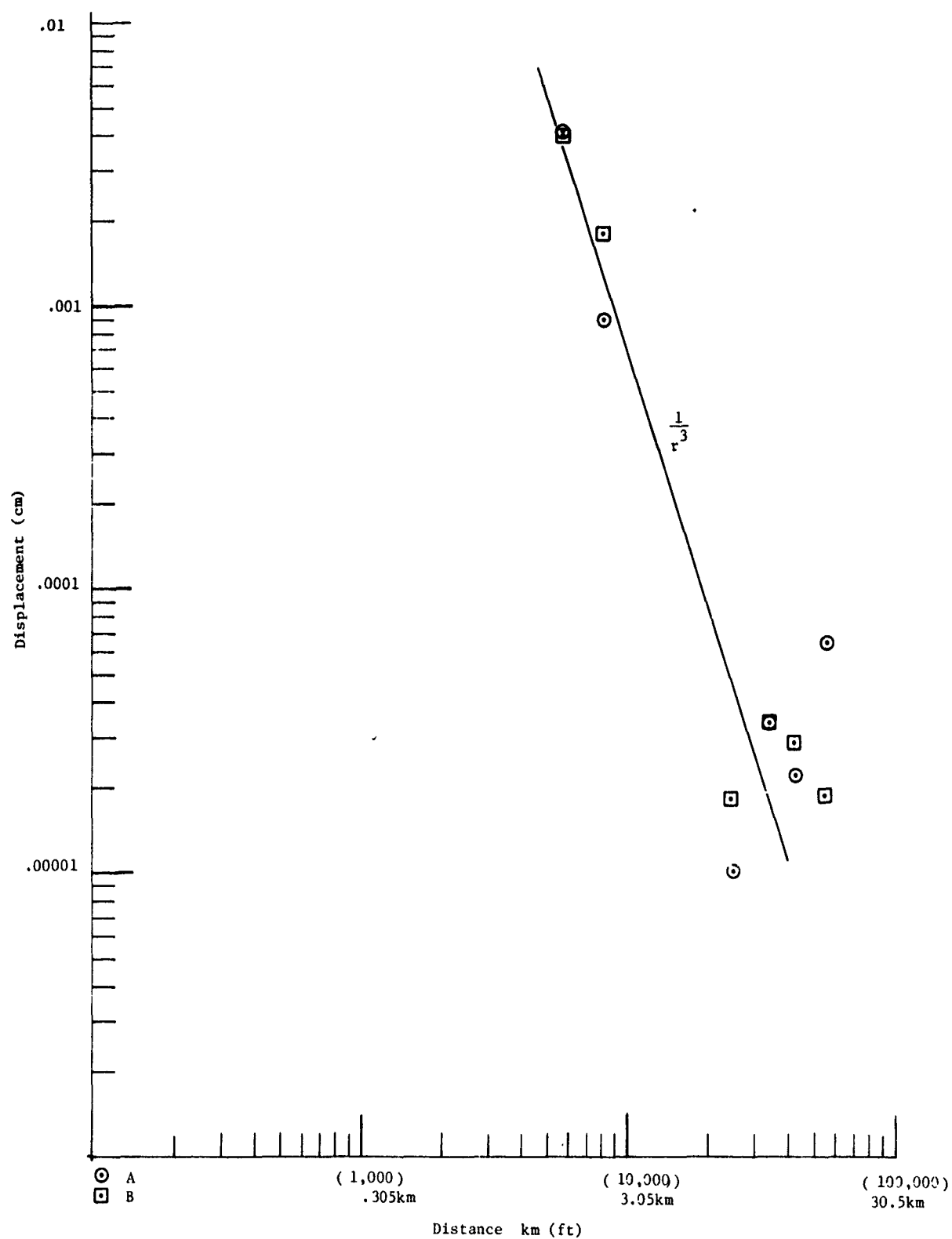


FIGURE 49. P-WAVE PARTICLE DISPLACEMENT, DICE THROW, LONGITUDINAL COMPONENT, SOUTH SITES

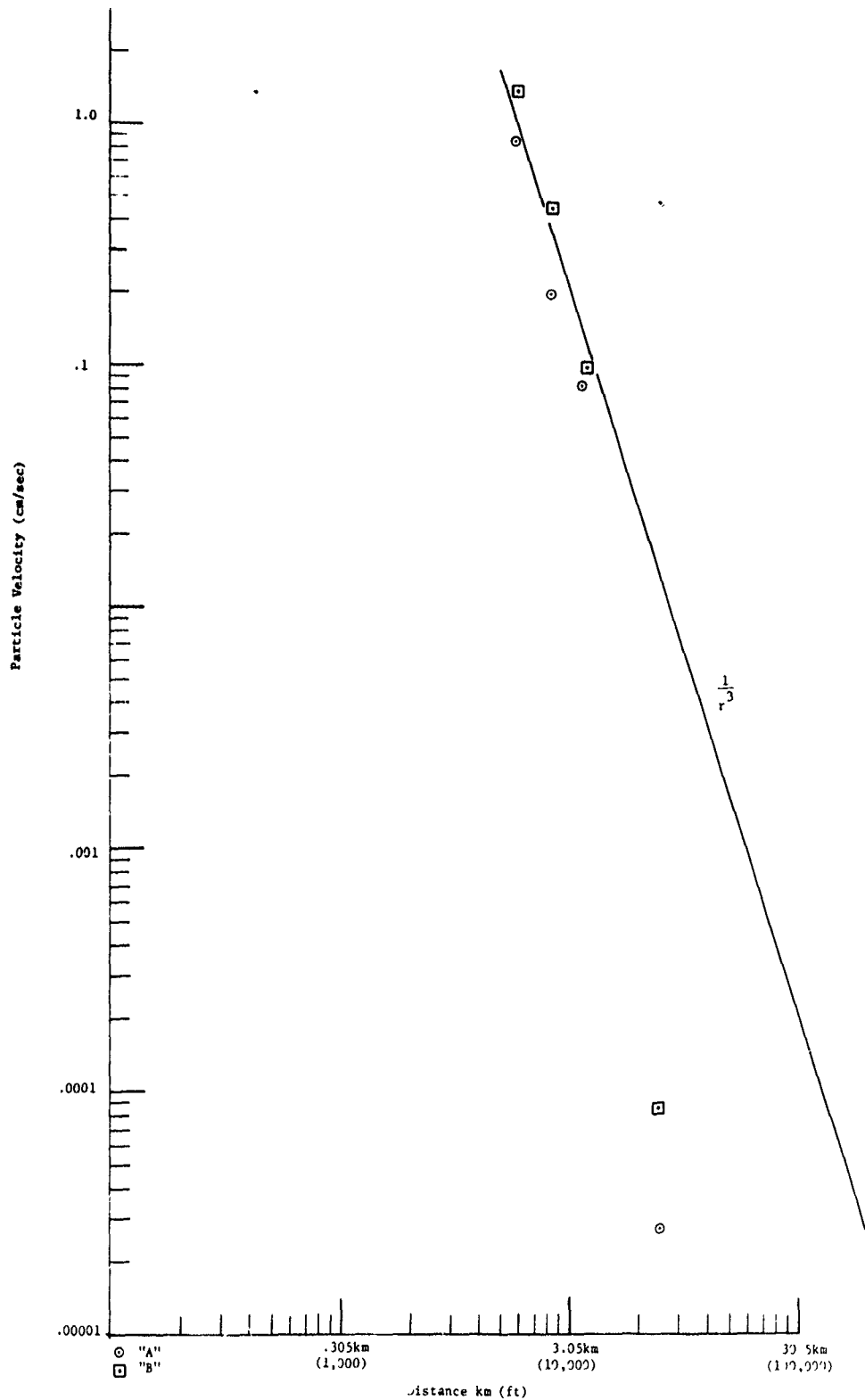


FIGURE 50. P-WAVE, PARTICLE VELOCITY, DICE THROW, VERTICAL COMPONENT, EAST SITES.

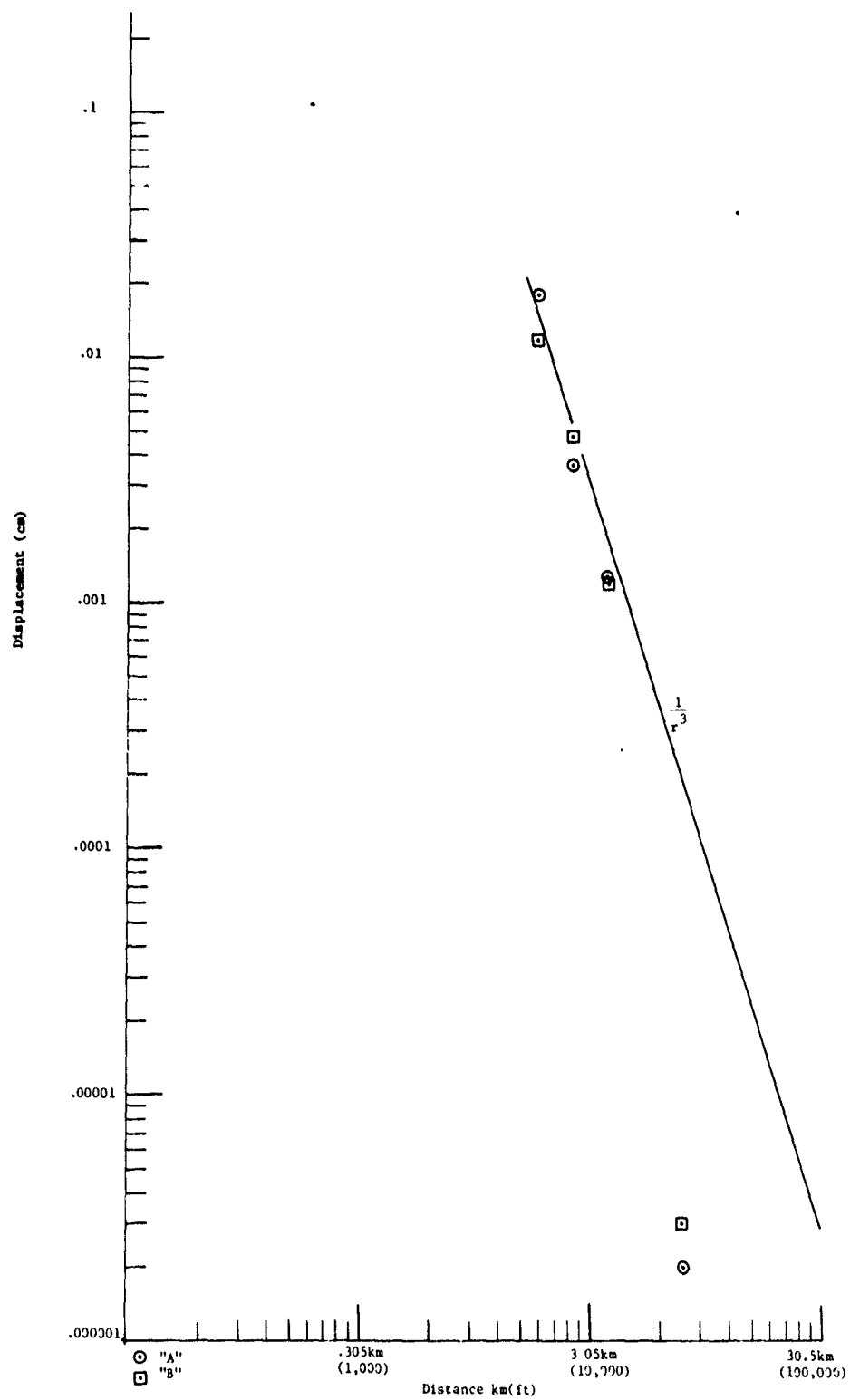


FIGURE 51. P-WAVE PARTICLE DISPLACEMENT, DICE THROW, VERTICAL COMPONENT, EAST SITES

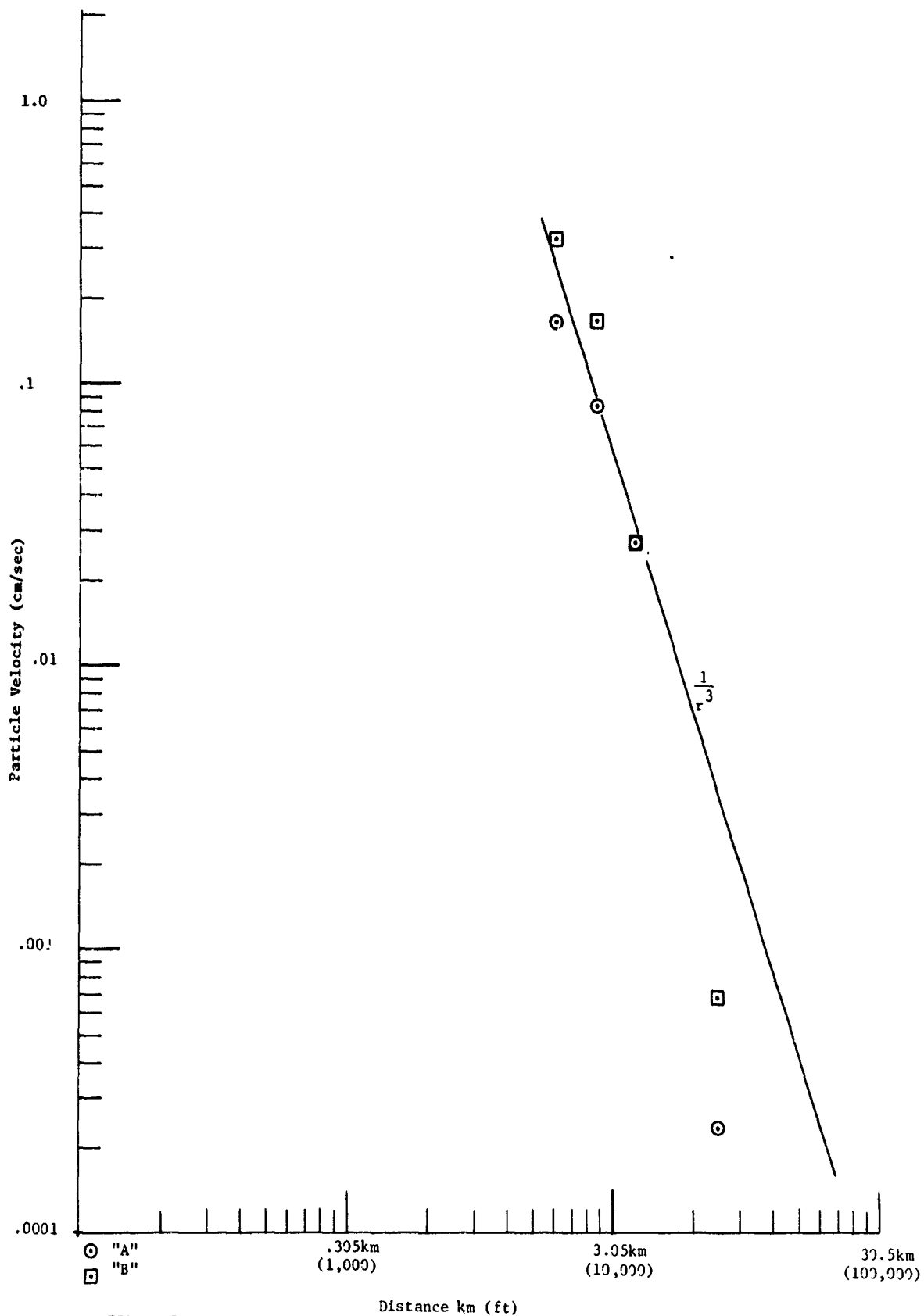


FIGURE 52. P-WAVE PARTICLE VELOCITY, DICE THROW, LONGITUDINAL COMPONENT, EAST SITES

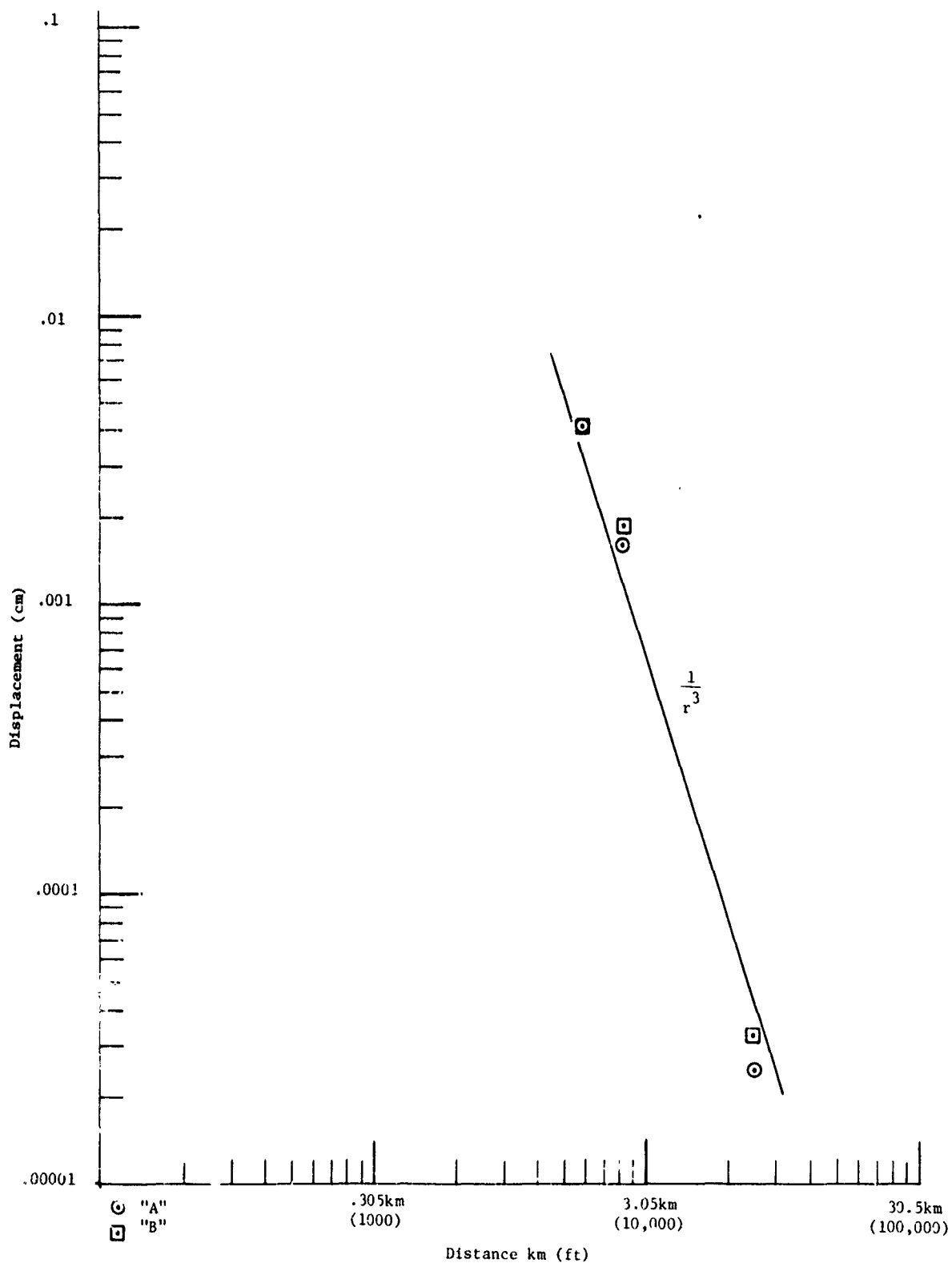


FIGURE 53. P-WAVE PARTICLE DISPLACEMENT, DICE THROW, LONGITUDINAL COMPONENT, EAST SITES



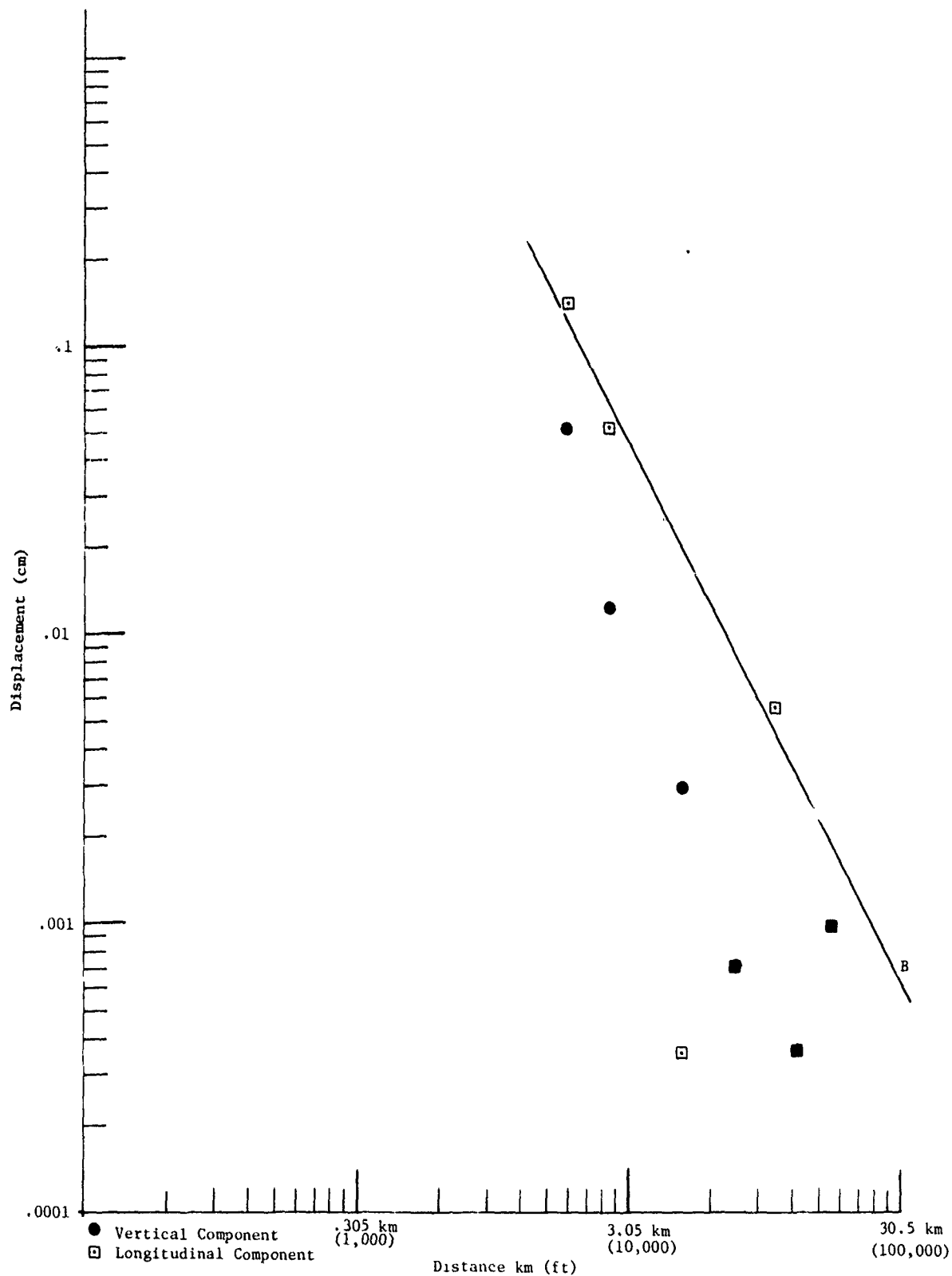


FIGURE 55. PARTICLE DISPLACEMENT FOR RAYLEIGH WAVE, DICE THROW, SOUTH SITES.

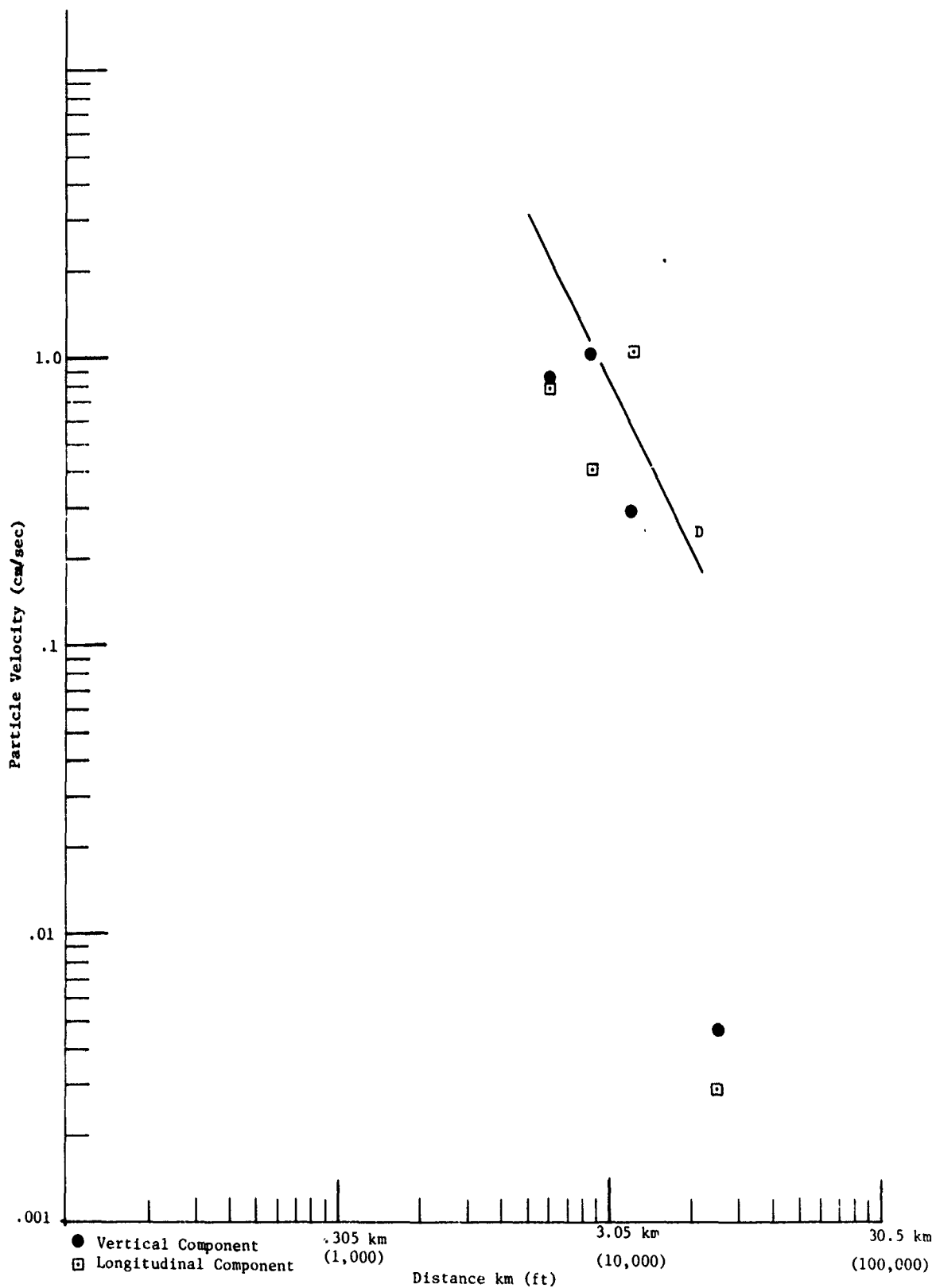


FIGURE 56. PARTICLE VELOCITY FOR RAYLEIGH WAVE, DICE THROW, EAST SITES.



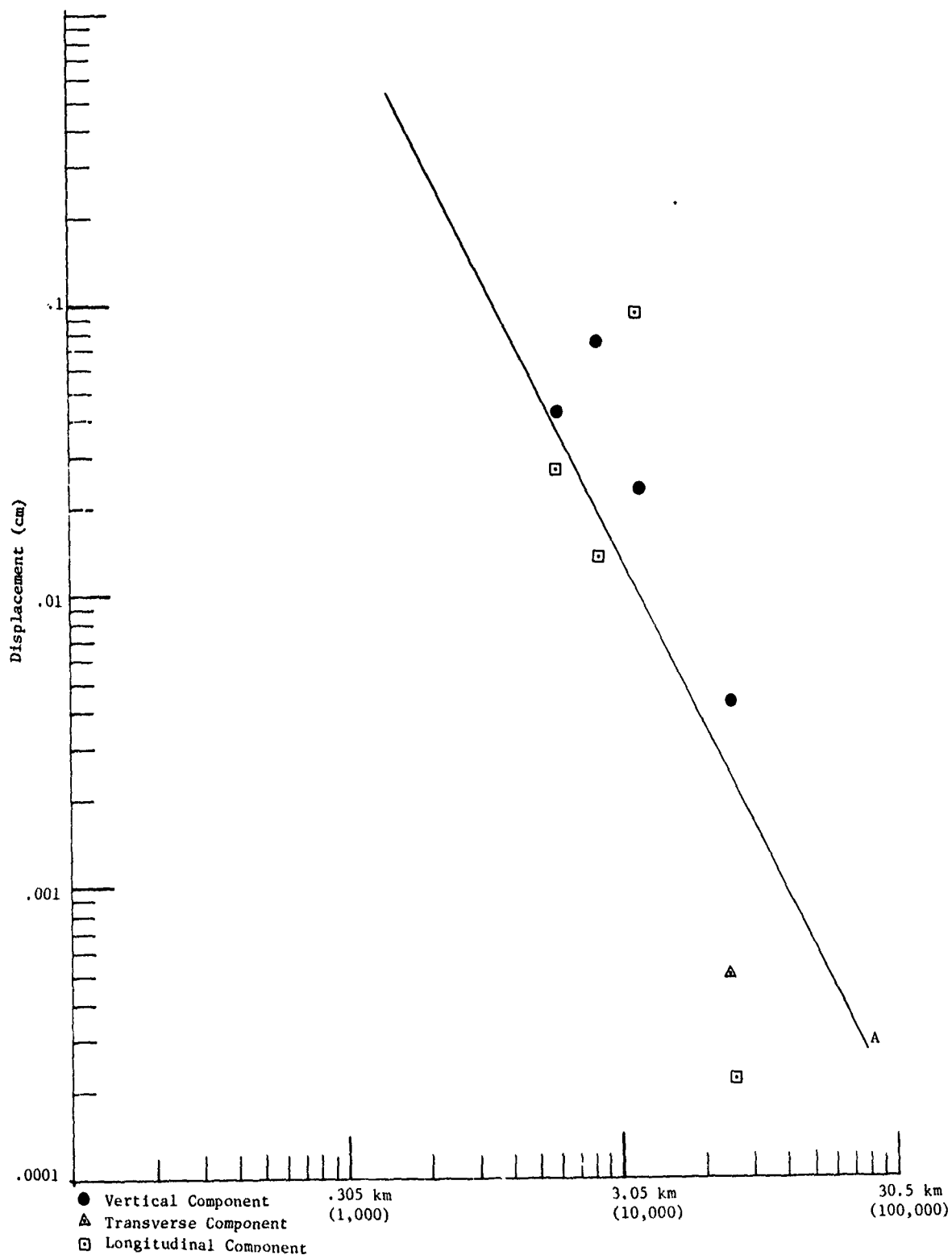


FIGURE 57. PARTICLE DISPLACEMENT FOR RAYLEIGH WAVE, DICE THROW, EAST SITES.

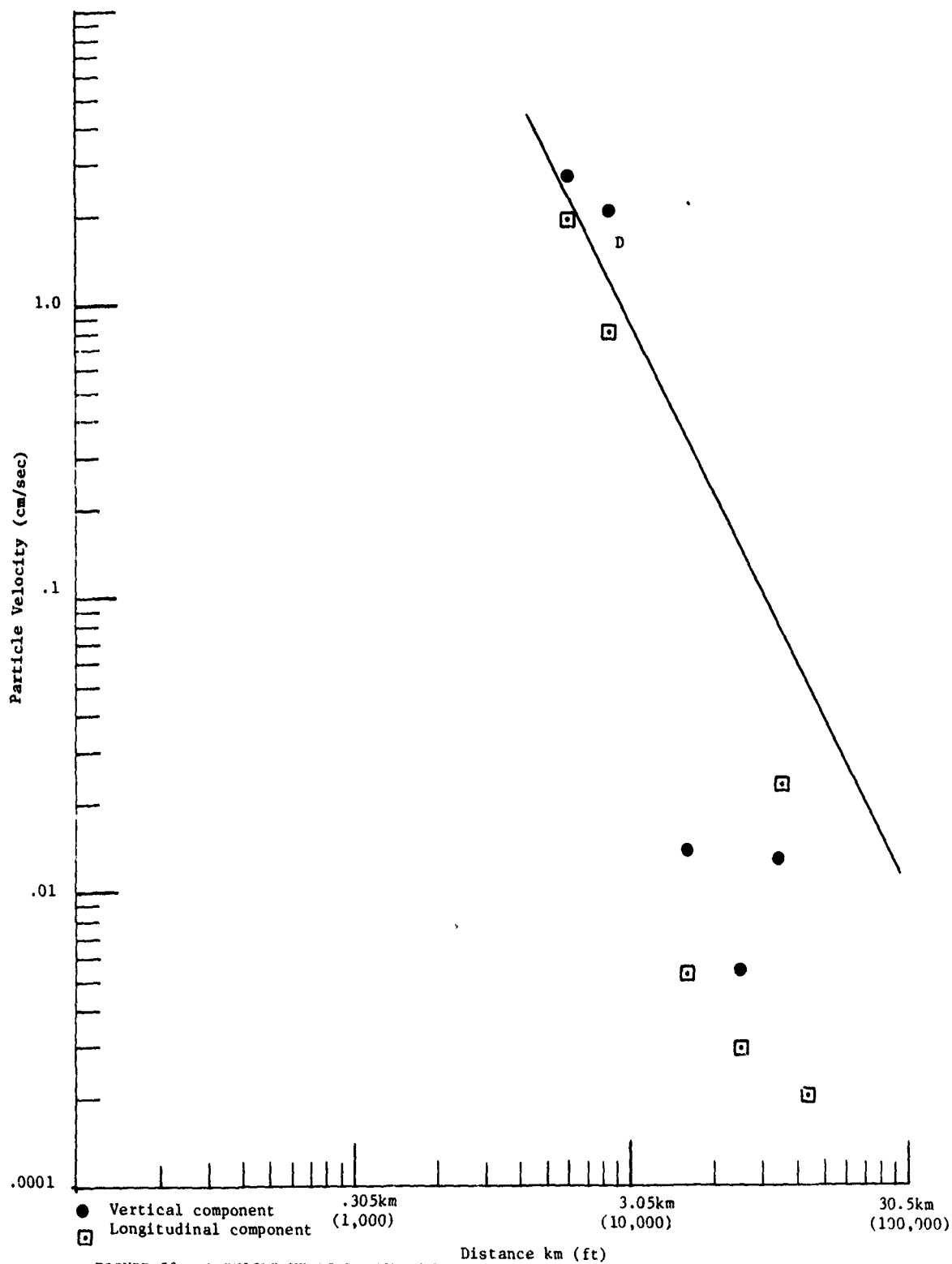


FIGURE 58. PARTICLE VELOCITY FOR FUNDAMENTAL MODE RAYLEIGH WAVE, DICE THROW, SOUTH SITES.

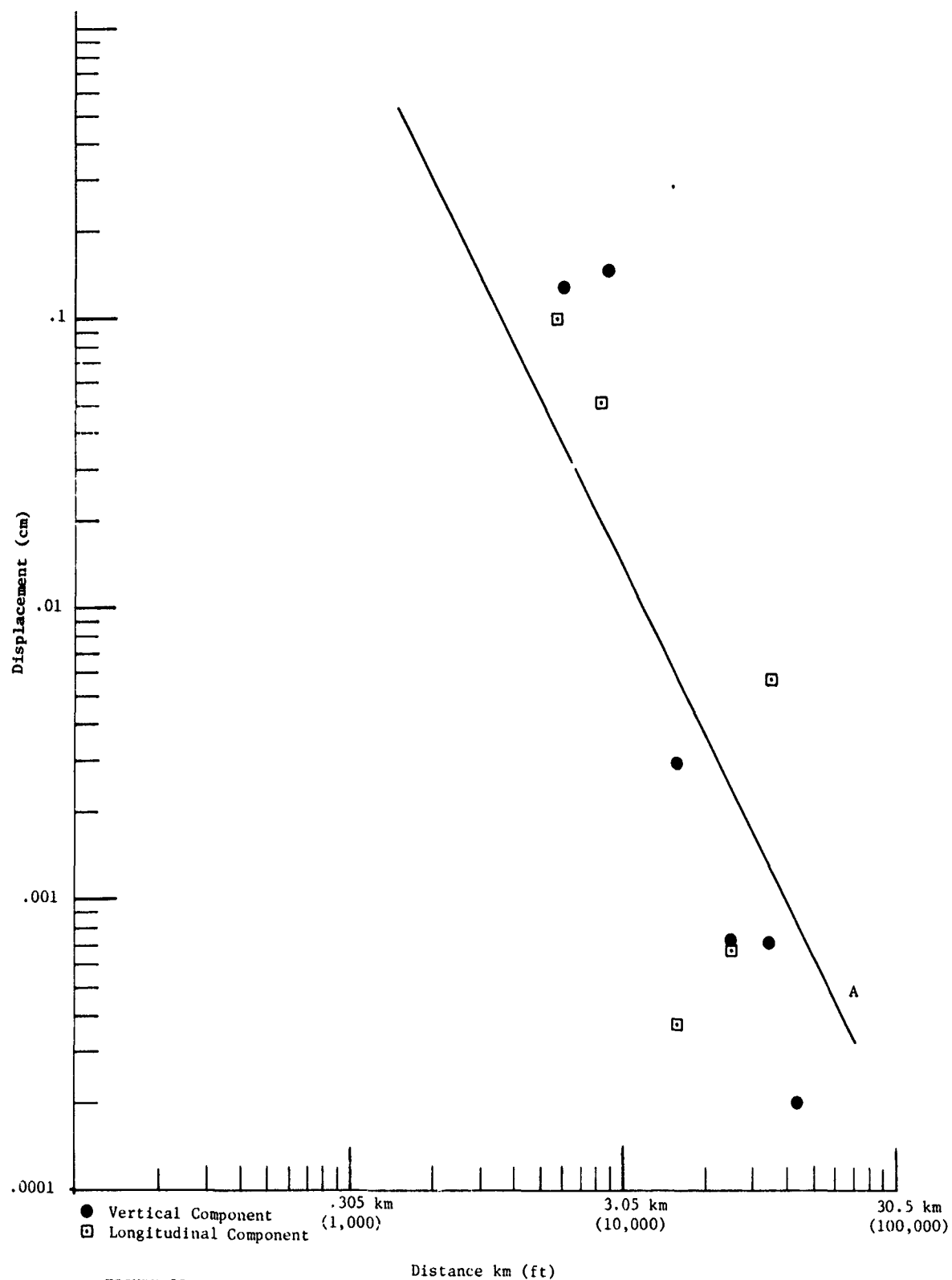


FIGURE 59. PARTICLE DISPLACEMENT FOR FUNDAMENTAL MODE RAYLEIGH WAVE, DICE THROW, SOUTH SITES.

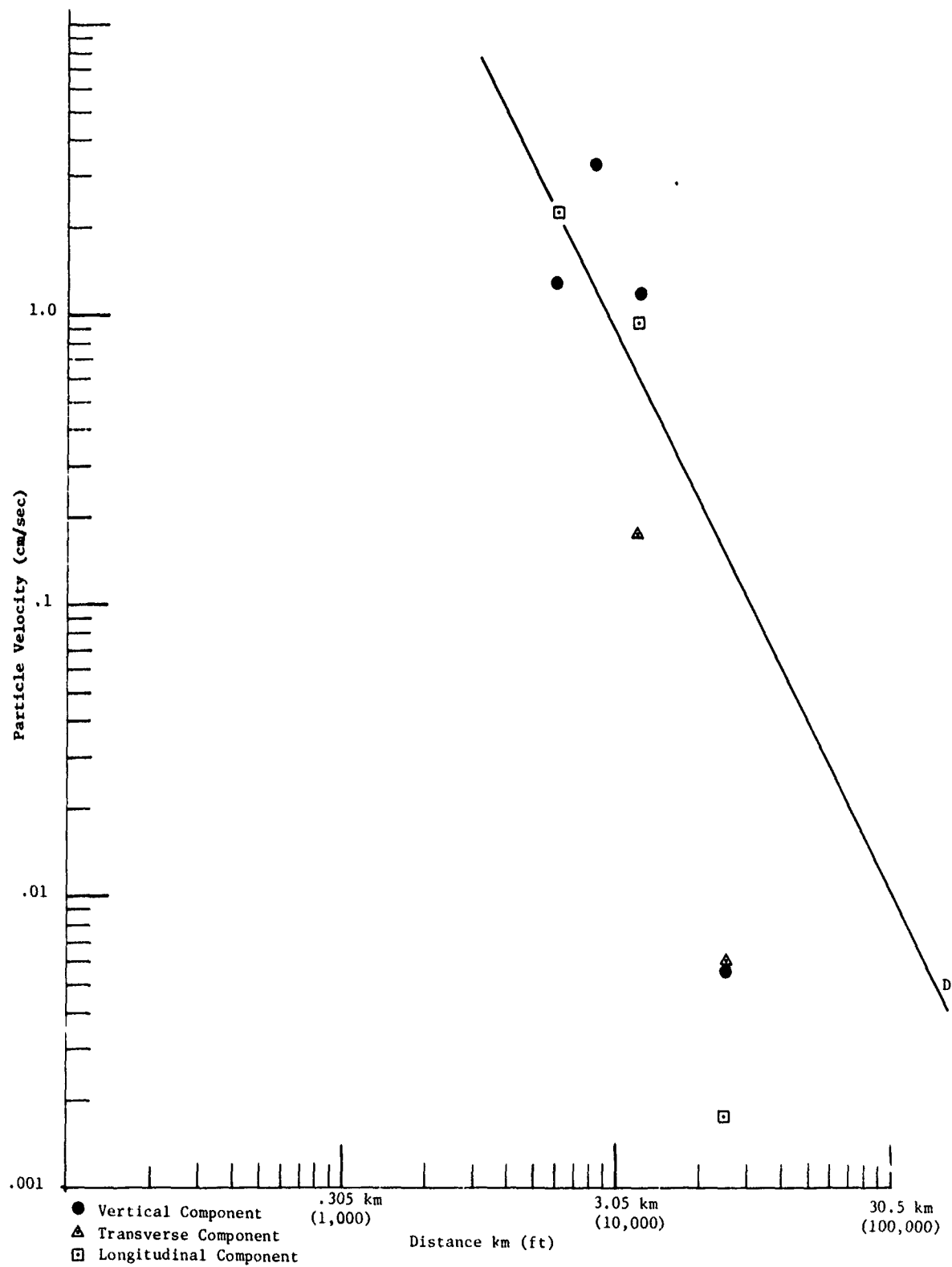
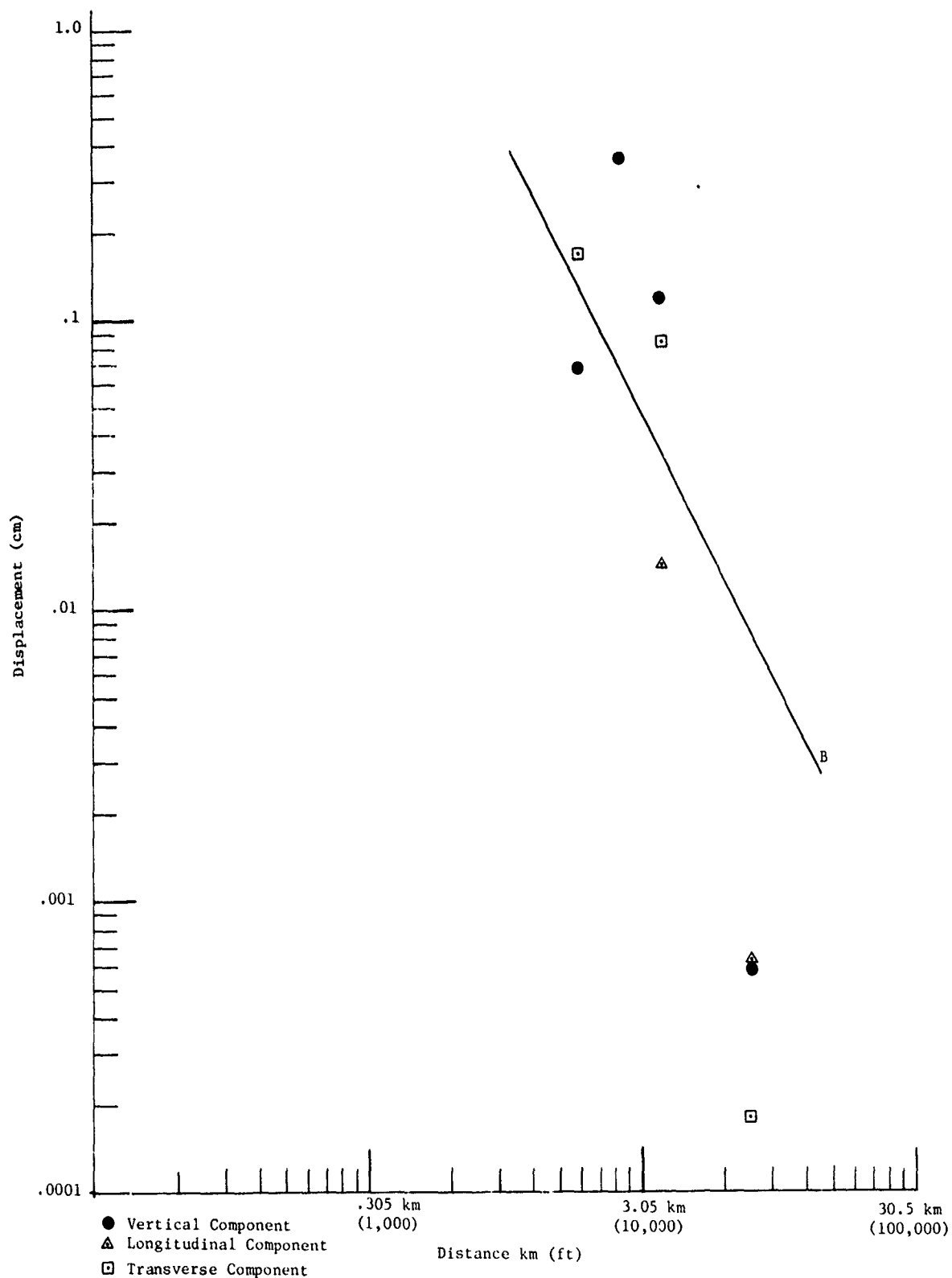


FIGURE 60. PARTICLE VELOCITY FOR FUNDAMENTAL MODE RAYLEIGH WAVE, DICE THROW, EAST SITES.



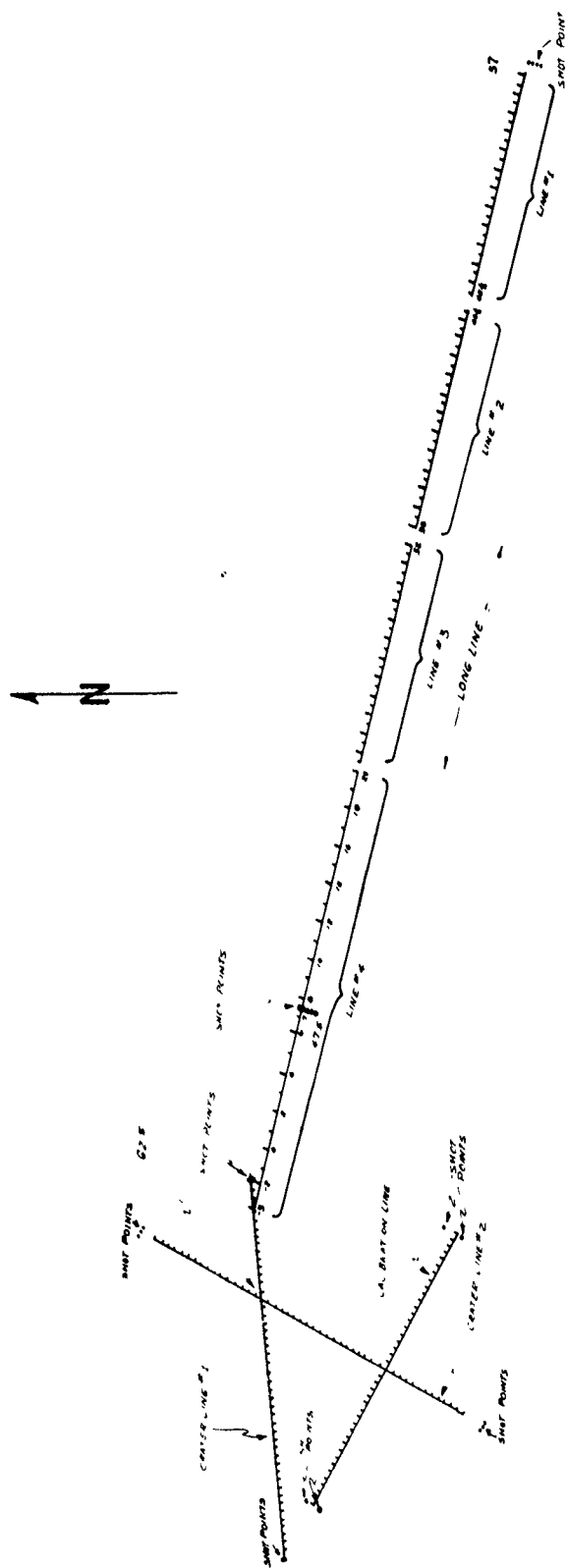


FIGURE 2. PLAN A. MAP LOCATIONS OF ALL T AND M RESECTION POINTS IN THE DEEP 13 AREA

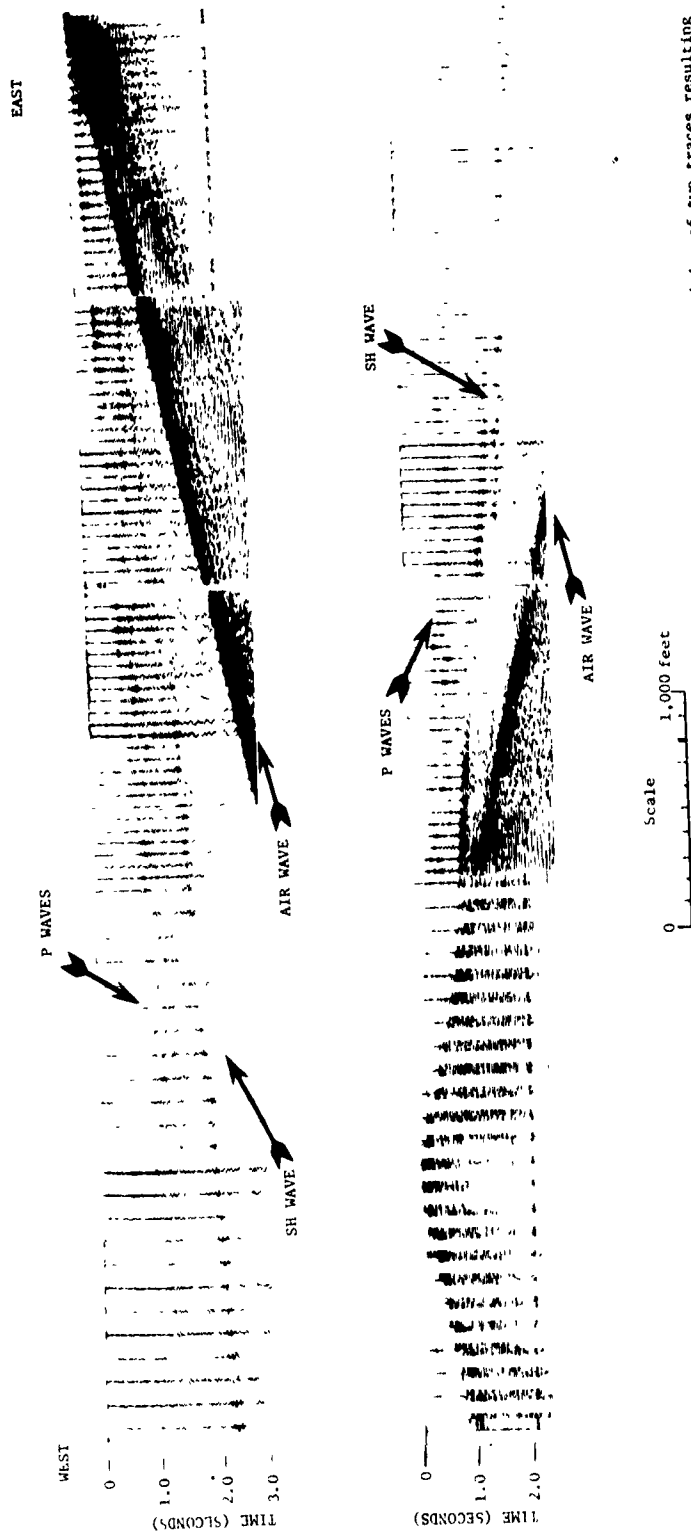


FIGURE 63. SH WAVE DATA FROM THE LONG REFRACTION PROFILE IN FIGURE 62. Each trace shown here is the superposition of two traces resulting from a 180° rotation of the shear wave source. The SH wave, therefore, is shown as the darker area between the polarity reversals.

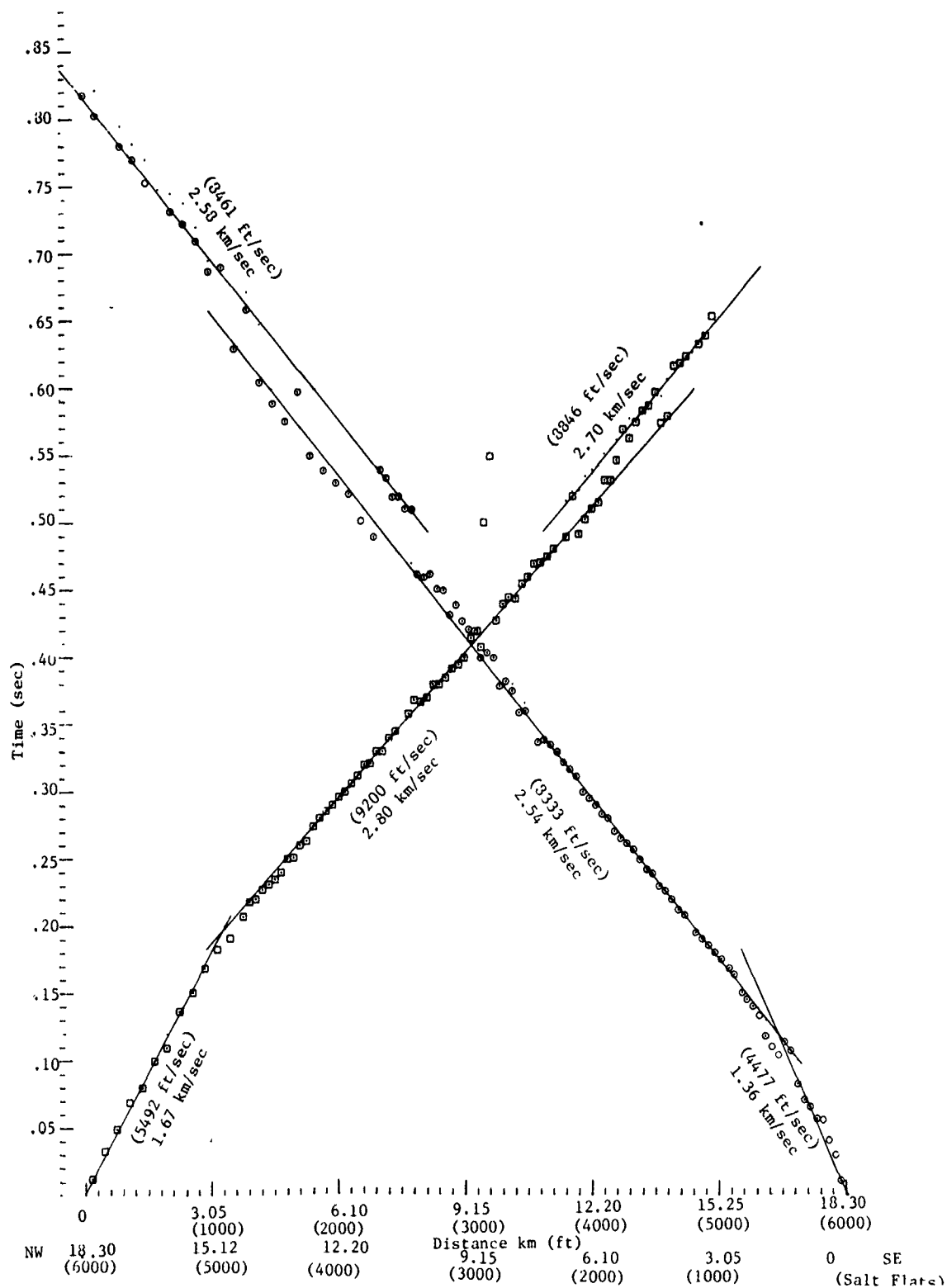


FIGURE 64. P-WAVE TRAVEL TIMES FOR LONG LINE (4 SEGMENTS) SHOWN IN FIGURE 62.



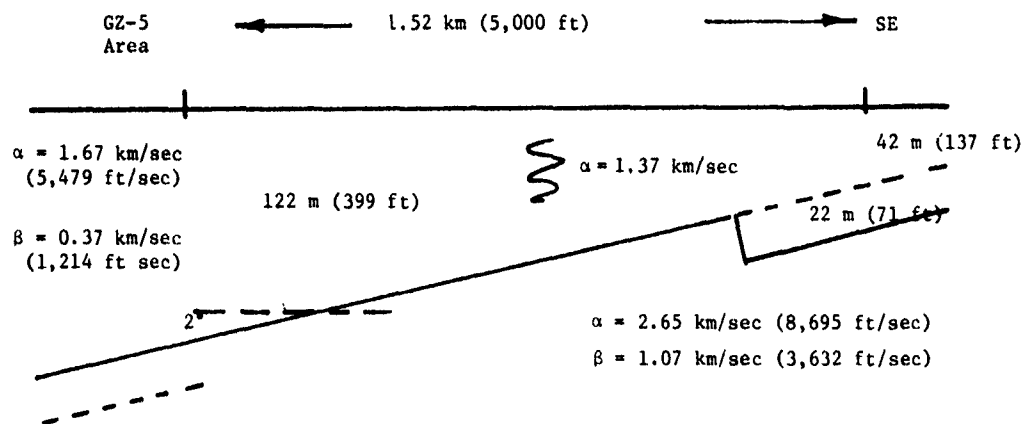


FIGURE 65. P ( $\alpha$ ) AND SH WAVE ( $\beta$ ) STRUCTURE ALONG THE LONG REFRACTION PROFILE SHOWN IN FIGURE 62. The SH travel time curve gives information on deeper structure shown in Figure 67.

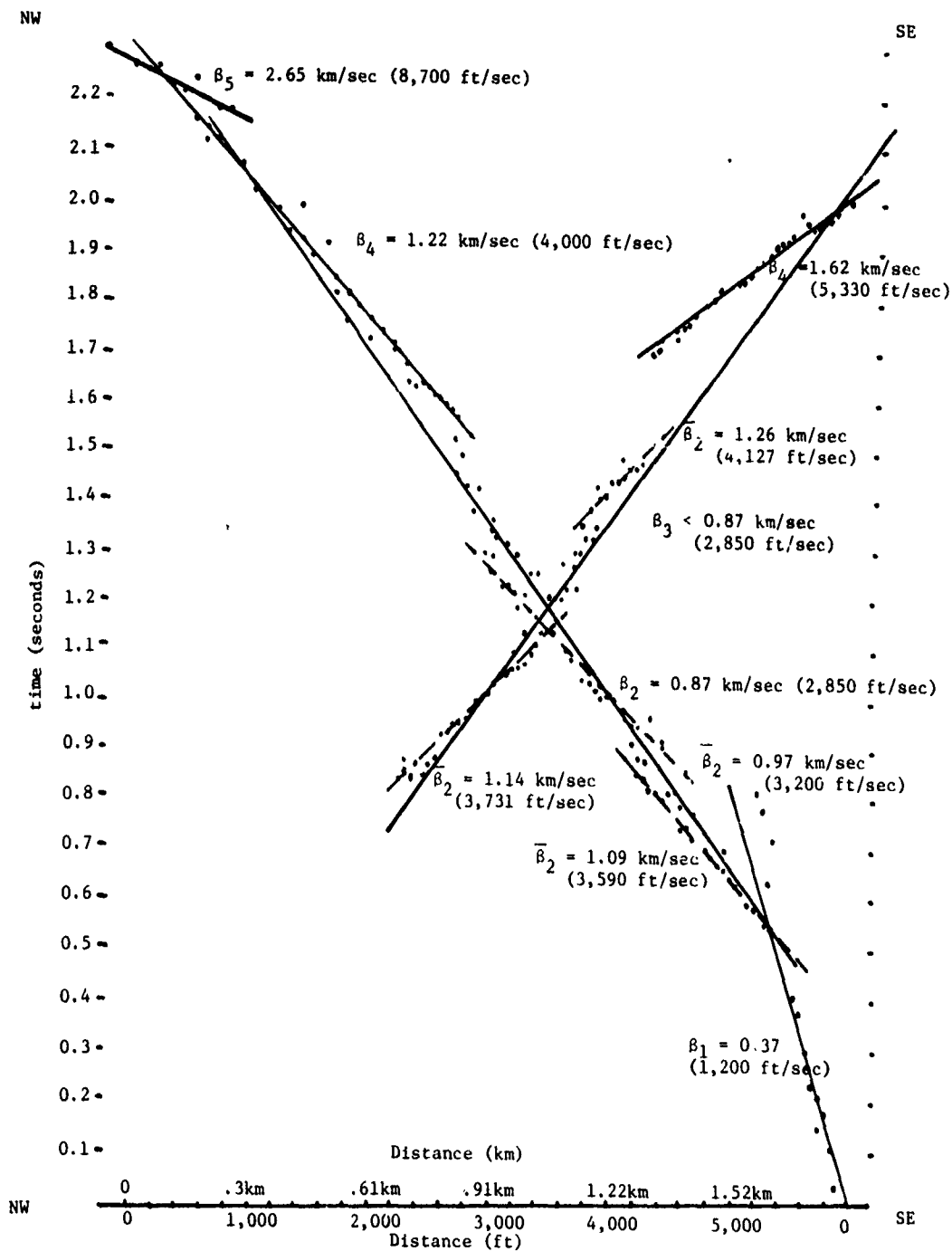


FIGURE 66. SH TRAVEL TIME CURVE FOR LONG REFRACTION PROFILE IN FIGURE 62. The solid lines are the analysis of Reinke (1977). The dashed lines are the travel time curves used in this report along with the agreed upon branches of  $\beta_1$ ,  $\beta_4$ , and  $\beta_5$ .

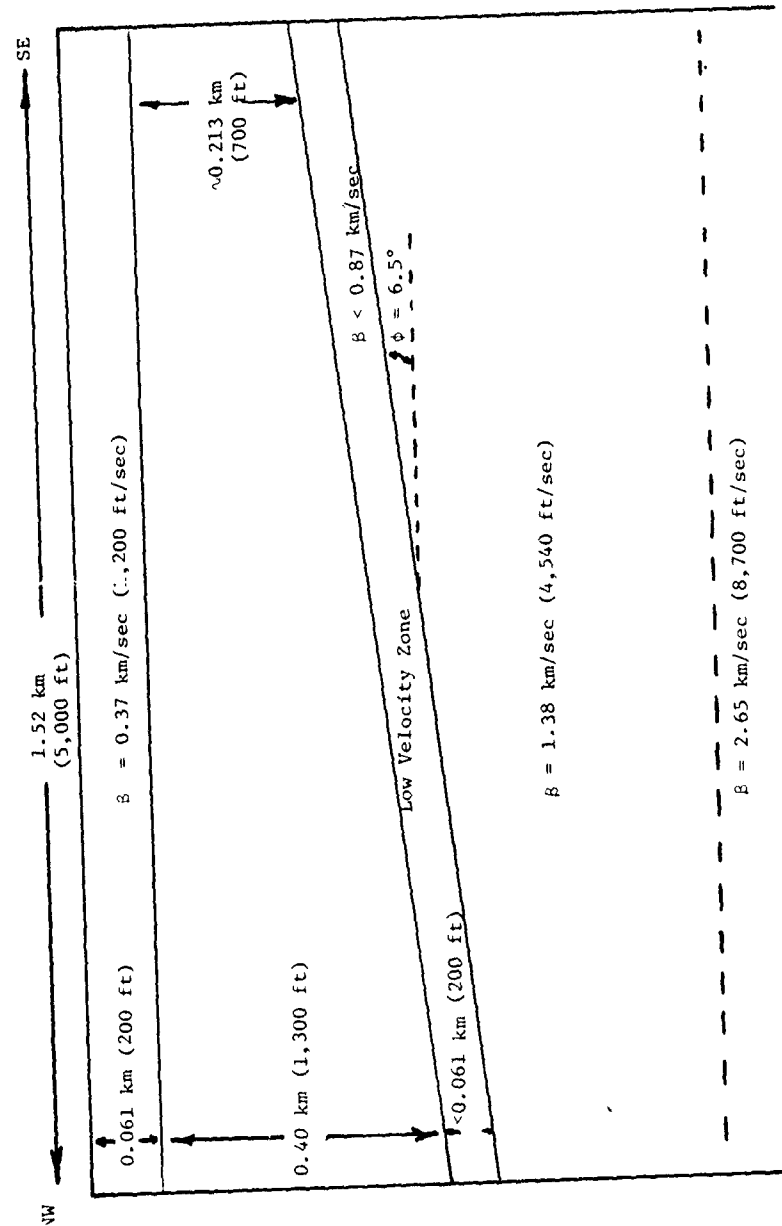


FIGURE 67. SH VELOCITY ( $\beta$ ) STRUCTURE NEAR QUEEN 15 AREA WHITE SANDS MISSILE RANGE (after Reinke, 1977). This structure was derived from a long double ended SH wave refraction profile.

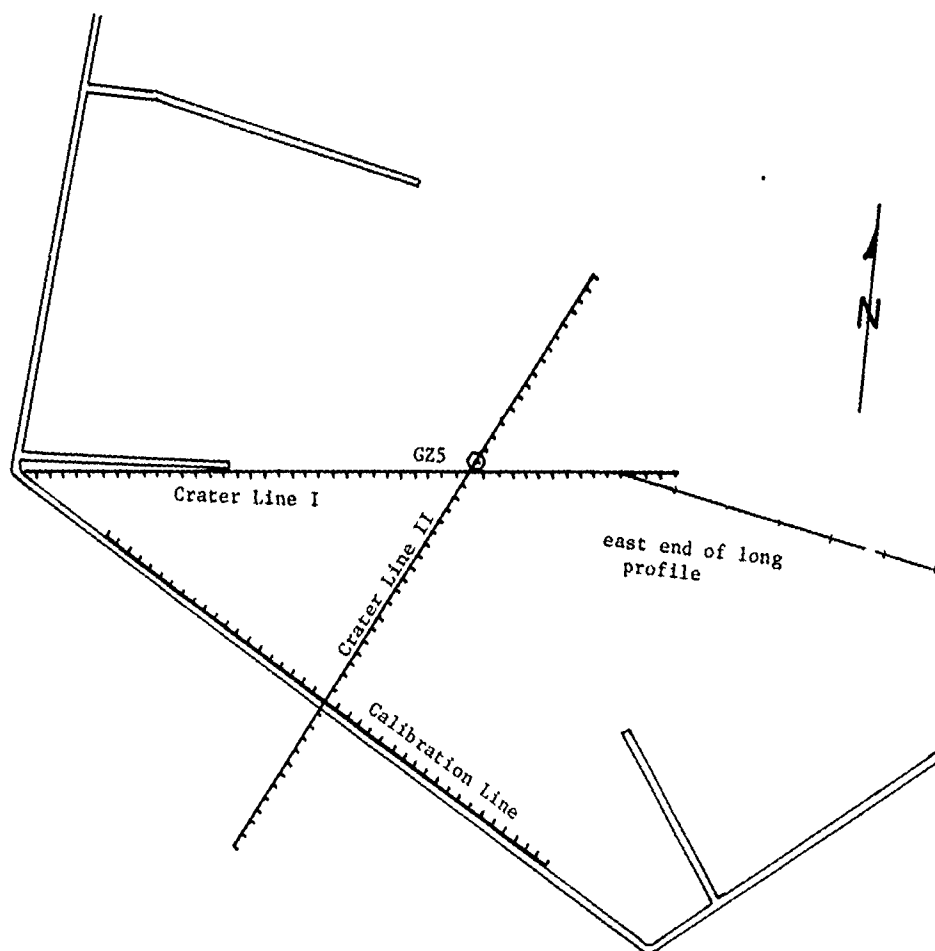


FIGURE 68.  
 POSITION OF SHORT P & SH REFRACTION  
 PROFILES AT GZ5 (QUEEN 15 AREA)  
 Shown in relation to the east end of  
 the long (6000 feet) SH refraction  
 profile

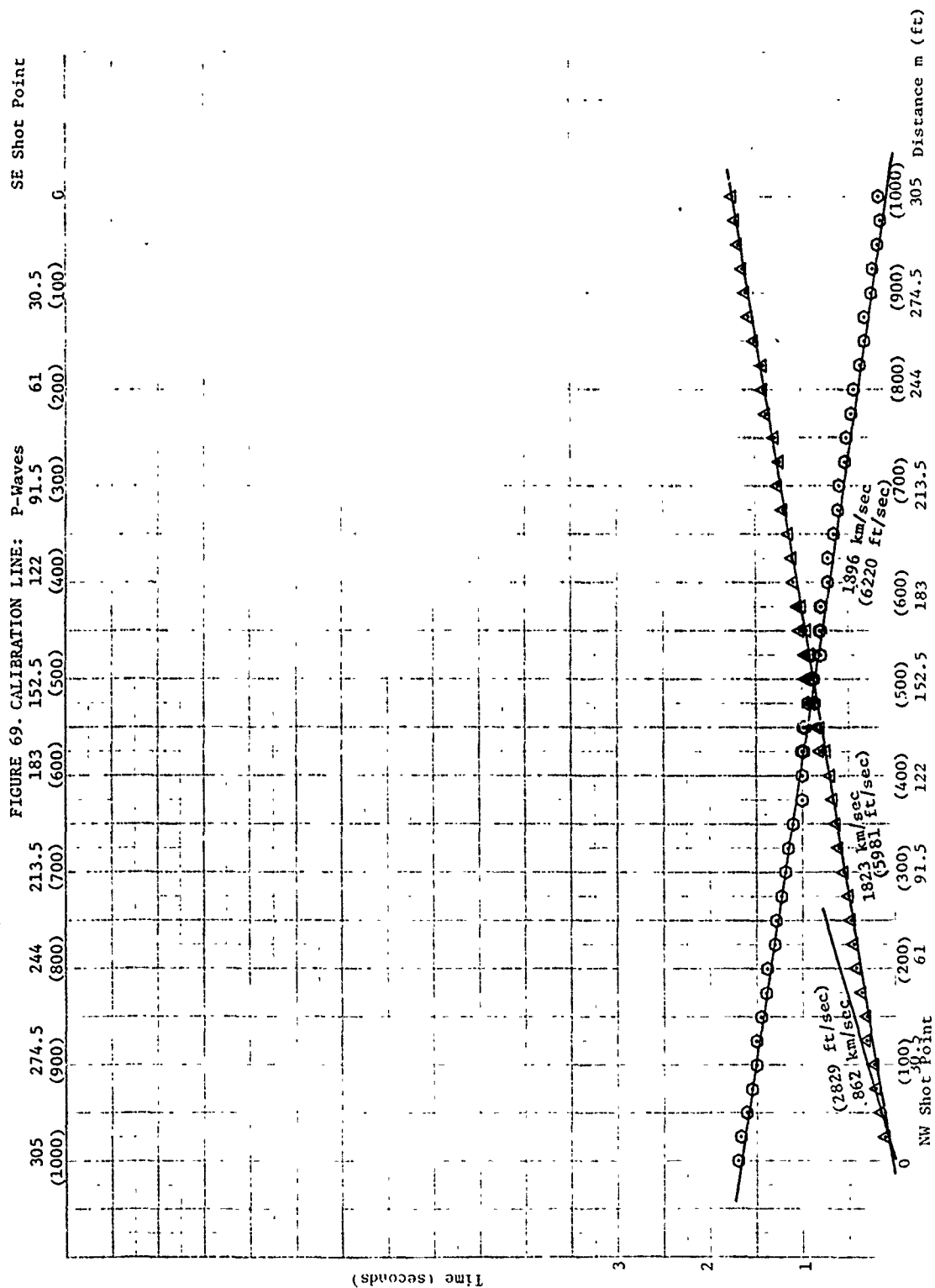
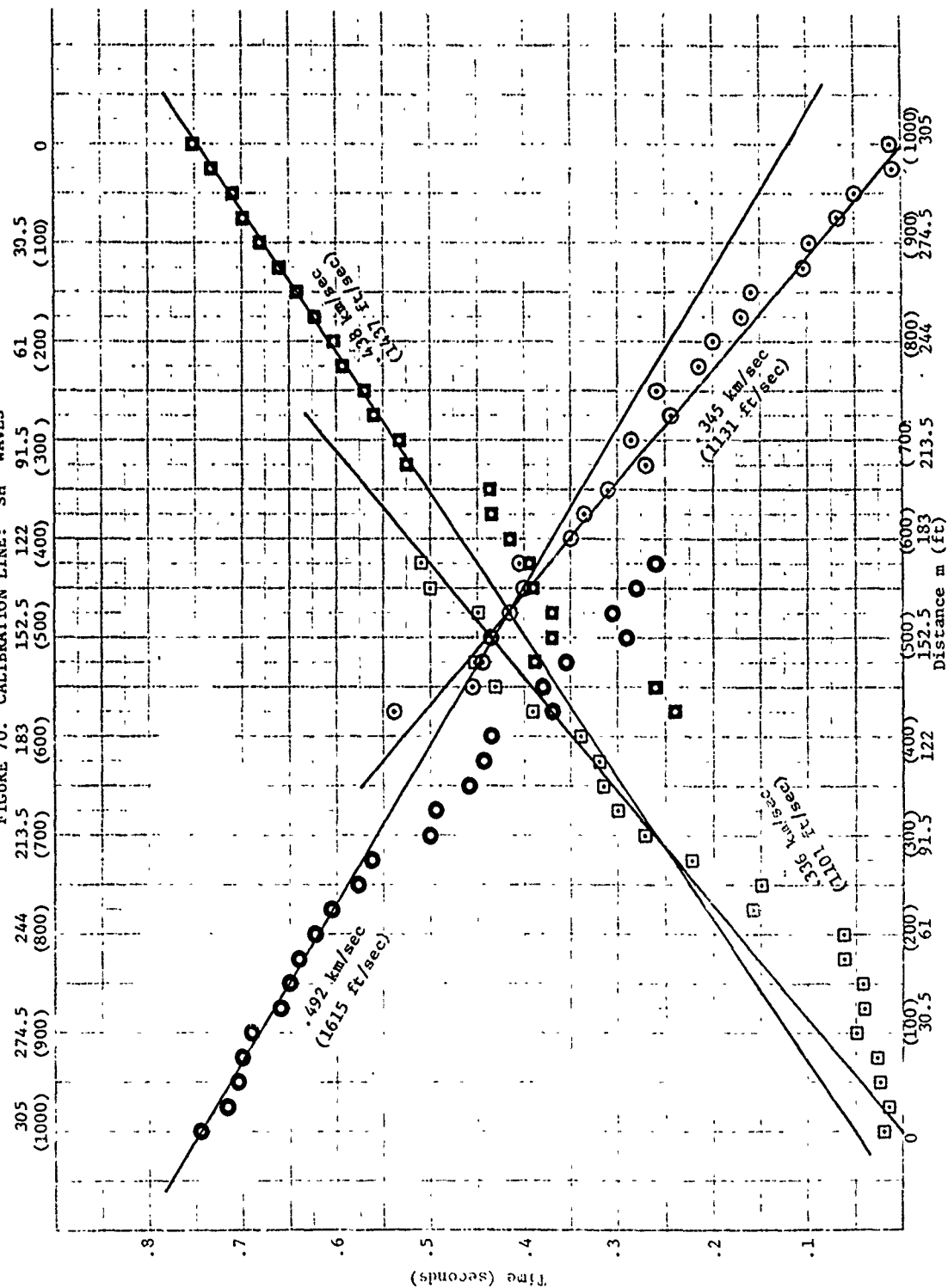


FIGURE 70. CALIBRATION LINE: SH WAVES



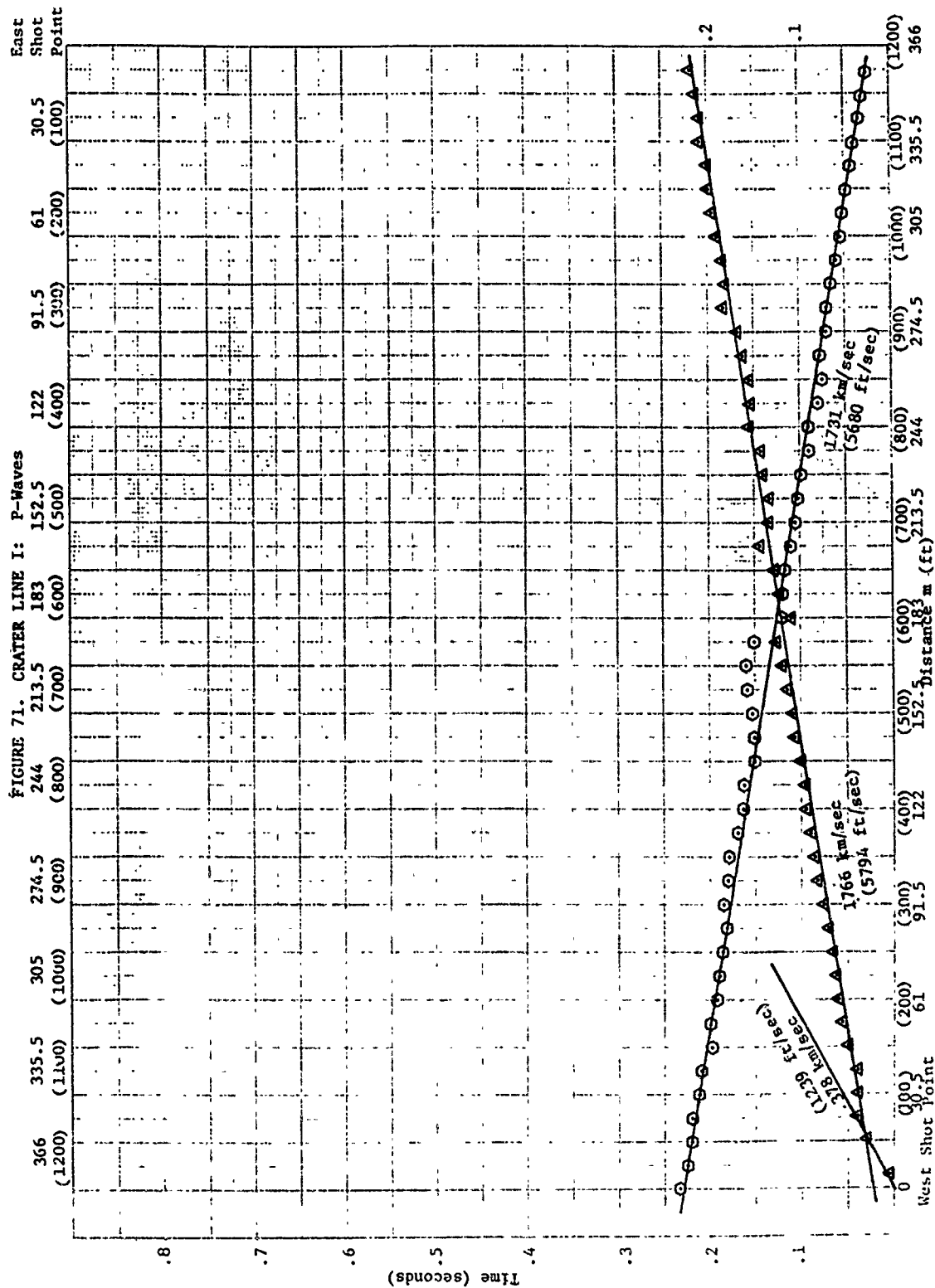


FIGURE 72. CRATER LINE I: SH-WAVES

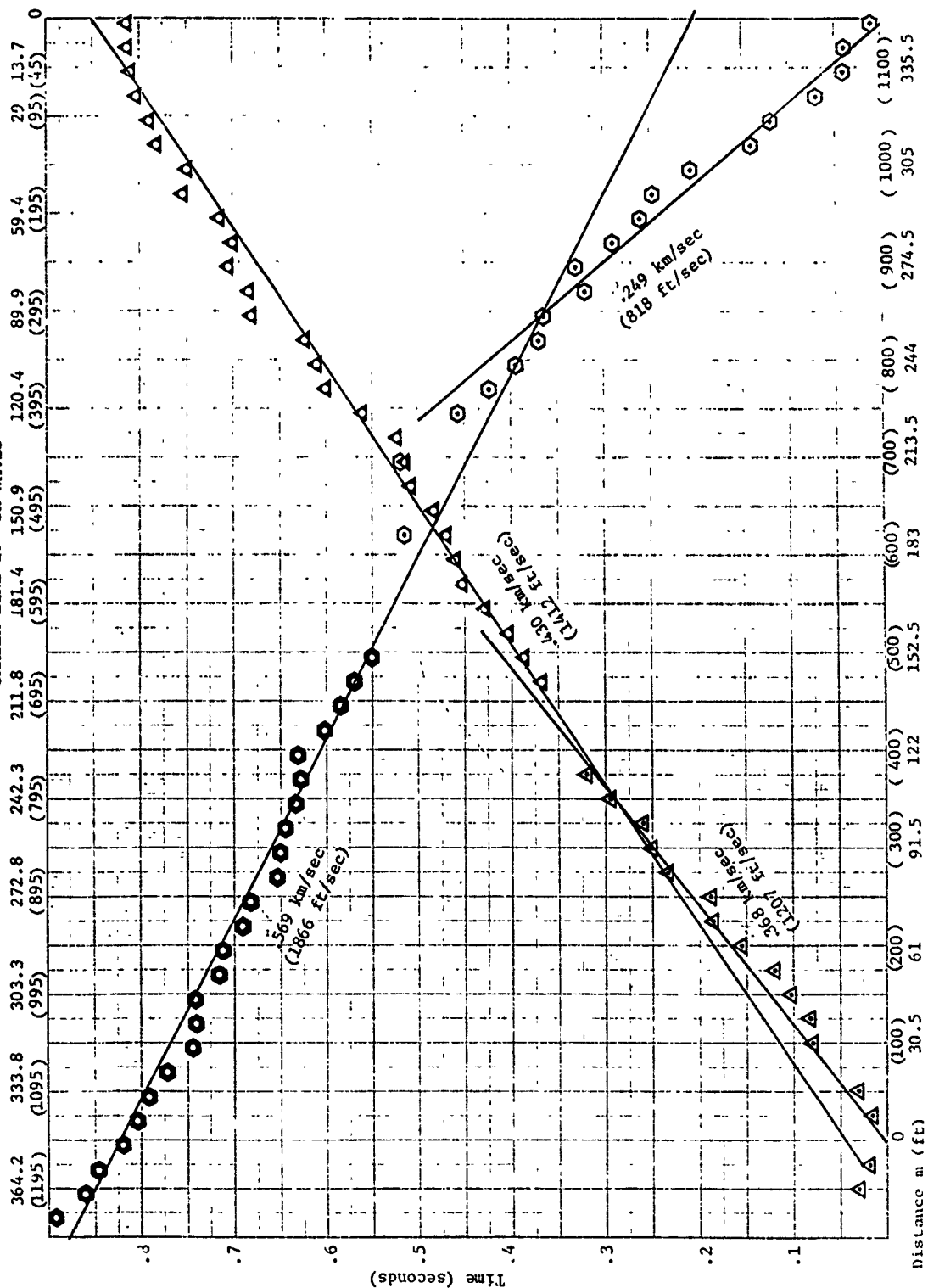
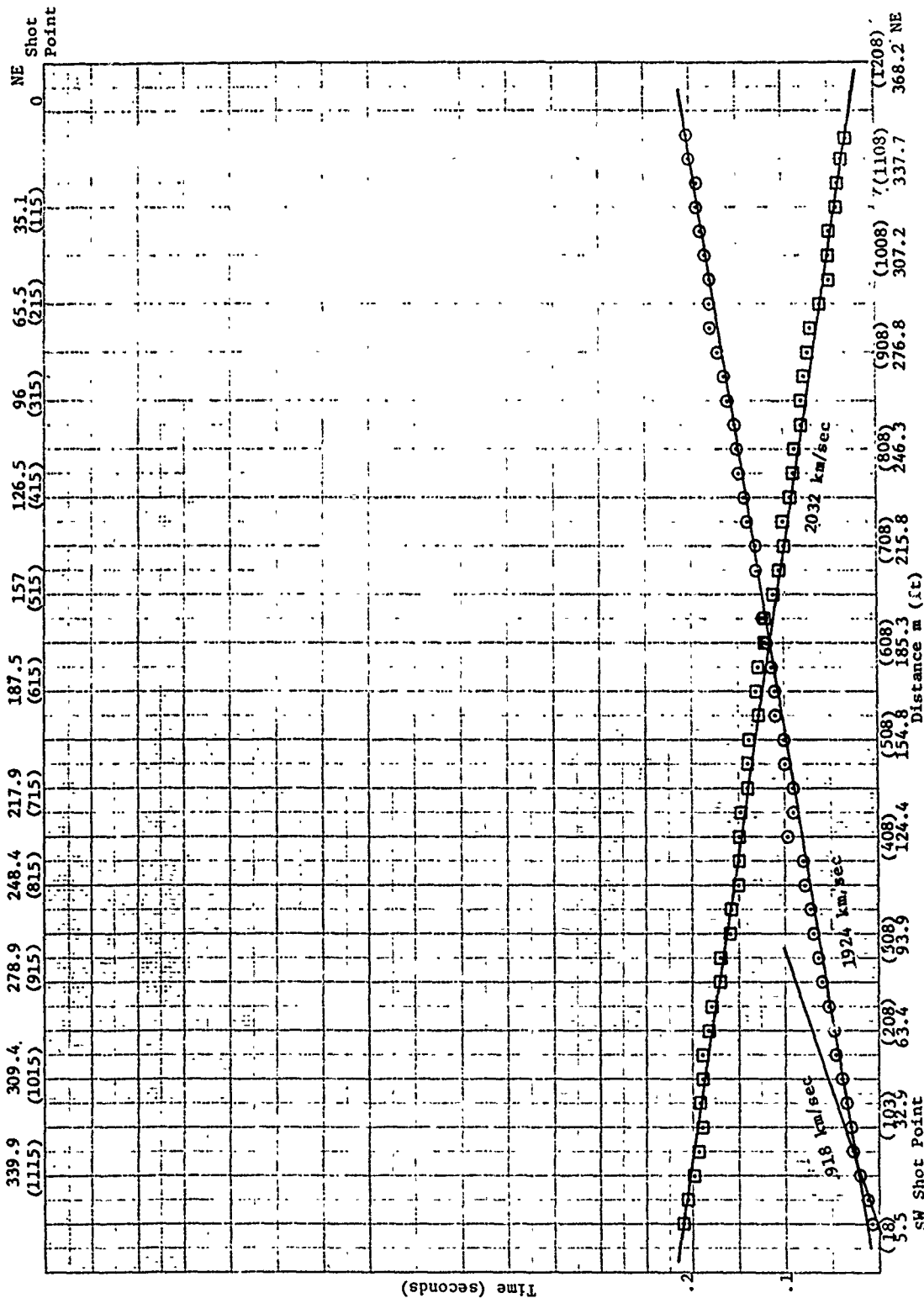
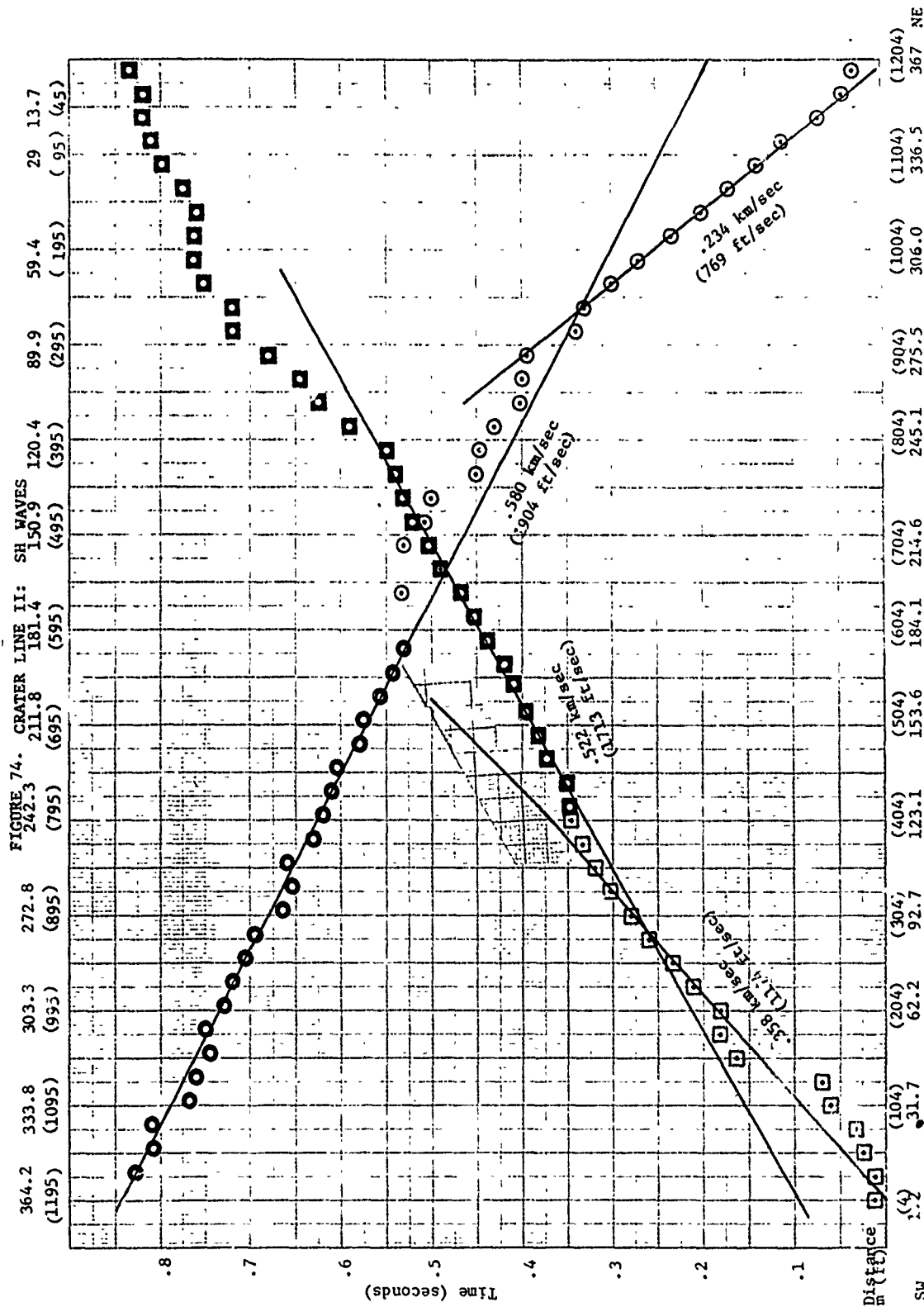




FIGURE 73. CRATER LINE II: P-WAVES





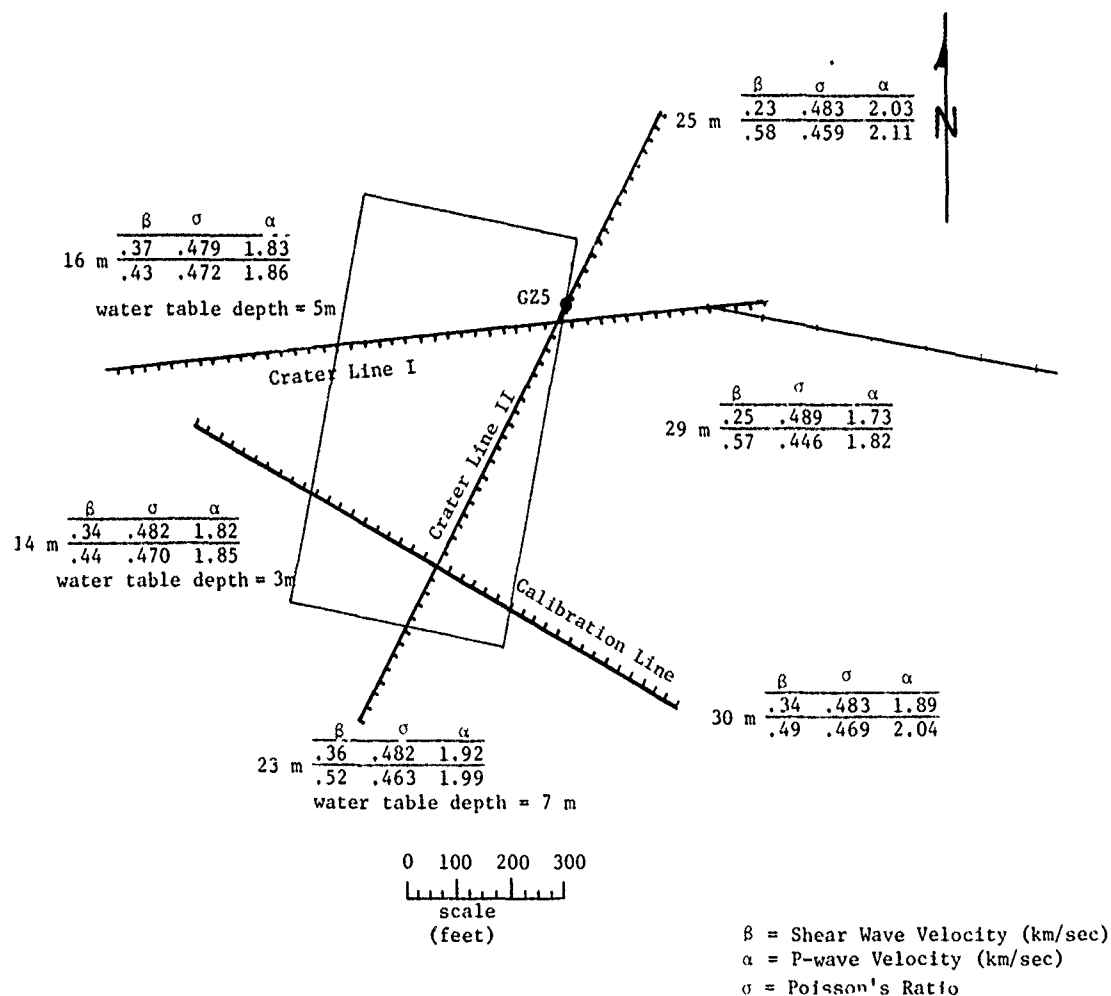


FIGURE 75. PLAN VIEW OF THREE SHORT P AND SH REFRACTION PROFILES NEAR GROUND ZERO AREA (GZ-5) OF PRE-DICE THROW I AREA. The P wave ( $\alpha$ ) and SH wave ( $\beta$ ) velocities are given for the travel time branches that emanate from the respective ends of each profile. The depth figure given beside these values is the depth to the next interface below the water table.

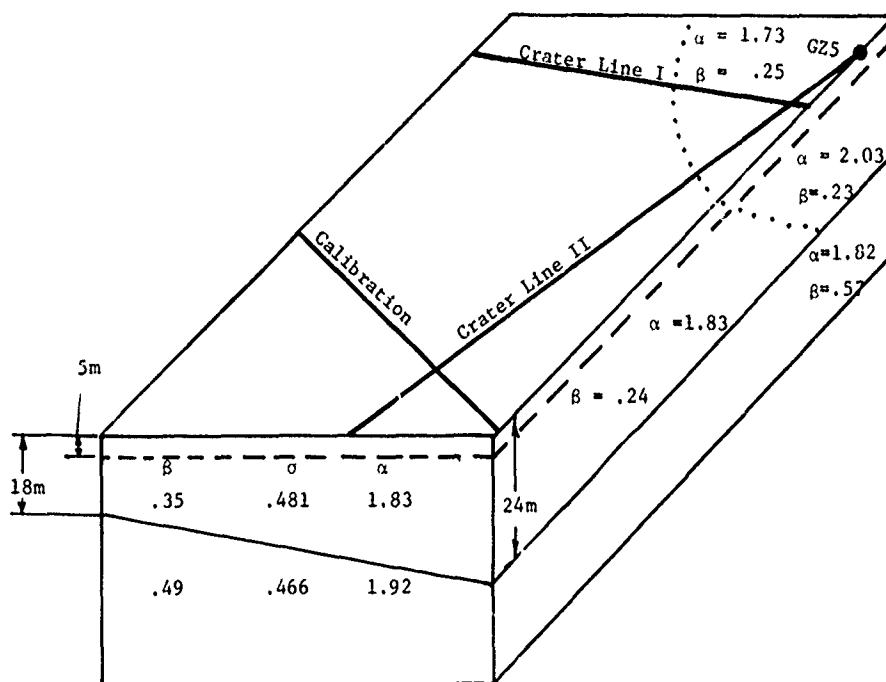


Figure 76. 3-D Model of Data Given in Figure 75.  
 ( $\beta$  and  $\alpha$  are S velocities and P velocities respectively  
 in km/sec)

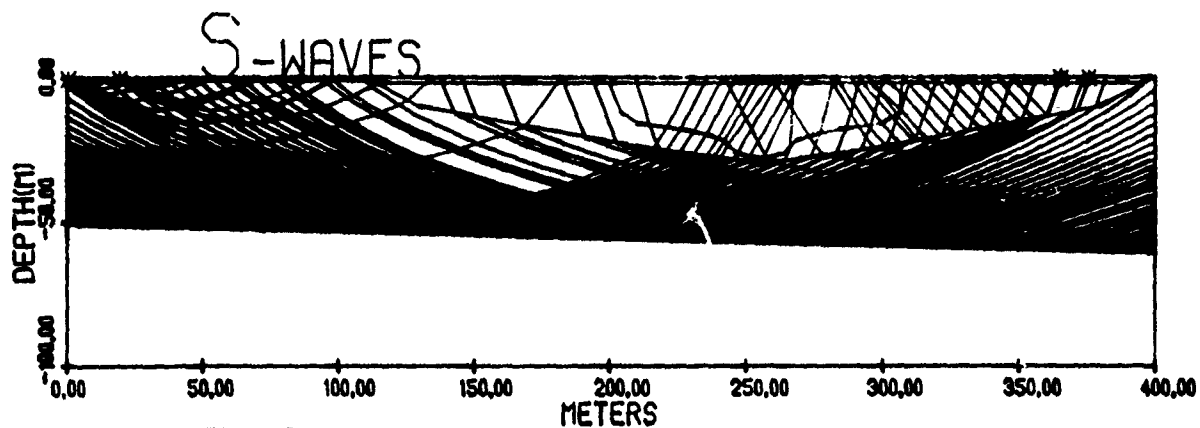
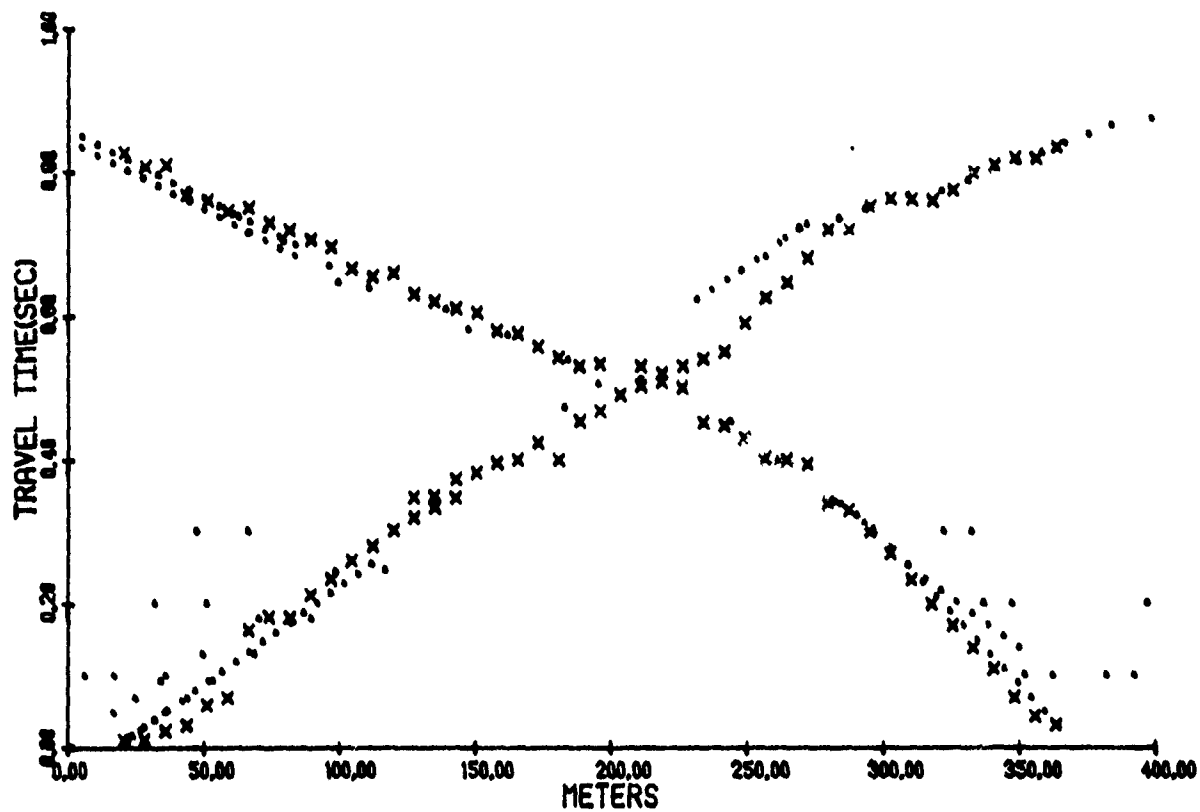


FIGURE 77. RAY TRACING ATTEMPT TO DETERMINE CRATER SIZE ON CRATER LINE II

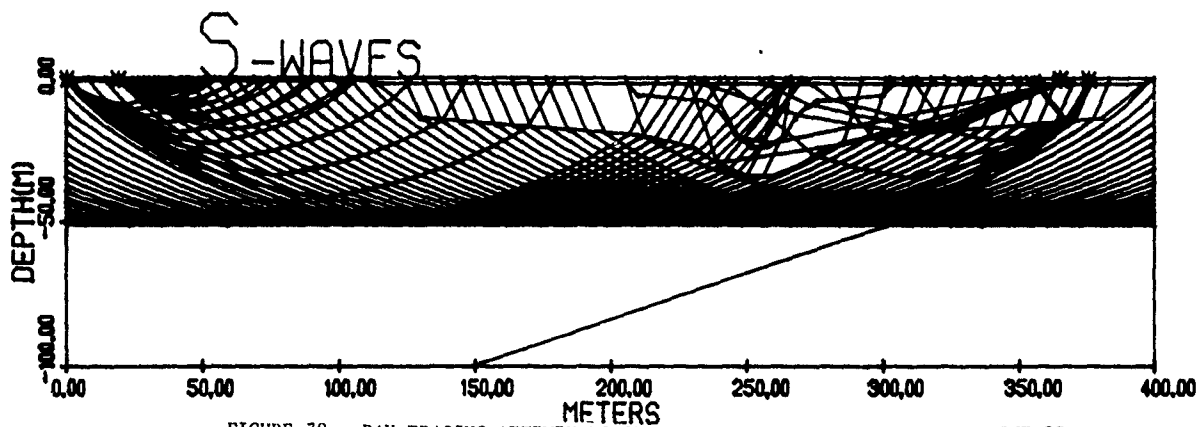
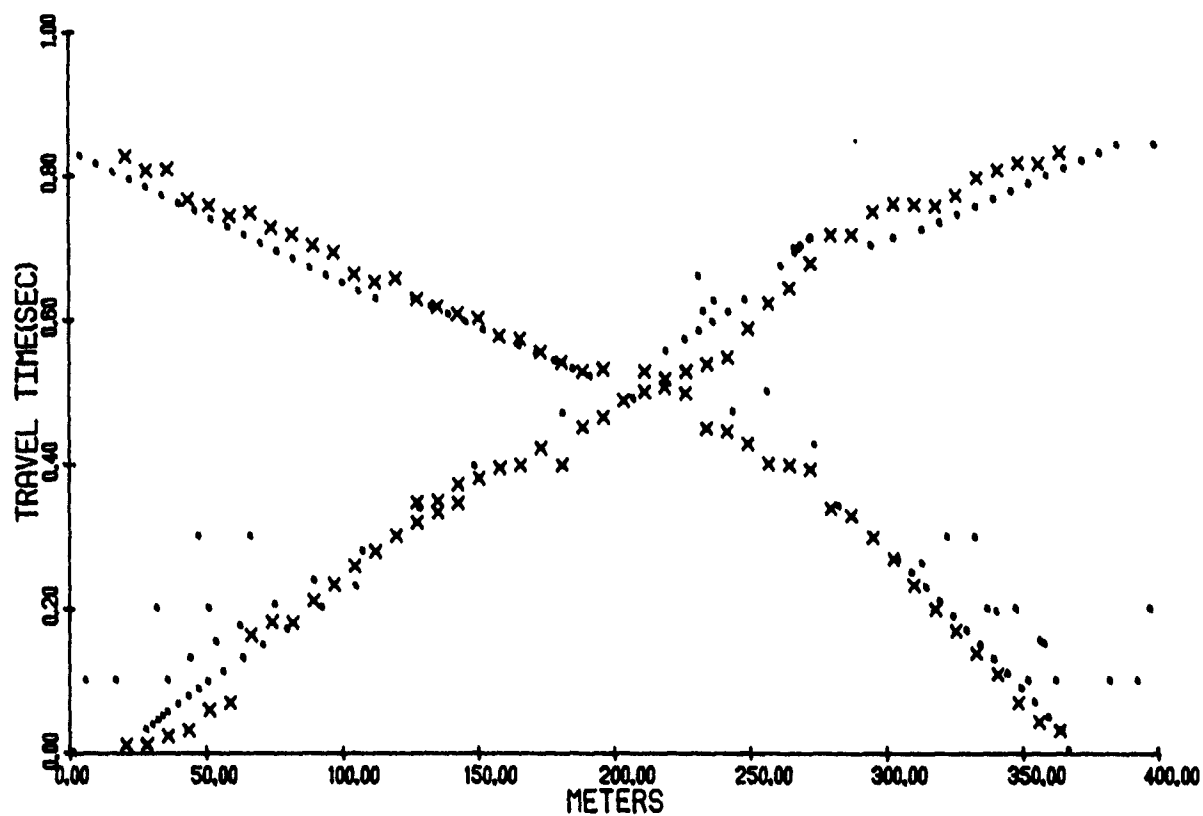


FIGURE 78. RAY TRACING ATTEMPT TO DETERMINE CRATER SIZE ON CRATER LINE II

## REFERENCES

- Herrin, E. and Reinke, R., 1976, personal communication.
- Jolly, R.N., 1956, Investigations of shear waves, *Geophysics*, Vol. 21, No. 4.
- O'Connell, R. and Budiansky, B. 1974. Seismic Velocities in Dry and Saturated Cracked Solids, *J.R.R.*, Vol. 79, No. 35.
- Reinke, R. 1976. unpublished Ph.D. Thesis, Southern Methodist University.
- Rodean, H. 1971. Nuclear Explosion Seismology, U.S. Atomic Energy Commission.
- Toksoz, M.N., Cheng, C.H. and Timur, A. 1976. Velocities of Seismic Waves in Porous Rocks, *Geophysics*, Vol. 41
- Turpening, R.M. 1976. Seismic Recording of the Dice Throw Events, Final Report, Environmental Research Institute of Michigan, Report No. 117200-1-F, AFOSR Contract F44620-76-C-0019.
- Zbur, R. 1975, personal communication.

### For General Reference

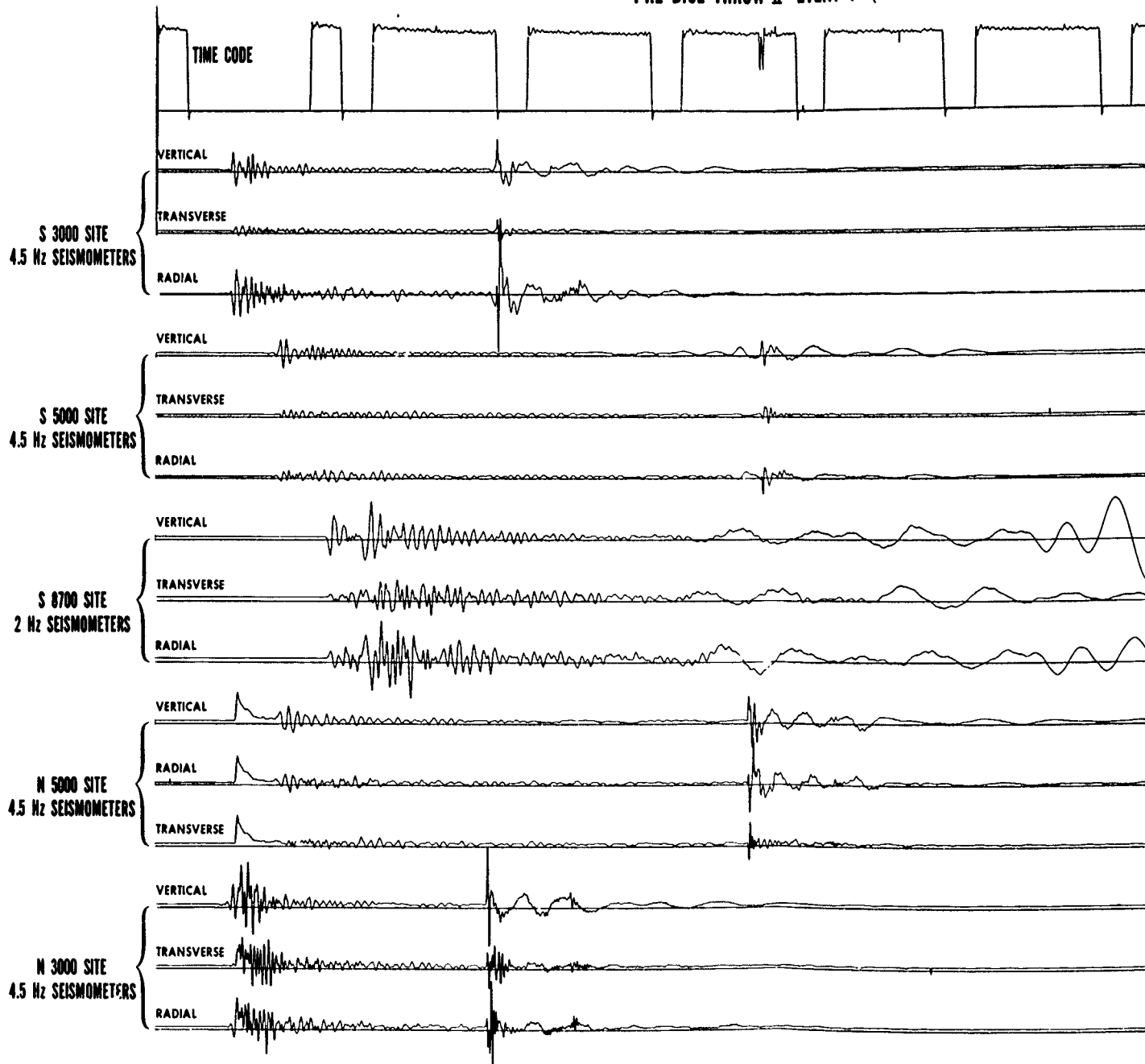
- Edwards, T.Y., G.L.E. Perry, 1976, Middle North, Series - Pre-Dice Throw II Events - Preliminary Results Report, Defense Nuclear Agency, POR 6904, September 1976.

APPENDIX

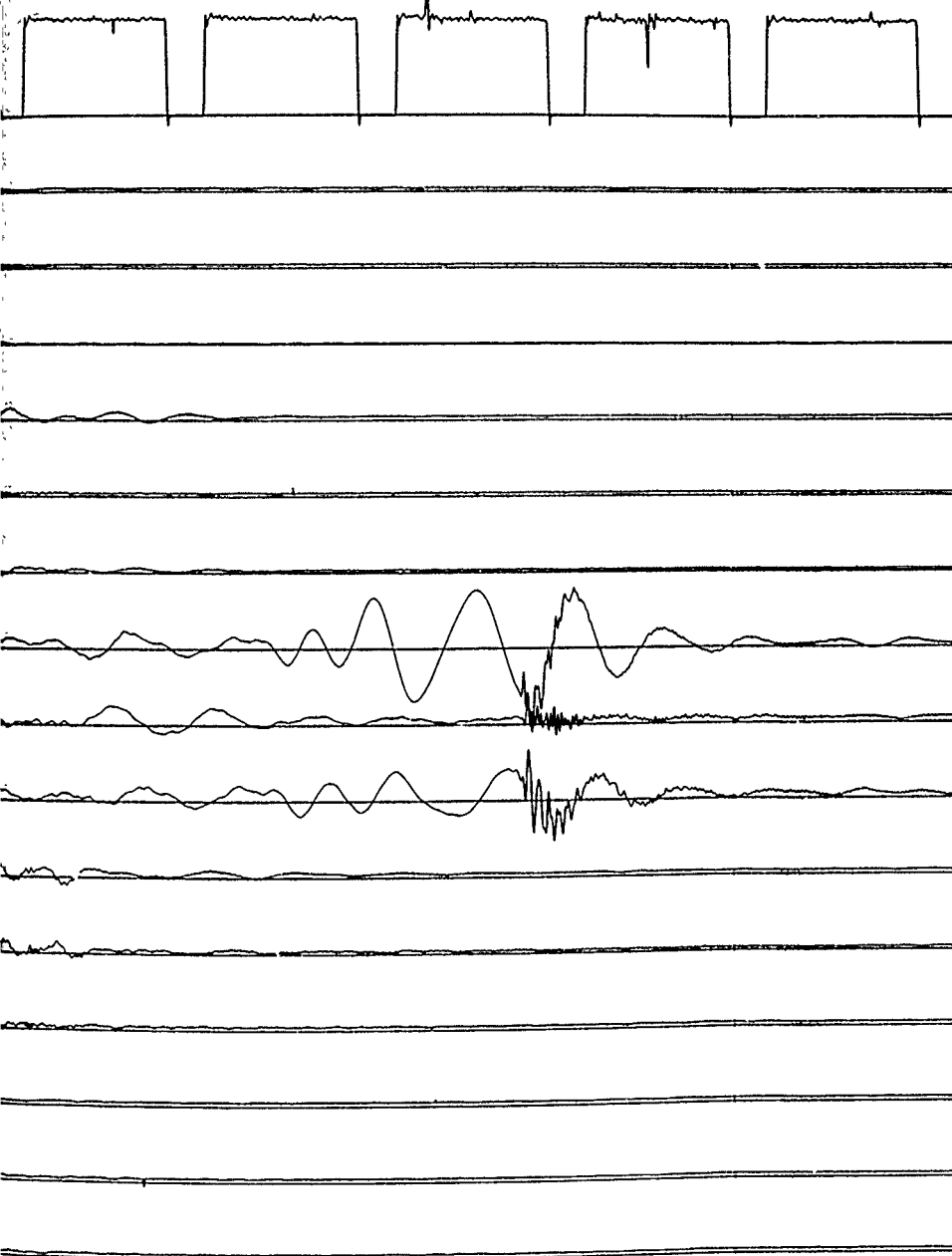
SEISMOGRAMS FROM THE PRE-DICE THROW II-1  
(TNT SHOT), PRE-DICE THROW II-2 (AN/FO SHOT)  
AND DICE THROW EVENTS



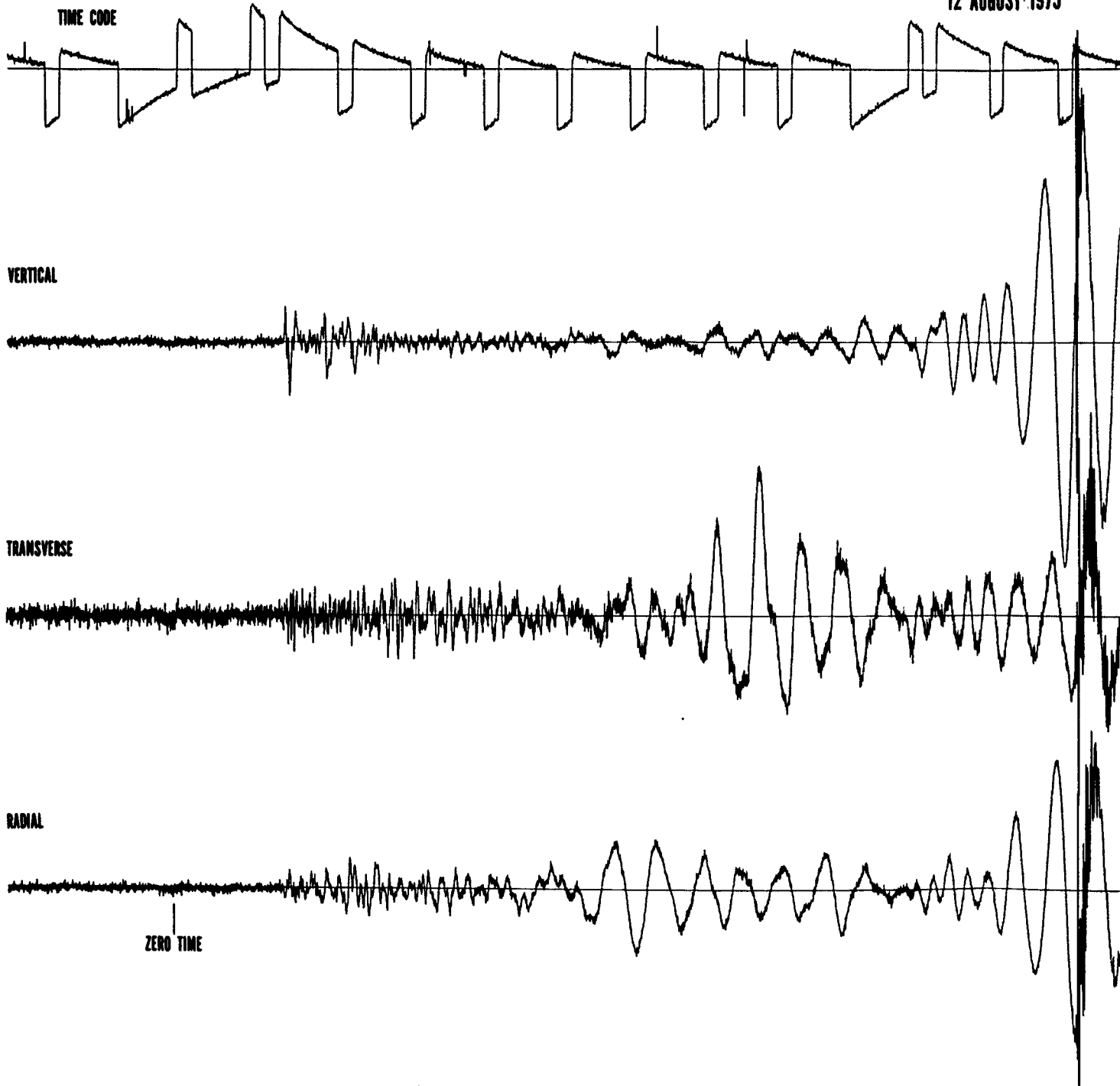
PRE DICE THROW II EVENT 1 (TNT EVENT) 12 AUGUST 1975



VENT 1 (TNT EVENT) 12 AUGUST 1975

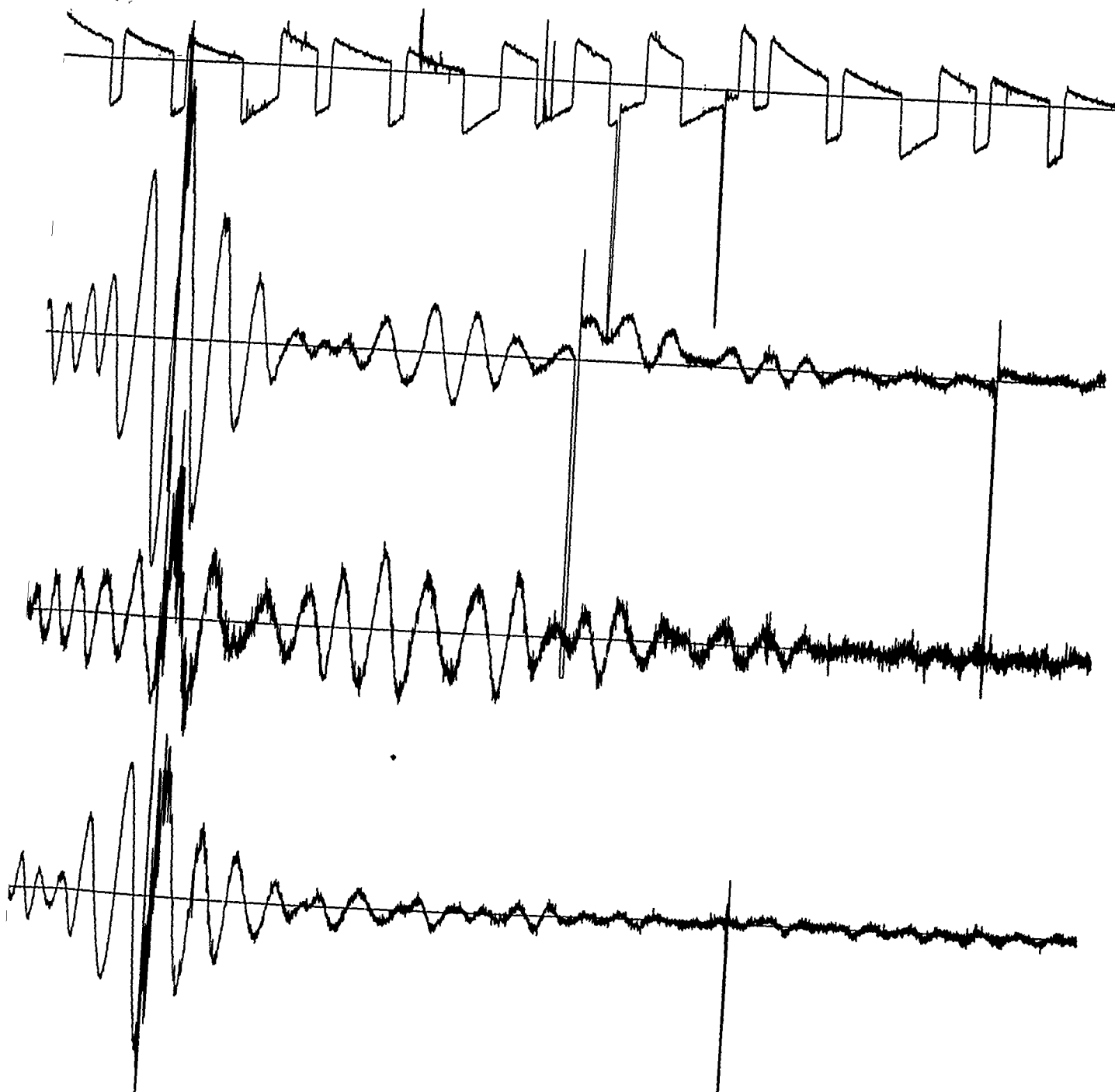


PRE DICE THROW II EVENT 1 (TNT E)  
2 Hz SEISMOMETERS  
N 15,000 SITE  
12 AUGUST 1975



/

ROW II EVENT 1 (TNT EVENT)  
Hz SEISMOMETERS  
N 15,000 SITE  
12 AUGUST 1975



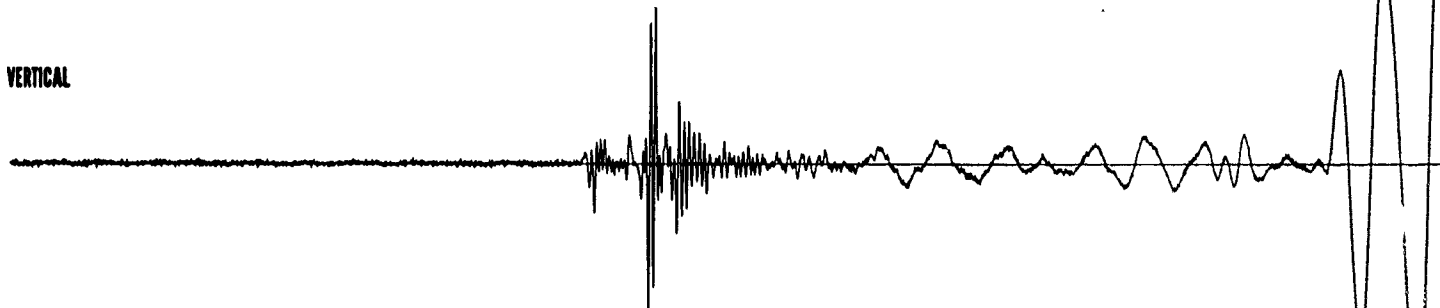
2

PRE DICE THROW II EVENT 1 (TNT)  
2 Hz SEISMOMETERS  
S 15,000 SITE  
12 AUGUST 1975

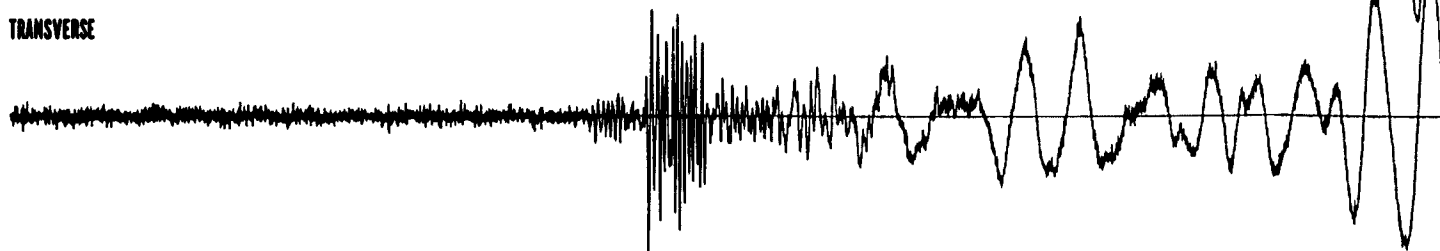
TIME CODE



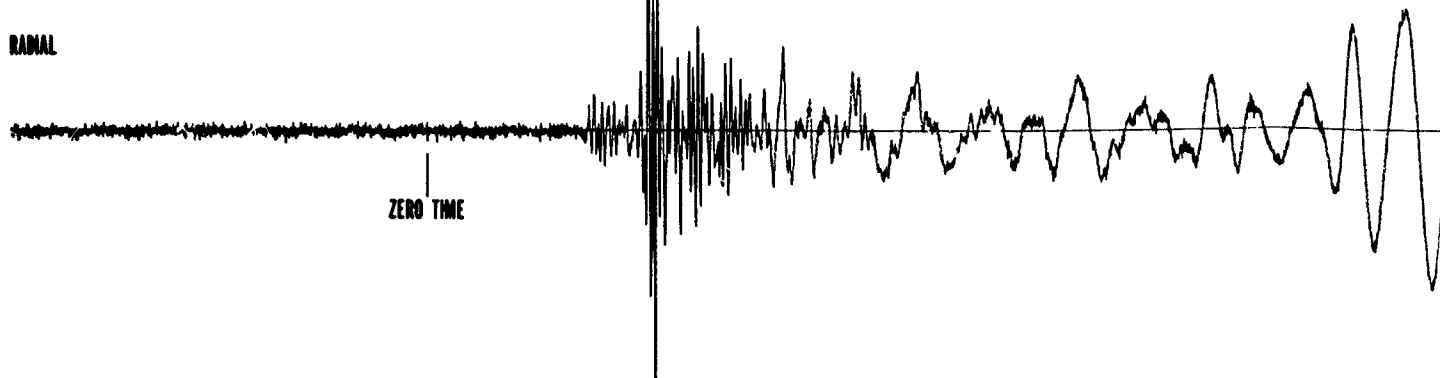
VERTICAL



TRANSVERSE

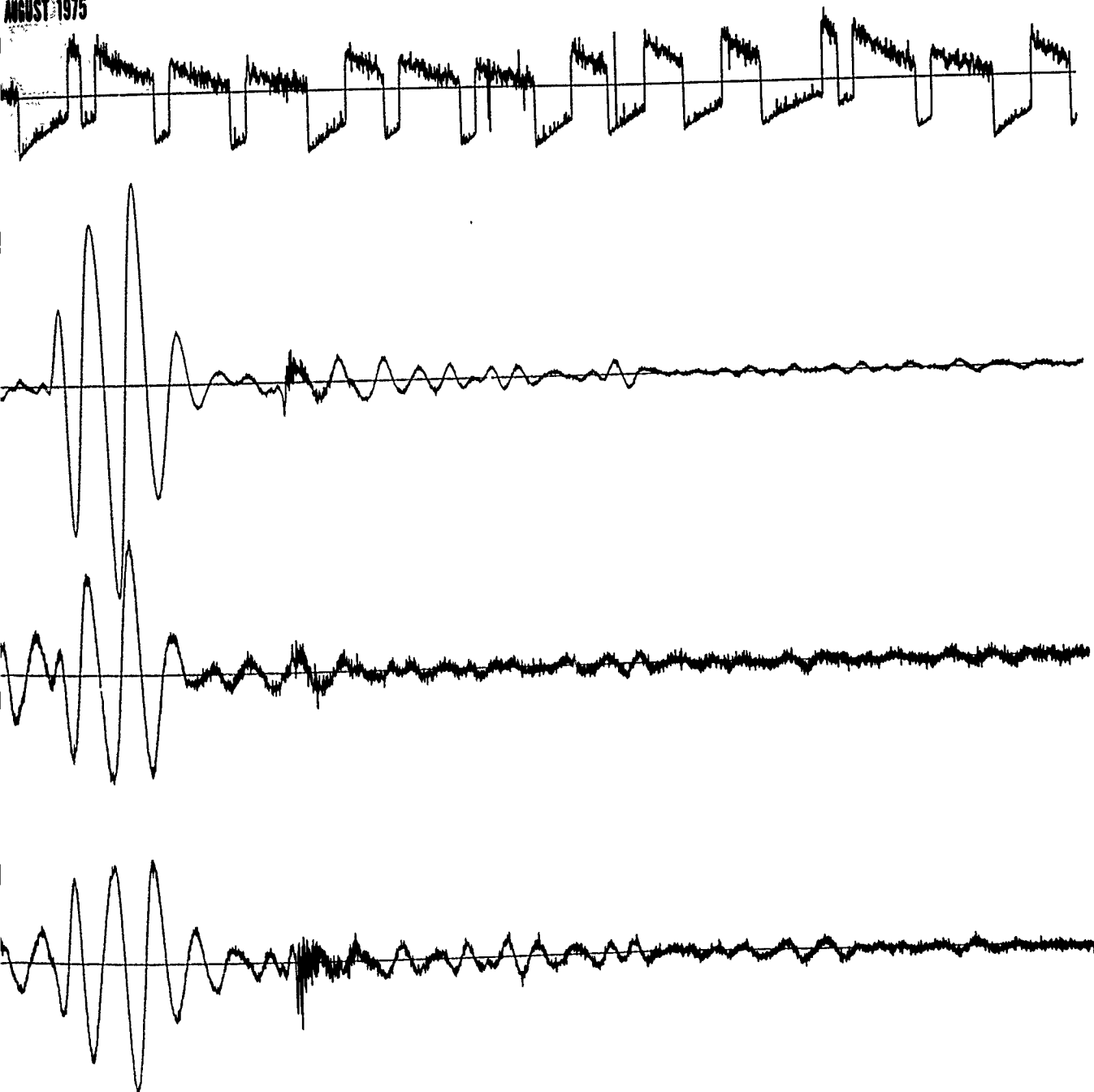


RADIAL



ZERO TIME

EVENT 1 (TNT EVENT)  
SEISMOMETERS  
15,000 SITE  
AUGUST 1975

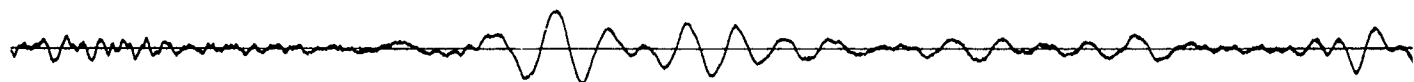


PRE DICE THROW II EVENT 1 (T  
2 Hz SEISMOMETERS  
N 25,000 SITE  
12 AUGUST 1975

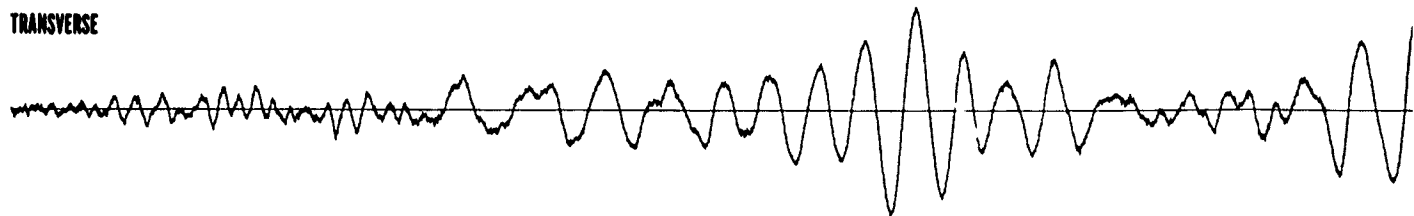
TIME CODE



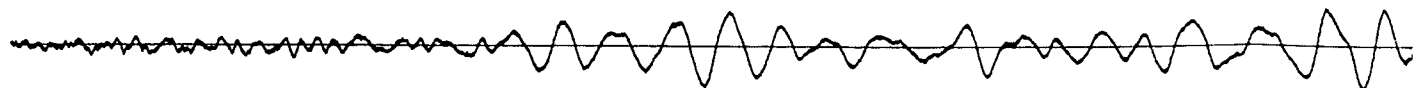
VERTICAL



TRANSVERSE



RADIAL

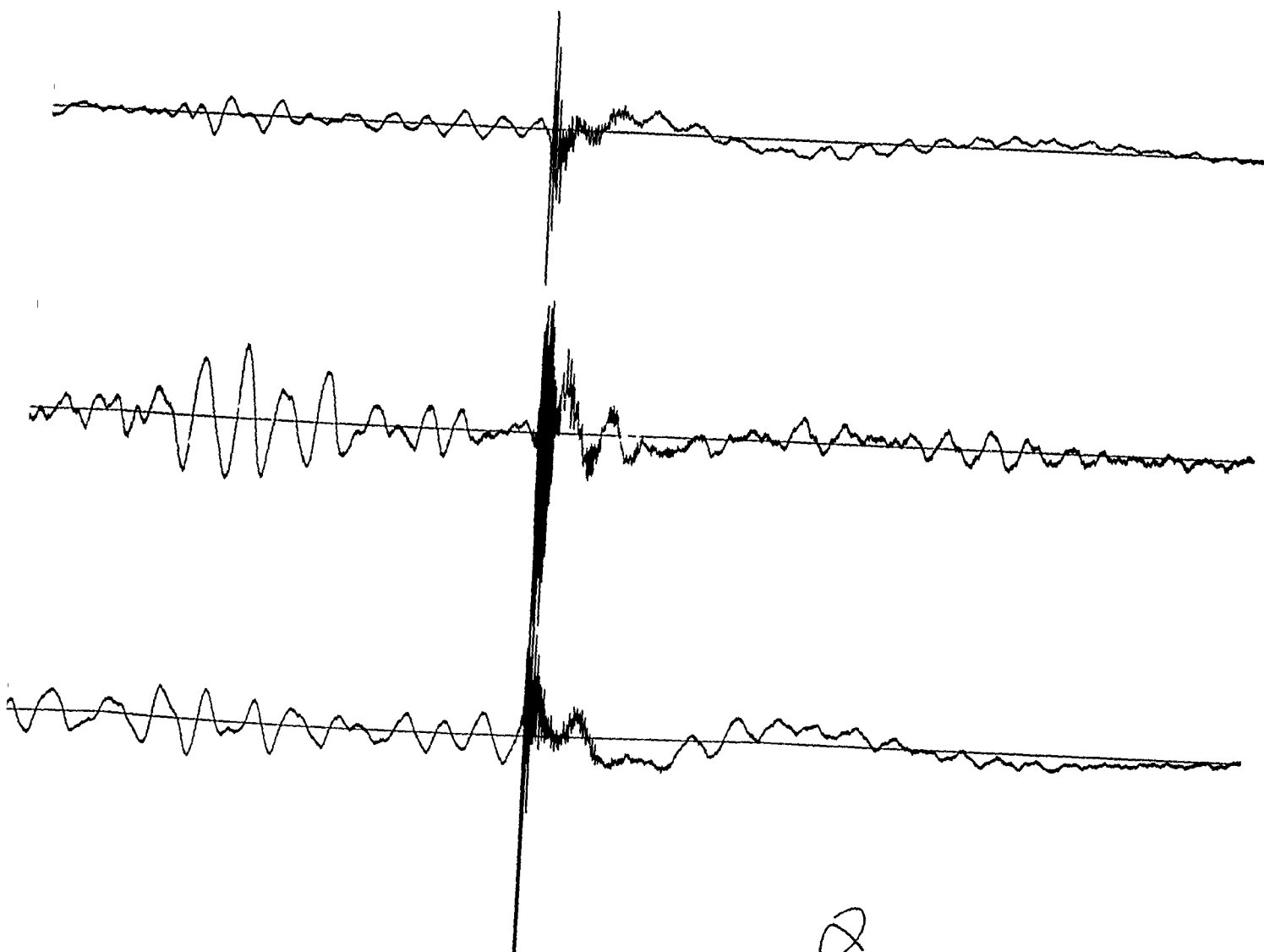
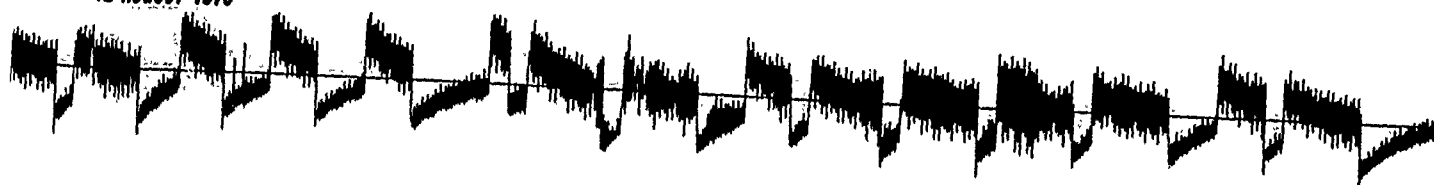


ICE THROW II EVENT 1 (TNT EVENT)

2 Hz SEISMOMETERS

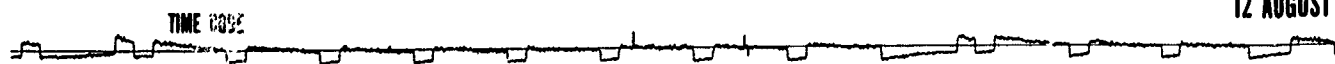
N 25,000 SITE

12 AUGUST 1975

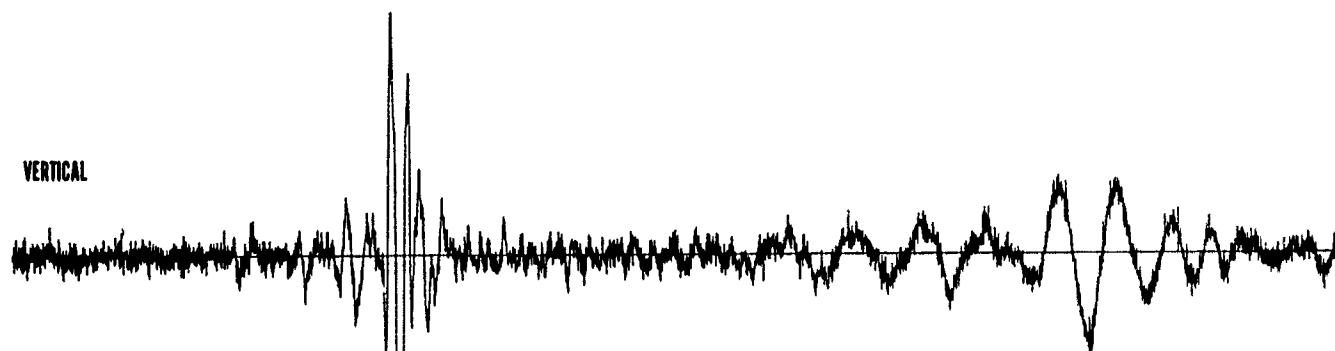




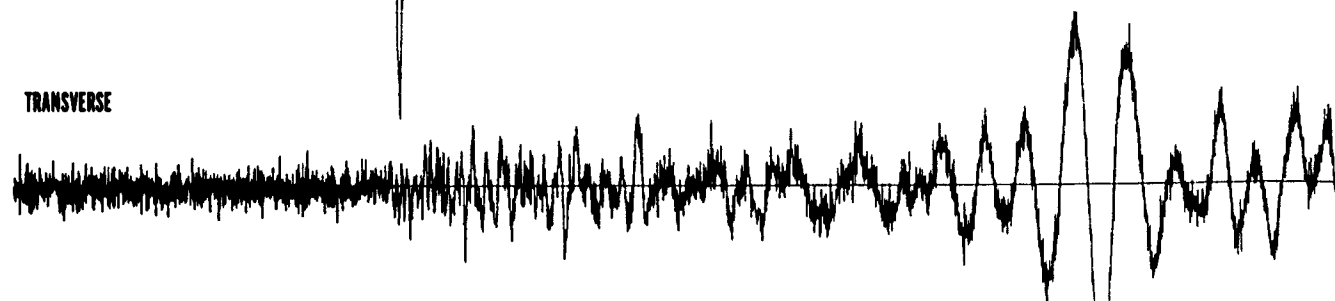
PRE DICE THROW II EVE  
2 Hz SEISMOI  
S 25,000  
12 AUGUST



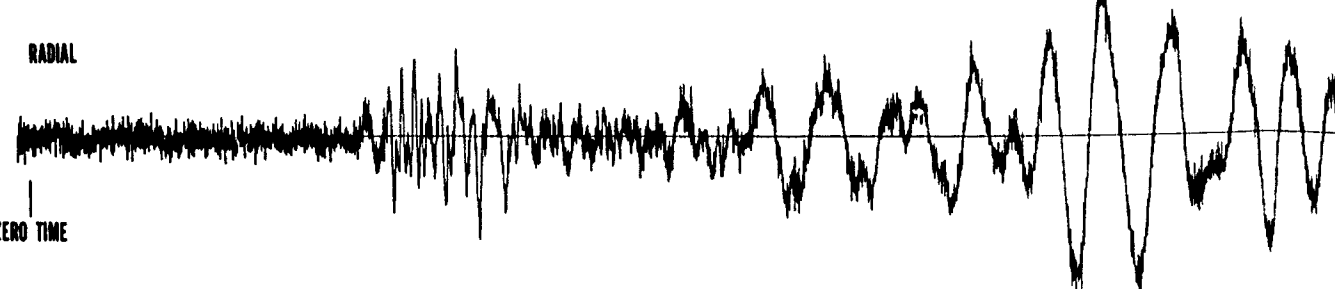
VERTICAL



TRANSVERSE



RADIAL



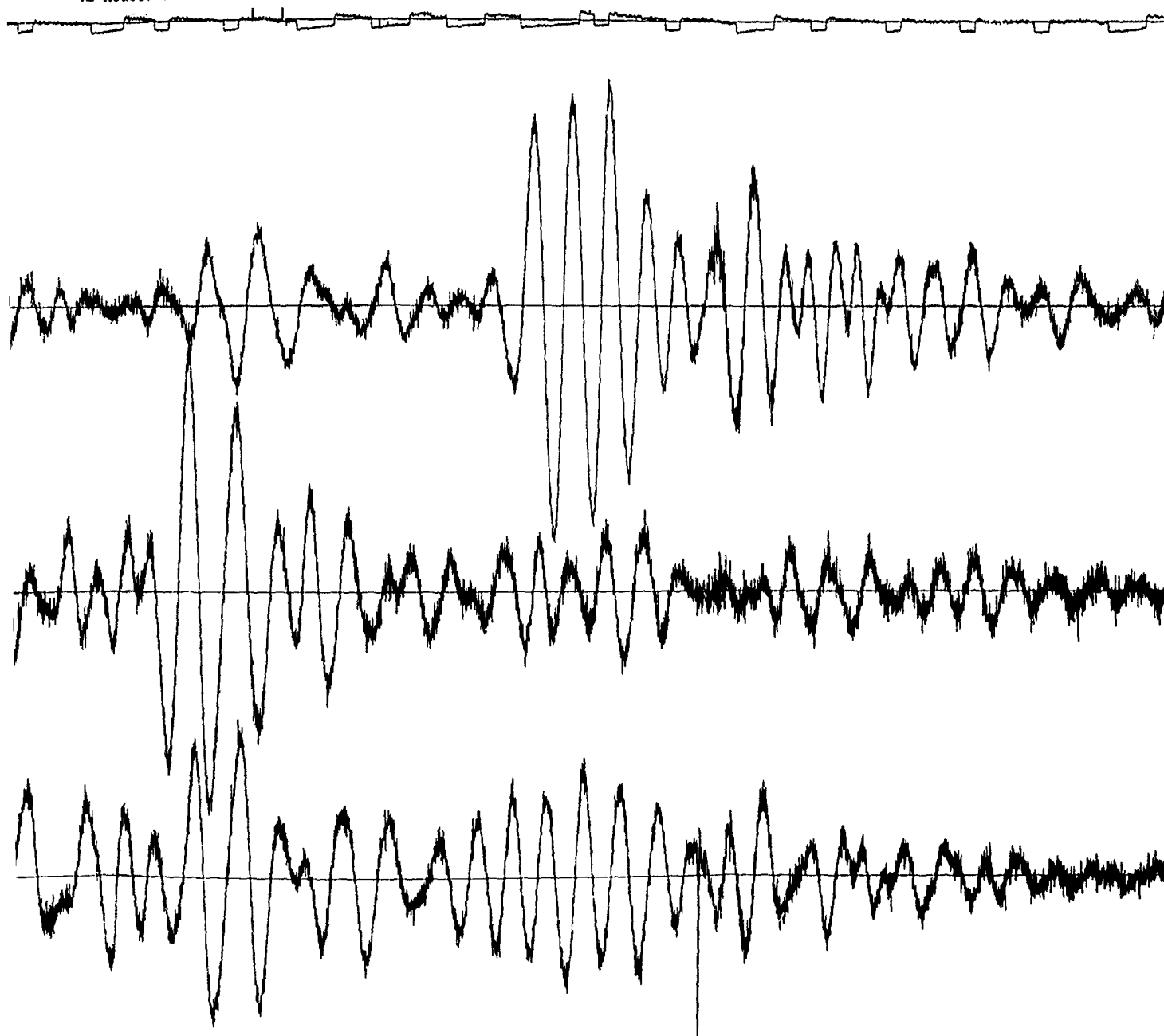
ZERO TIME

DICE THROW II EVENT 1 (TNT EVENT)

2 Hz SEISMOMETERS

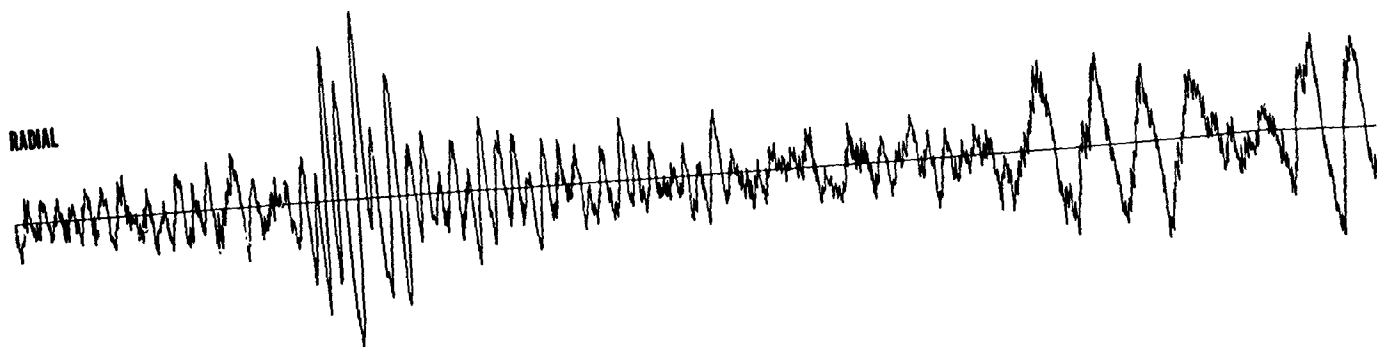
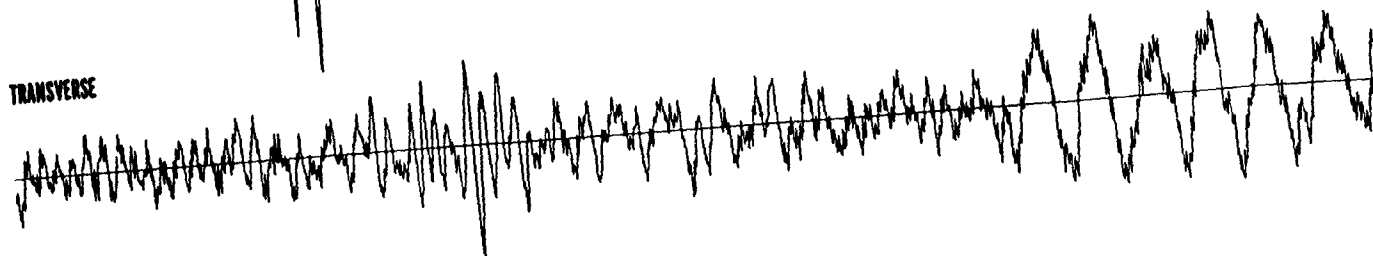
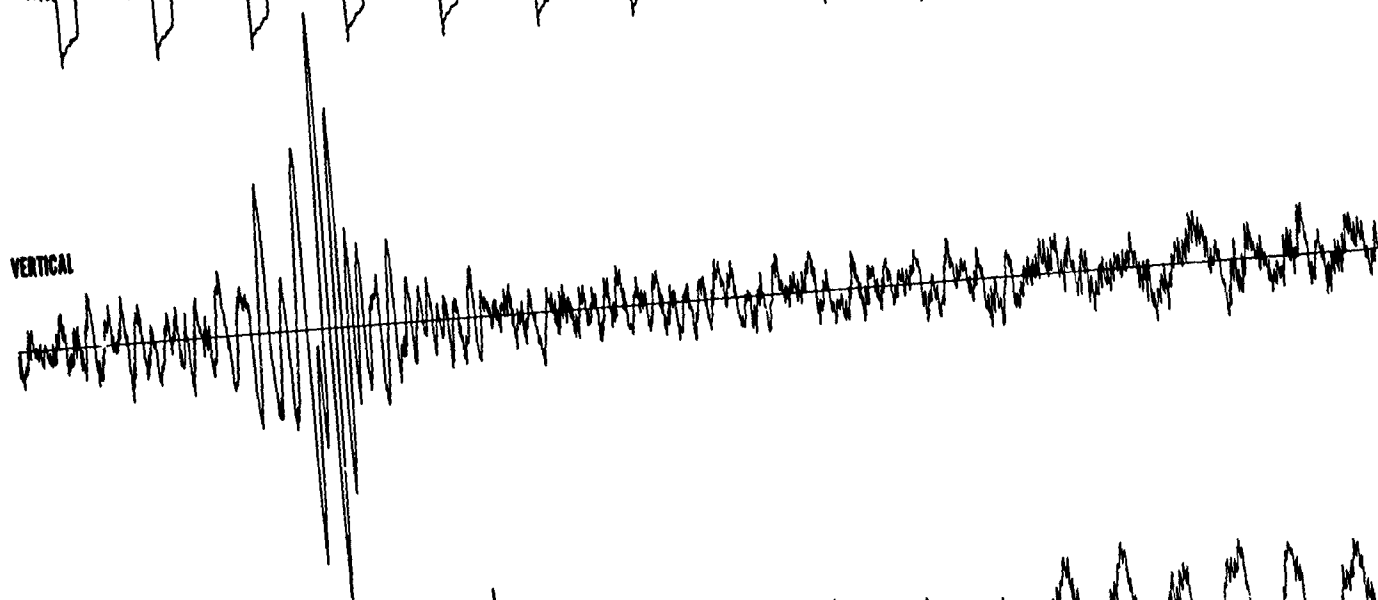
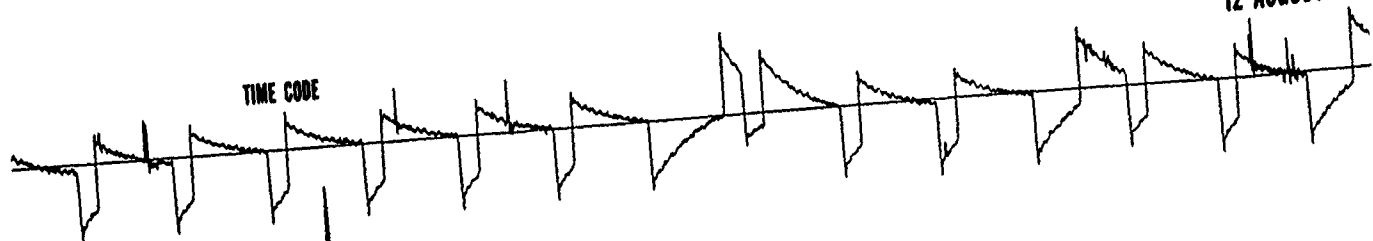
S 25,000 SITE

12 AUGUST 1975



2

PRE DICE THROW II EVENT 1  
2 Hz SEISMOMETER  
S 35,000 SITE  
12 AUGUST 197

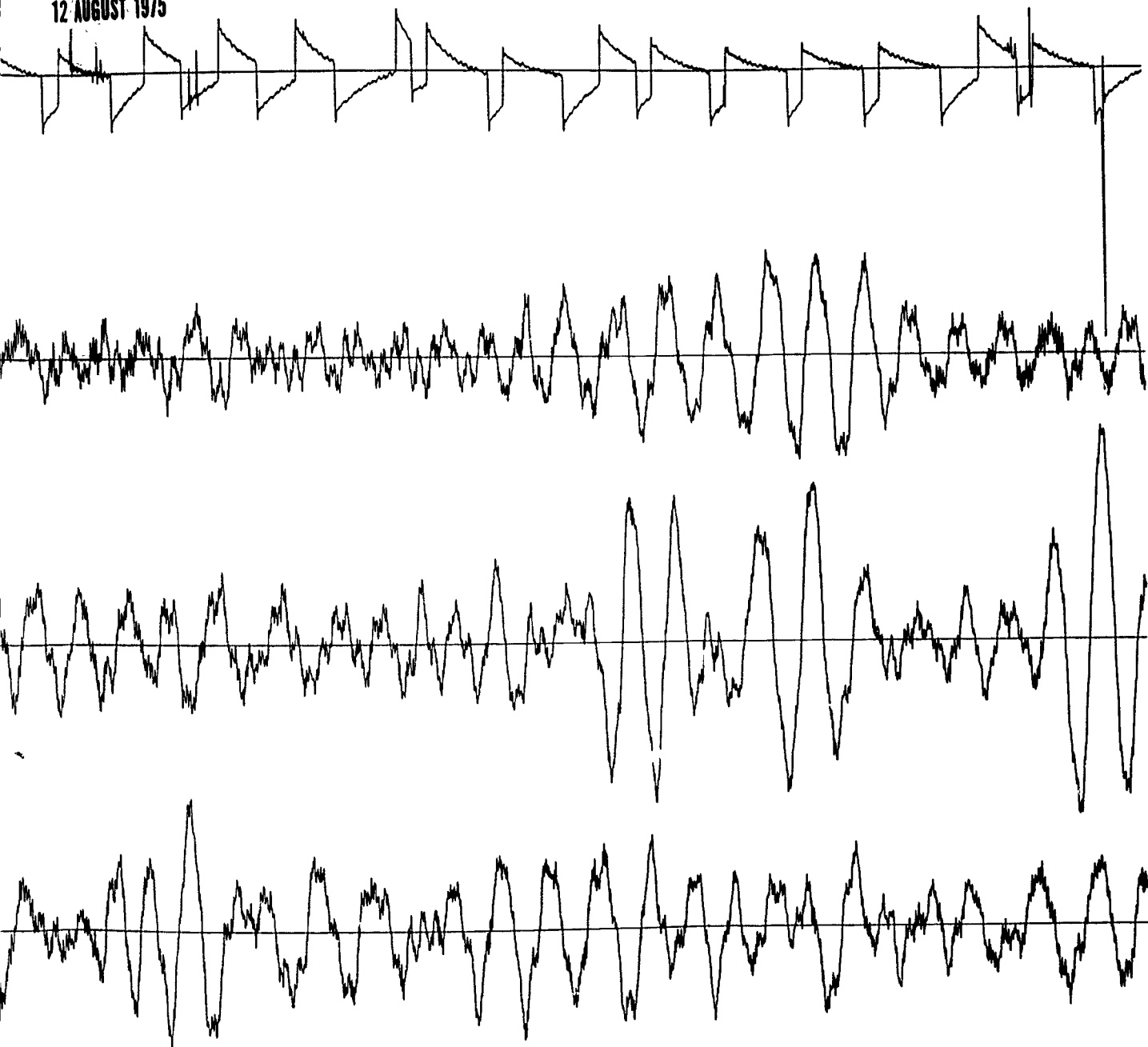


CE THROW II EVENT 1 (TNT EVENT)

2 Hz SEISMOMETERS

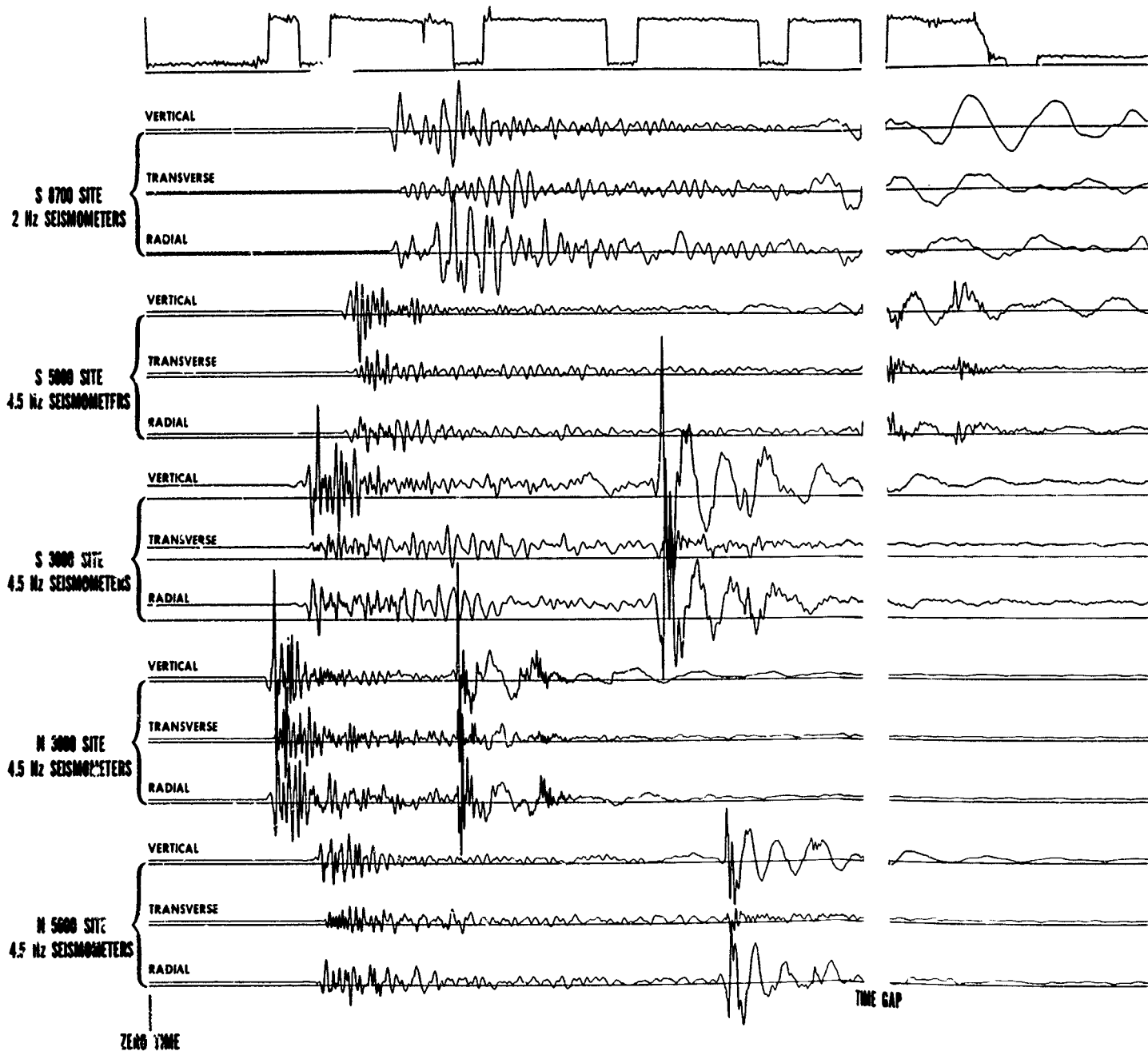
S 35,000 SITE

12 AUGUST 1975

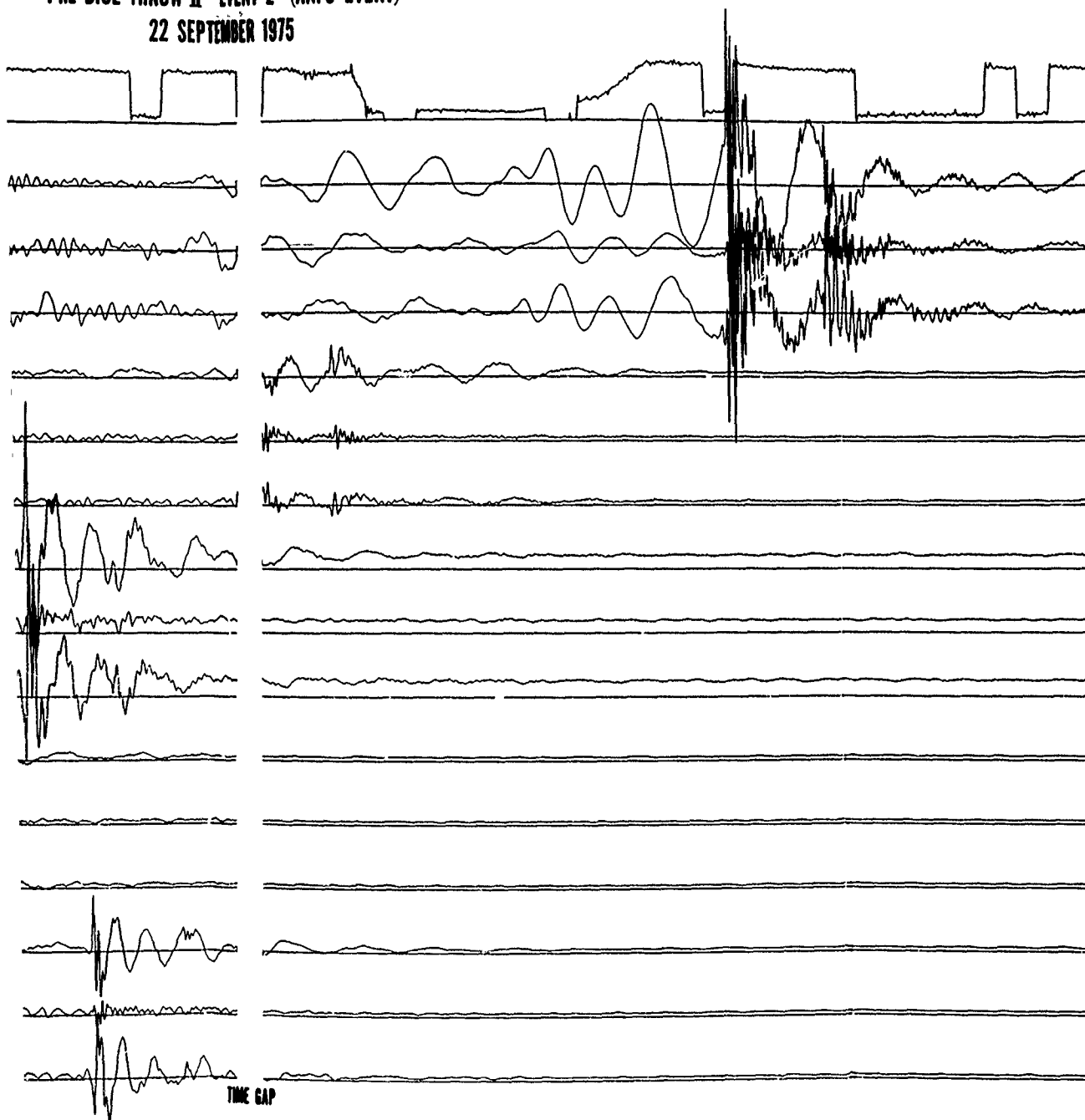


2

PRE DICE THROW II EVENT 2 (ANFO EVENT)  
22 SEPTEMBER 1975

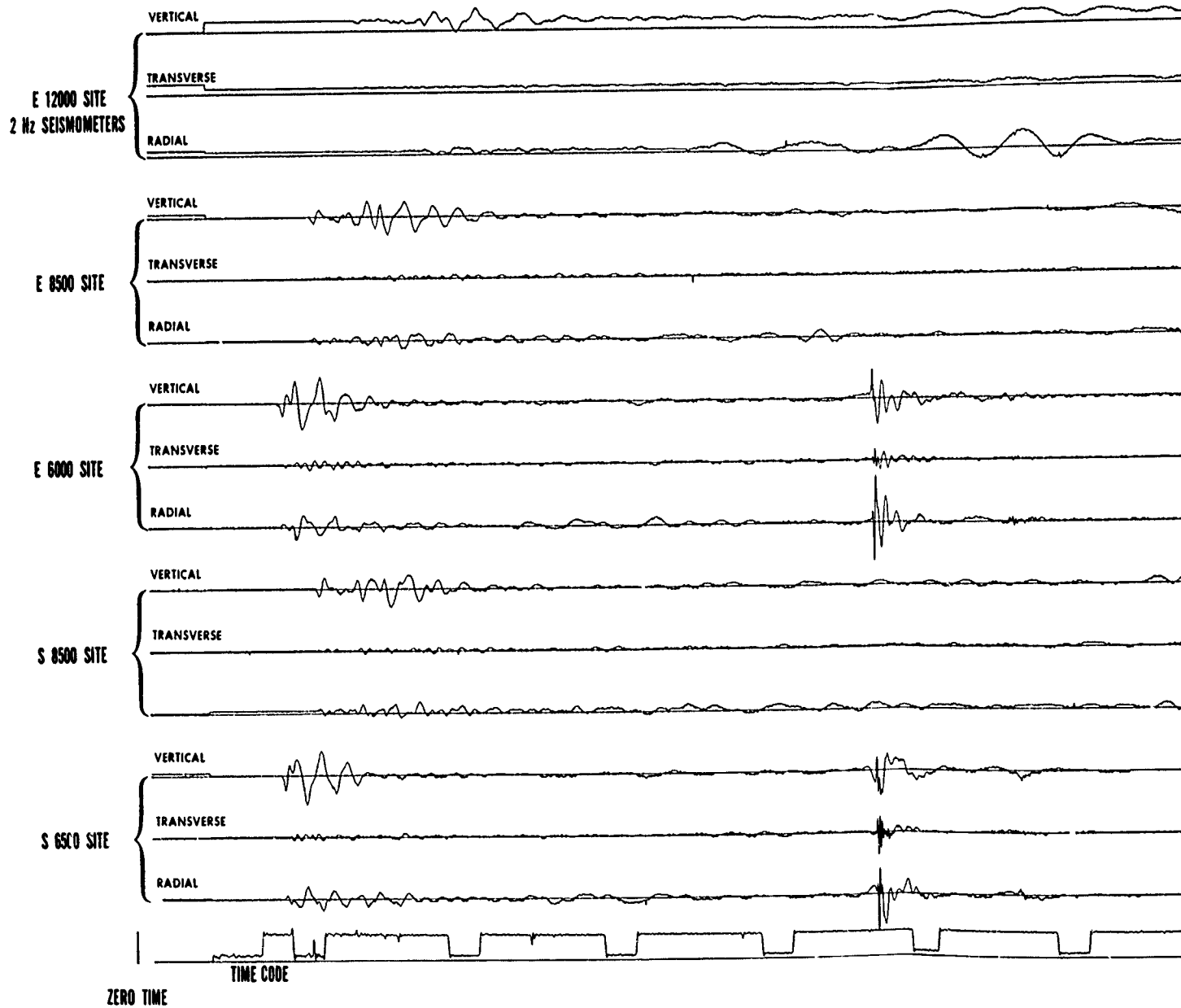


PRE DICE THROW II EVENT 2 (ANFO EVENT)  
22 SEPTEMBER 1975

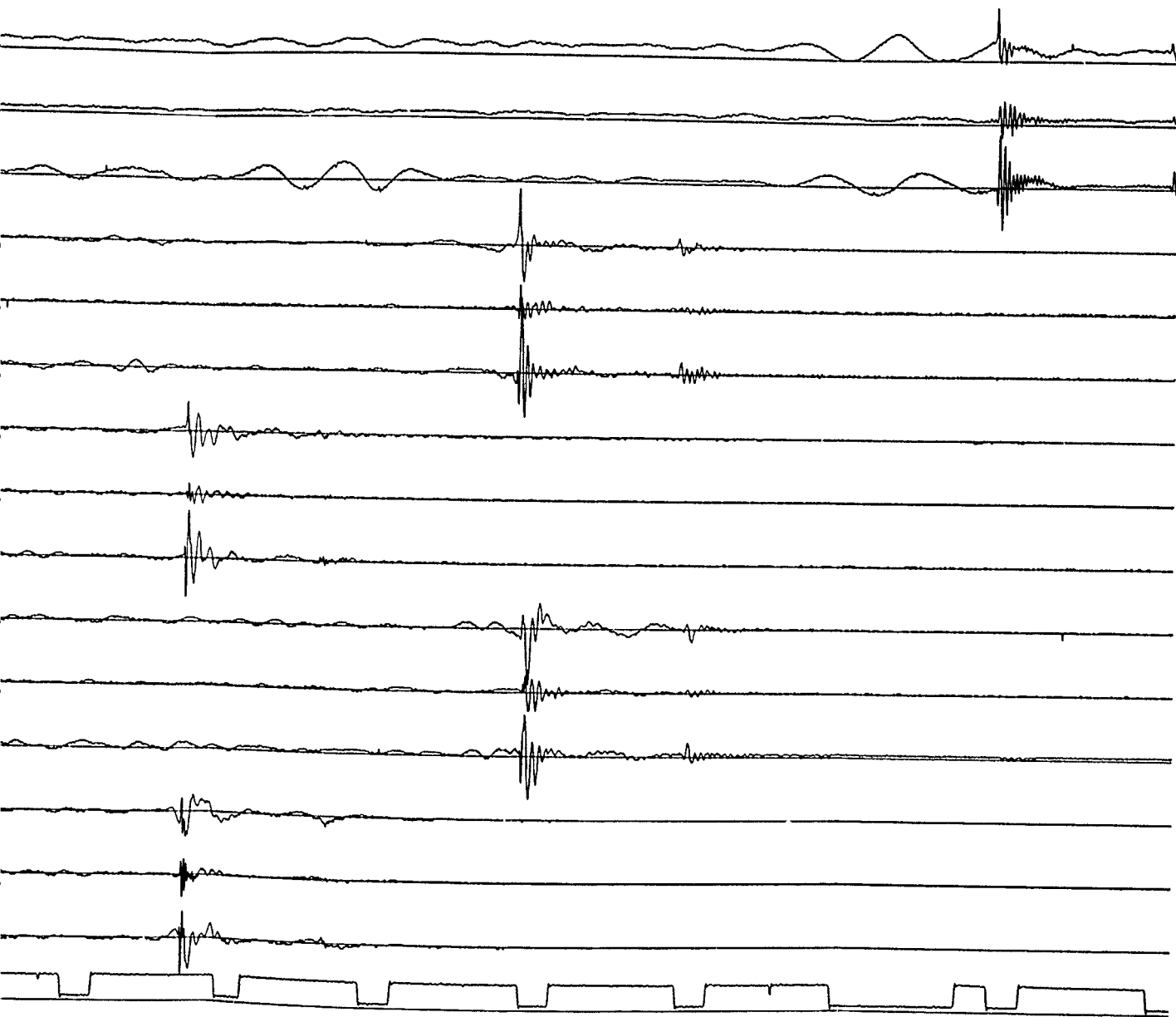


2

1976 DICE THROW (ANFO EVENT)  
OCT. 6, 1976



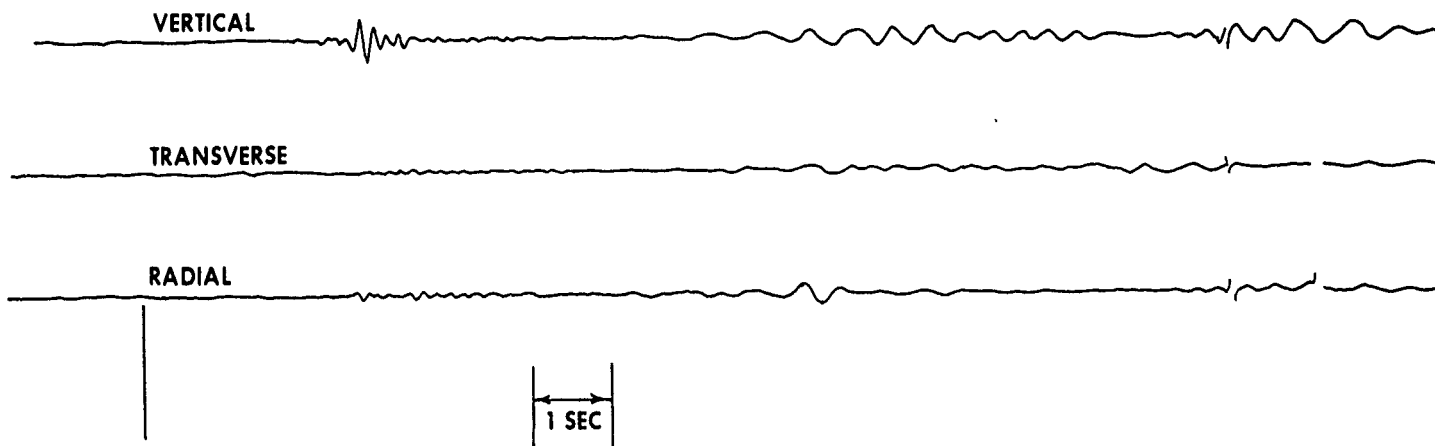
1976 DICE THROW (ANFO EVENT)  
OCT. 6, 1976



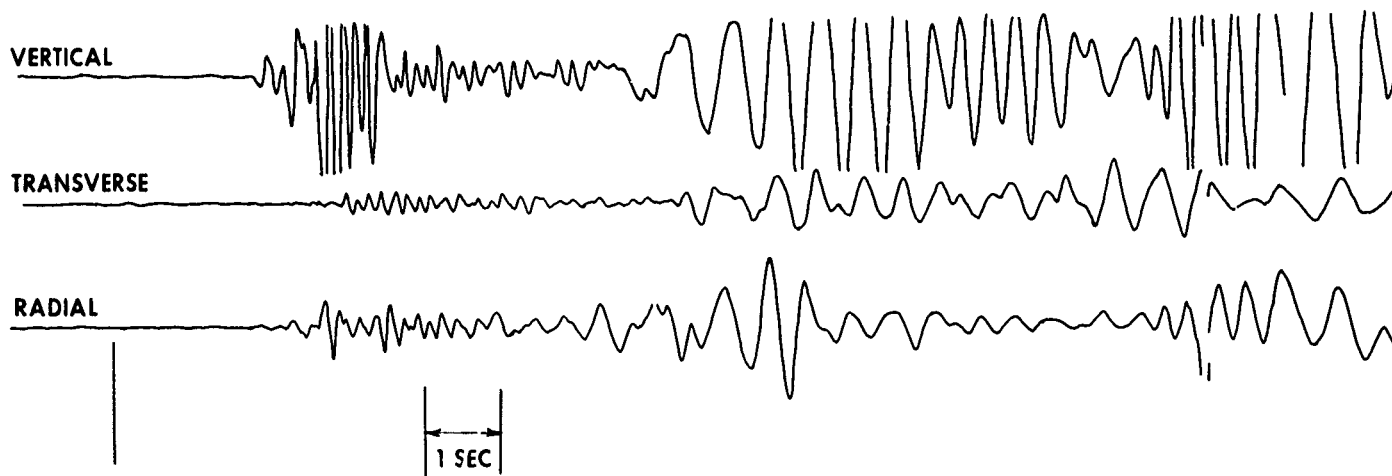
2



**DICE THROW  
S 16,000 SITE  
HIGH GAIN CHANNELS**



**LOW GAIN CHANNELS**



ELS

~~~~~

~~~~~

~~~~~

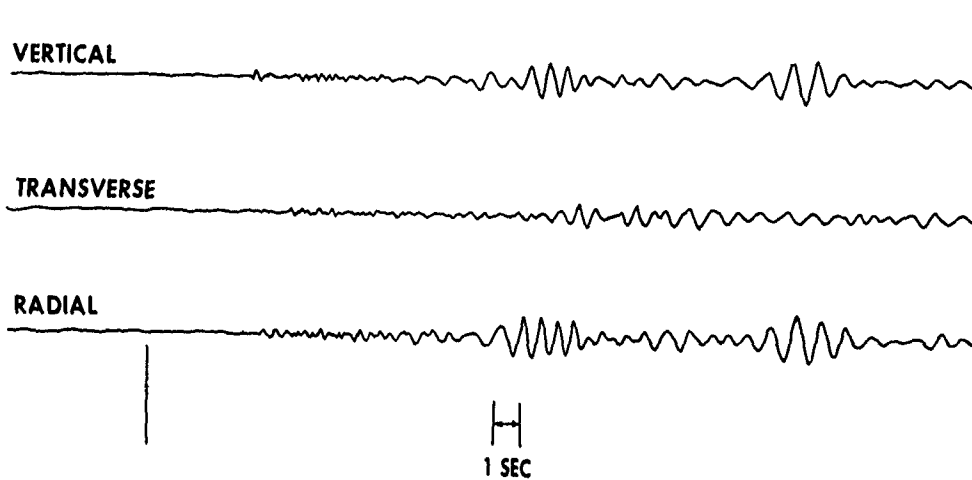
LS

~~~~~

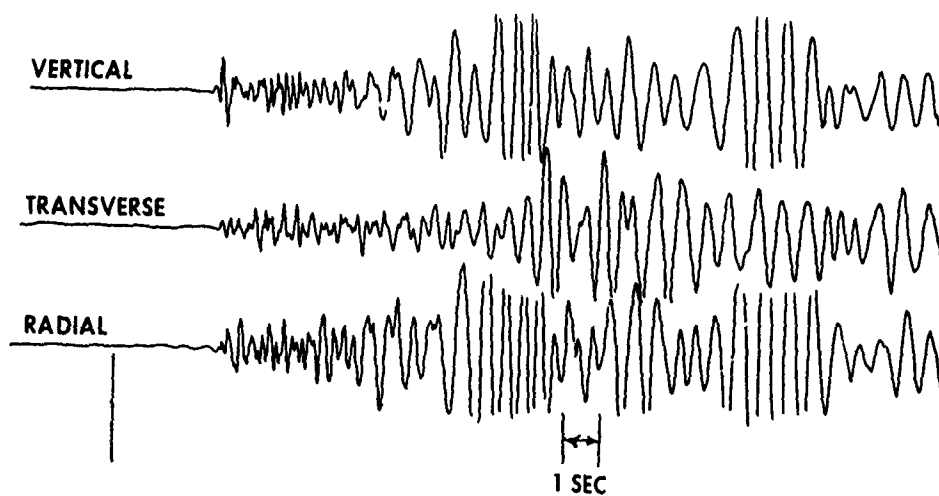
~~~~~

~~~~~

DICE THROW  
E 25,000 SITE  
HIGH GAIN CHANNELS



LOW GAIN CHANNELS



DICE THROW  
S 25,000 SITE  
HIGH GAIN CHANNELS

VERTICAL

TRANSVERSE

RADIAL

1 SEC

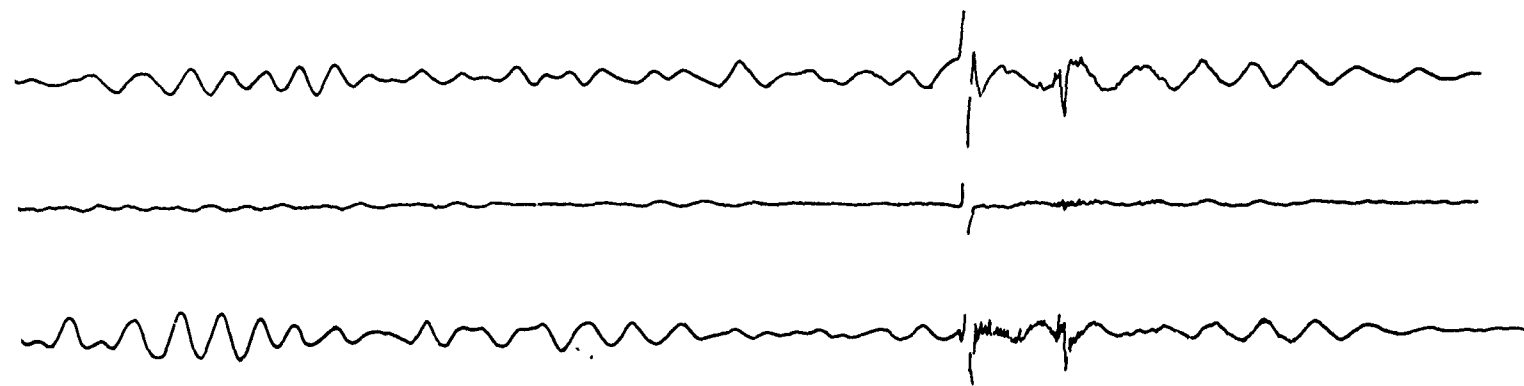
VERTICAL

TRANSVERSE

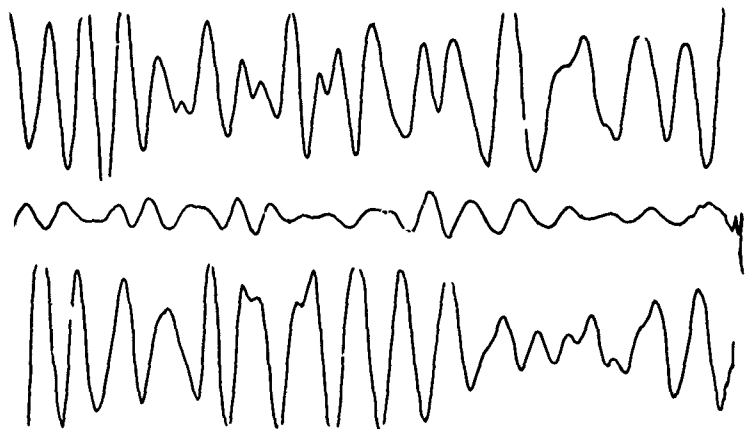
RADIAL 2

1

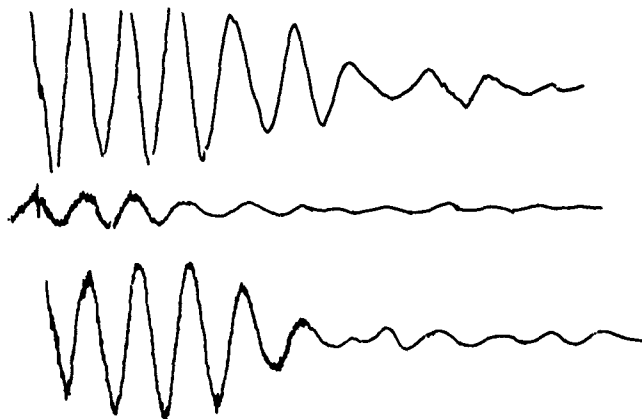
DICE THROW  
S 25,000 SITE  
HIGH GAIN CHANNELS



1 SEC



1 SEC



2

**DICE THROW  
S 35,000 SITE  
HIGH GAIN CHANNELS**

**VERTICAL**



**TRANSVERSE**

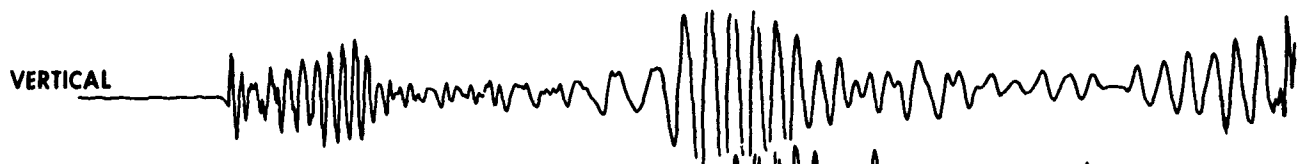


**RADIAL**



**LOW GAIN CHANNELS**

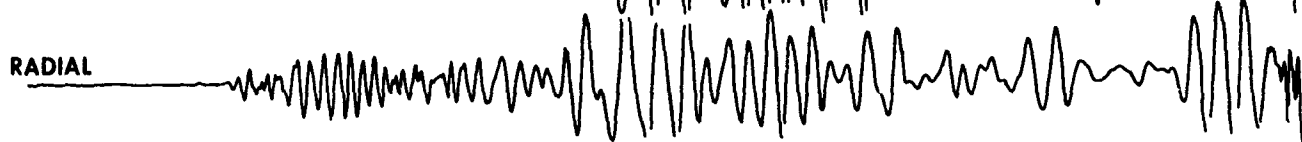
**VERTICAL**



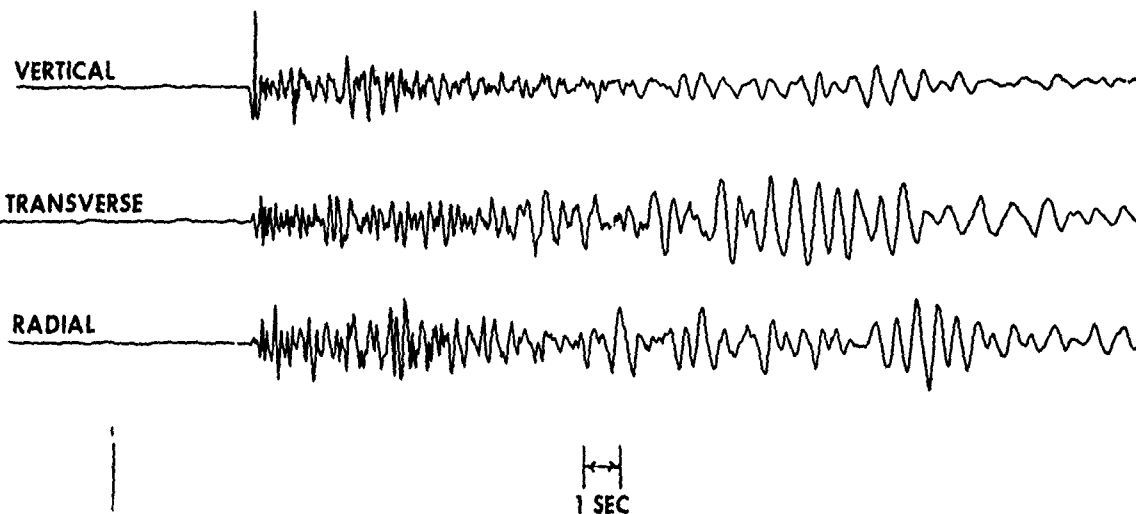
**TRANSVERSE**



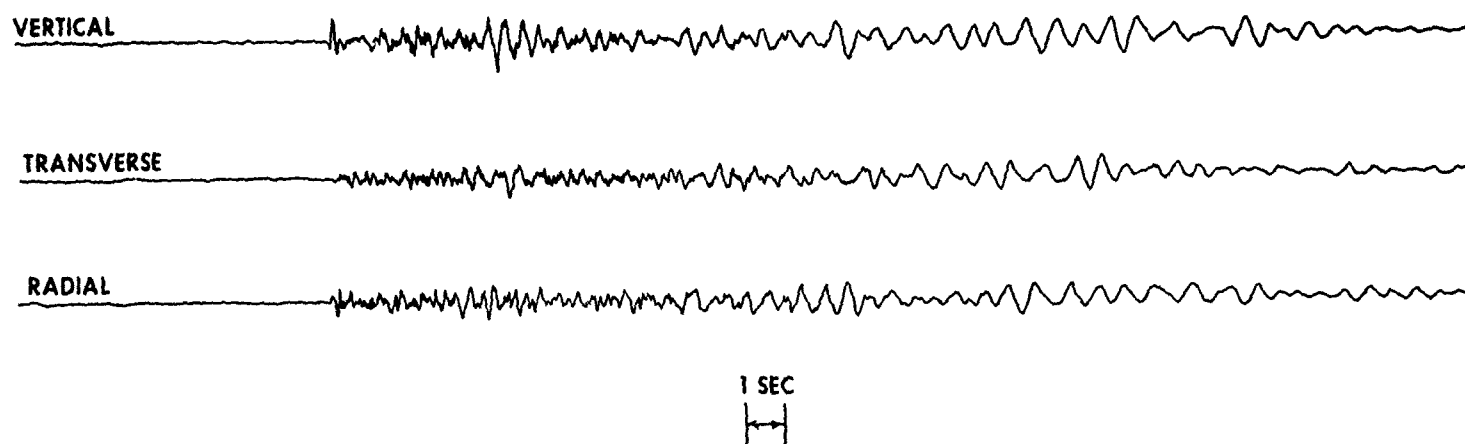
**RADIAL**



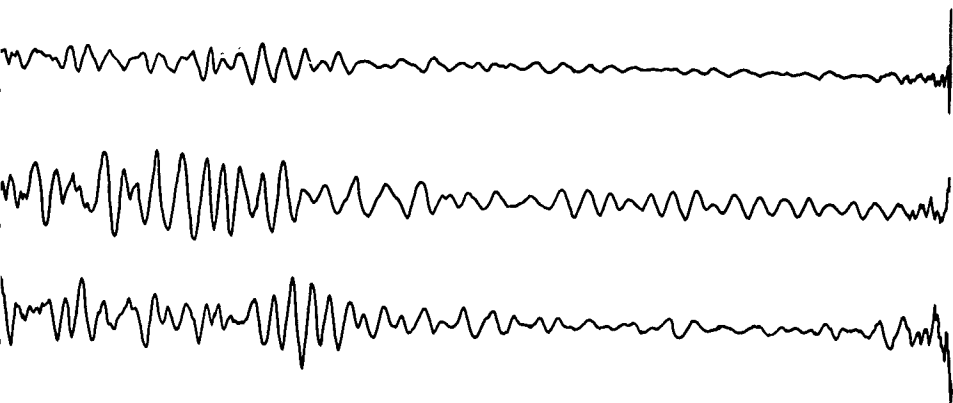
DICE THROW S 43,000 SITE HIGH GAIN CHANNELS



DICE THROW  
S 57,000 SITE  
HIGH GAIN CHANNELS



13,000 SITE HIGH GAIN CHANNELS



DICE THROW  
S 57,000 SITE  
HIGH GAIN CHANNELS

